REPORT DOCUMENTATION PAGE

Form Approved
OMB No. 0704-0188

1. AGENCY USE ONLY (Leave blank)	2. REPORT DATE	3. REPORT TYPE AND DATES COVERED
	29 Sept., 1997	Final Report

4. TITLE AND SUBTITLE

Autoignition and combustion in Diesel Engines Under Cold Starting conditions.

5. FUNDING NUMBERS

DAAL 03-88-K-0016

6. AUTHOR(S)

Naeim A. Henein

7. PERFORMING ORGANIZATION NAME(S) AND ADDRESS(ES)

Center for Automotive Research
Wayne State University
Detroit, Michigan

8. PERFORMING ORGANIZATION REPORT NUMBER

9. SPONSORING / MONITORING AGENCY NAME(S) AND ADDRESS(ES)

U. S. Army Research Office
P. O. Box 12211
Research Triangle Park, NC 27709-2211

10. SPONSORING / MONITORING AGENCY REPORT NUMBER

ARO 25190.2-EG

11. SUPPLEMENTARY NOTES

The view, opinions and/or findings contained in this report are those of the author(s) and should not be construed as an official Department of the Army position, policy, or decision, unless so designated by other documentation.

12a. DISTRIBUTION / AVAILABILITY STATEMENT

Approved for public release; distribution unlimited.

12b. DISTRIBUTION CODE

13. ABSTRACT *(Maximum 200 words)*

This report includes the results of an investigation on the autoignition and combustion processes in diesel engines at low ambient temperatures. Experiments were conducted on three different single-cylinder direct-injection, four-stroke engines, using fuels of different cetane numbers and physical properties. Tests covered ambient temperatures ranging from 25°C to -25°C. The engines were soaked at least eight hours before a cold start test. The analysis indicated that the difficulty in starting diesel engines is caused by combustion instability at low temperatures. Combustion instability will cause the engine to misfire once before it fires again. This is referred to as 8-stroke-cycle operation. If it misfires twice , it is referred to as 12-stroke-cycle operation, and so on. This pattern was found to be reproducable. The engine may start on a 12-stroke-cycle operation at low temperatures, shift to an 8-stroke-cycle, and finally shifts to the regular 4-stroke-cycle. This pattern has been found not to be engine or fuel specific. A detailed thermodynamic and combustion analysis of the experimental data indicated that the cause for combustion instability is a combination of dynamic, physical and chemical kinetics factors. Recommendations are made to reduce combustion instability by using the electronic controls already available on engines.

14. SUBJECT TERMS

Diesel engines, cold starting, combustion instability, white smoke

15. NUMBER OF PAGES

78

16. PRICE CODE

17. SECURITY CLASSIFICATION OF REPORT	18. SECURITY CLASSIFICATION OF THIS PAGE	19. SECURITY CLASSIFICATION OF ABSTRACT	20. LIMITATION OF ABSTRACT
UNCLASSIFIED	UNCLASSIFIED	UNCLASSIFIED	UL

NSN 7540-01-280-5500

Standard Form 298 (Rev 2-89)
Prescribed by ANSI Std Z39-18
298-102

Autoignition and Combustion in Diesel Engines Under Cold Starting Conditions

Final Report

Naeim A. Henein

September 26, 1997

U. S. Army Research Office
Contract Number
DAAL 03-88-K-0016

Center for Automotive Research
Detroit, MI 48202

Approved for Publication Release:

Executive Summary

Military diesel engines should have quick and reliable starting characteristics, without the emission of visible white smoke. This is particularly important in the field where every effort is made to assure prompt starting and reduce the vehicle signature. The goal of this program is to gain more insight and a better understanding of the autoignition and combustion processes in diesel engines under low ambient temperatures, in order to improve the startability of military dieasel engines.

The approach taken in this project is experimental supported by detailed analytical investigation aimed at identifying the nature and causes of engine misfiring. Experiments were conducted on three different single-cylinder engines to assure that the findings are not related only to any specific engine. All these engines are of the four-stroke type with direct injection combustion chambers, the type used in military engines. The first engines is a stand-alone air-cooled engine complete with its electric starter and fuel tank, installed in the cold room. The tests on this engines were under actual starting conditions where the engine dynamics play a key role in the thermodynamic and combustion processes. The second engine is a TACOM-LABECO research engine installed in the cold room, and connected to an electric dynamometer. The tests on this engine were conducted at constant speed to eliminate the effect of engine dynamics on combustion. The third engine was a modified research engine with a transparent piston top and a reflecting mirror to photograph the fuel spray and observe its development, evaporation, mixing with air, autoignition and combustion. The engines were soaked for at least eight hours before conducting a start test.

The tests covered a wide range of ambient temperatures, from 25°C to -25°C. Fuels of different physical and chemical properties were tested. These included Diesel fuel DF2, JP5 fuel, and two military fuels: Ref1 (volatile) and Ref2 (less volatile).

This investigation showed that combustion instability at low temperatures is the source of the difficulty in cold starting and the emission of large amounts of white smoke. Combustion instability has been found not to be a random phenomenon because it can be reproduced. The engine may start firing and misfire once before it fires again. This is referred to as an eight-stroke-cycle operation. If it misfires twice, it is considered to be in a twelve stroke operation, and so on. The engine may start on a twelve-stroke-cycle at low temperatures, and shifts to an eight-stroke-cycle, and finally to the regular four-stroke-cycle. This pattern was found to be repeatable, and not specific to any engine or any fuel. The reasons for such instability were identified and found to be related to a combination of dynamic, physical and chemical kinetics factors.

It is recommended that further research be conducted to understand the details of the chemical autoignition reactions by using laser based diagnostic techniques. Also, it is recommended that the results of this research be applied to develop a strategy for starting the engine. This strategy will be implemented by using the electronic controls, already available in heavy duty diesel engines. This will assure an improvement in the starting of military diesel engines, without the emission of white smoke.

Table of Contents

Introduction

The diesel engine cold start conditions represent the worst of all engine conditions for the autoignition and combustion processes. The ambient temperature, low rotating speeds during cranking, and the resulting low compression temperatures and pressures contribute to the difficulties experienced in cold-starting diesel engines. These difficulties may become severe and result in unreliable starting when fuels which are slightly off specifications, such as JP8, are used instead of regular diesel fuel. The problems encountered during starting are :

1- Complete failure to start.
2- Successful firing but failure to sustain running.
3- Successful starting and sustained running with the emission of excessive amounts of unburned hydrocarbons which appear as white smoke.

For military engines the conditions are more severe, and the situation is more serious. Starting reliability should be very high, and the engines may be required to start and successfully run on fuels having off-specifications for Cetane Number and other physical properties. In addition, the emission of excessive amounts of white smoke during starting of military diesel engines may be undesirable or even dangerous. This is particularly the case in the field, where every effort is made to reduce vehicle signature.

Most of the research on autoignition and combustion of fuel sprays in diesel engines has been conducted at high temperatures, with the goal of improving thermal efficiency and reducing undesirable gaseous and particulate emissions. The investigations on cold starting have been limited to the overall engine performance parameters, without analysis of the processes which lead to such performance. The parameters included time-to-first fire, time required for the engine to reach idle speed, time to achieve sustained running, the minimum unaided starting temperature, and the time required for the disappearance of white smoke. No work has been done to investigate the autoignition and combustion processes under the cold start conditions.

The goal of this investigation is to conduct a detailed cycle-by-cycle analysis of the thermodynamic, autoignition and combustion processes during cold starting, identify the different cold-start phenomena, determine the cause(s) of combustion instability, and propose approaches to improve the reliability of starting military diesel engines.

Research Approach

The approach is a to run experiments under controlled conditions on different engines, using different fuels under a wide range of ambient room temperatures.

Experimental engines used in the investigation:

1- A stand-alone single cylinder, air cooled, four-stroke-cycle, direct injection diesel engine, installed in the cold room , complete with its electric starter and fuel tank.

2- A TACOM-LABECO single cylinder research engine, installed in the cold room and connected to an electric dynamometer.
3- An optical access modified single-cylinder diesel engine installed outside the cold room for starting tests at normal room temperature.

Fuels :
The following fuels were tested :
1- DF2 diesel fuel.
2- JP5 fuel.
3- REF1 military reference fuel.
4- REF2 military reference fuel.

Ambient temperatures:
Cold-start tests were conducted with the engines soaked for at least eight hours, under the temperatures ranging from 25°C to -20°C.

Experimental Results and Discussions:

The details of the experimental work, including instrumentation, samples of experimental data, samples of theoretical analysis, discussions and conclusions are given in the following publications which are included in the Appendix:

Appendix 1:
"Diesel Cold Starting: A Phenomenological Model," ASME Energy-Sources Technology Conference, paper No. 93-ICE-24, 1993.

Appendix 2:
" Diesel Cold Starting: Actual Cycle Analysis Under Border-Line Conditions," Zahdeh, A. R., Henein, N. A., and Bryzik, W., SAE paper No. 900441.
Appendix 3:
"Diesel Engine Cold Starting: Combustion Instability," Henein, N. A., Zahdeh, A. R., Yassine, M. K., and Bryzik, SAE paper No. 92005.
Appendix 4:
"Diesel Cold Starting: White Smoke," Zahdeh, A. R., and Henein, N. A., SAE 920032
Appendix 5:
"Fundamental Cold Start Phenomena Within Advanced Military Diesel Engines," Bryzik, W., and Henein, N. A., 19th Army Science Conference, Orlando, Florida, 20-23 June ,1994.

Conclusions:

The following are the main conclusions reached in this project and detailed in the above five publications:

1- The phenomenological model developed, explains the effect of ambient temperature and cetane number on the startability of single-cylinder and multi-cylinder diesel engines. In addition it indicates the need for a better understanding of the different processes which contributes to the difficulty in starting military diesel engines, and the resulting white smoke emissions.

2- The phenomenon of combustion instability has been identified and investigated in tests on a single cylinder stand-alone diesel engine running on diesel fuel. The engine experienced the following modes of operation:

a- regular 4-stroke-cycle.
b- single-skip cycle before refiring, referred to as an 8-stroke-cycle.
c- double-skip cycle before refiring, referred to as 12-stroke-cycle operation.
d- triple-skip cycle before refiring, referred to as 16-stroke-cycle.

The 4-stroke cycle operation was observed at temperatures above 0°C. Lowering the ambient temperature resulted in the operation on the 8-stroke-cycle. Lowering the temperature further, resulted in the operation on the 12-stroke-cycle and the 16-stroke cycle. At certain temperatures the engine operated on a combination of the different cycles.

3- Combustion instability during cold starting of diesel engines is not a random phenomenon. It follows a repeated pattern, where the engine may skip one or more cycles. The engine shifts from one mode to another with less skip cycles. Finally it runs on the regular 4-stroke-cycle.

4- Combustion instability is not fuel specific. All the hydrocarbon fuels tested in this program experienced combustion instability during diesel cold starting. The tested fuels have a wide range of properties, including volatility, cetane number, and specific gravity.

5- Combustion instability is not engine specific. It has been observed and documented on the stand-alone single-cylinder engines, the transparent single-cylinder engine, and a production 4-cylinder engine. These engines are four-stroke-cycle, direct injection, and of different designs and makes.

6- Cool flames were observed before the sharp pressure rise in the firing cycle. Cool flames were also observed in the misfiring cycles.

7- The cause of the first misfiring after acceleration appears to be a combination of the following dynamic, and chemical and physical factors:

a- Engine dynamics which result in acceleration after a firing cycle, allow less time at top dead center for the processes which lead to ignition to be completed. This results in late start of combustion reactions in the expansion stroke.
b- The rate of the combustion reactions is reduced because of the decreasing gas temperature of the expanding gases. This is in addition to the drop in the reaction rates caused by the charge dilution by the exhaust gases from the firing cycle.
c- Misfiring when running on less volatile fuels, such as Ref 2, can also be contributed to the lack of fuel vapor, mixed with oxygen, ready to carry on the combustion process after autoignition. Detailed analysis of the cylinder gas pressure traces and rates of heat release indicated that autoignition exothermic reactions started but combustion failed.

8- The causes of sequential misfiring appear to be an imbalance between the following:
a- energy released from exothermic reactions which depend on the concentration of the fuel vapor, dilution with residual gases which still remain after the first misfiring, and the gas temperature.
b- energy absorbed in fuel evaporation, endothermic reactions, heat losses to the walls, and blowby losses.

Recommendations:

1- Investigate the chemical factors which cause combustion instability by using advanced laser based diagnostic techniques in the optical access engine.

2- Develop a new technique to measure the mass of the white smoke emitted during the cold start of heavy duty engines.

3- Apply the research findings to develop a strategy for the fast and reliable starting of multi-cylinder military diesel engines, without the emission of white smoke. Apply this strategy, by using the electronic controls already available on current production heavy duty engines. Conduct tests to verify the effectiveness of the new strategy.

Appendix 1

"Diesel Cold Starting: A Phenomenological Model," Henein, N. A.

ASME Energy-Sources Technology Conference , Paper No. 93-ICE-24, 1993

THE AMERICAN SOCIETY OF MECHANICAL ENGINEERS
345 E. 47th St., New York, N.Y. 10017

93-ICE-24

DIESEL COLD STARTING: A PHENOMENOLOGICAL MODEL

N. A. Henein
Department of Mechanical Engineering
Center of Automotive Research
Wayne State University
Detroit, Michigan

ABSTRACT

A phenomenological model is developed to bring more insight in the interrelationships between the engine dynamics and the autoignition and combustion processes, under low ambient temperatures. The parameters which affect the engine dynamics during cranking are: the cranking torque, engine frictional losses and inertia of moving parts. The parameters which affect the autoignition are the air pressure and air temperature near the end of the compression process, and the cetane number of the fuel. The parameters which affect the combustion process are the mass of fuel injected, fuel volatility and rates of combustion reactions. The net driving torque on the crank shaft of the engine is a function of the starter torque, gas torque, and the frictional torque.

The interdependency of these parameters is explained and illustrated graphically in a diagrammic format.

INTRODUCTION

The difficulties in the cold starting of diesel engines arise from the fact that they rely on the autoignition process to start combustion. Unlike the spark ignited (gasoline) engine, the diesel engine does not use an electric spark to ignite a premixed charge of fuel-vapour and air. The diesel fuel has a very low volatility if compared with gasoline and is not premixed with the intake air, but it is much easier to autoignite than gasoline.

Many factors affect the startability of automotive diesel engines. These factors are related to the starting system, engine dynamics and the autoignition and combustion processes. The following is a list of some important parameters which affect the startability of the diesel engine.

a. Starting system: battery charge and starter characteristics.

b. Engine design:

   i- Combustion chamber:
      . Surface to volume ratio
      . Turbulence
      . Material

   ii- Compression Ratio:

. Nominal
. Valve timing

iii- Inertia of the rotating and reciprocating parts

iv- Frictional Torque:
. Piston assembly
. Bearings
. Valve gear
. Pumps
. Accessories
. Lubricating oil viscosity, viscosity index and additives

v- Injection system type and design

vi- Engine deterioration and blowby rate:
. Piston rings wear
. Cylinder wear
. ...

c- Fuel properties:
. Cetane number
. Volatility
. Heating value

d- Compressed air properties:
. Temperature
. Pressure

Other parameters affect diesel engine startability. In the following sections the major parameters which affect engine dynamics autoignition and combustion will be explained.

ENGINE DYNAMICS

The air temperature and pressure at the end of the compression stroke, in any engine, depends mainly on the cranking speed.

The acceleration of the engine to the cranking speed depends on the torques acting on the crankshaft, which include the starter torque, the net gas torque, the friction torque, the load torque and the inertia torque of the rotating and reciprocating parts.

$$\frac{d\omega}{dt} = \frac{T_s + T_g - T_f - T_L - mr^2\omega^2(TK)\frac{d(TK)}{d\theta}}{I_e + mr^2(TK)^2}$$

The gas torque varies during the engine cycle and reaches a peak value in the early part of the expansion stroke. The net gas torque of the cycle depends on the total amount of energy released from fuel combustion, rate of energy release, the heat transfer losses to the cylinder walls and the blowby losses. The net cycle torque may be positive or negative. If combustion fails or does not release enough energy to overcome the losses, the net gas torque can be negative.

The engine frictional torque is the sum of the frictional torques of the moving components. During starting the frictional torques may be high because of the high oil viscosity, and the absence of the formation of a continuous oil film. In addition ancillary frictional losses may be high.

The load torque is usually zero during starting, if the engine is decoupled from the driven equipment.

The inertia torque is due to the acceleration or deceleration of the rotating and reciprocating components.

The starter torque is a function of the battery voltage and current, the load on the starter and its efficiency. It is related to the starter speed by an exponential function (1). In this analysis the starter torque will be considered to be a constant.

AUTOIGNITION

The preignition processes consist mainly

of the injection and spray formation, heat and mass transfer between the air and the spray leading to the formation of an ignitable mixture, endothermic reactions leading to the formation of intermediate radicals and exthothermic reactions leading to the formation of ignition nuclei and the release of enough detectable energy. The start of the increase in pressure due to combustion is generally considered as an indication of the start of combustion. The details of these processes are not well understood and many empirical correlations have been developed for their description. The period of time between the start of injection and the pressure rise due to combustion is known as the ignition delay and can be expressed in terms of the gas temperature T and pressure P (2):

$$I.D. = \frac{A e^{\frac{E}{RT}}}{P^n}$$

During starting of compression temperatures and pressures are low because the relatively high heat transfer and blowby losses. As the engine is motored the walls get warmer and these losses decrease.

COMBUSTION PROCESSES

The success of the combustion process, after autoignition takes place, depends on the availability of a property premixed fuel-vapour and air in the vicinity of the ignition nuclei. The fuel volatility, air temperature and spray characteristics play major roles in the formation of the ignitable mixture. The rate of release of the energy of combustion during the early stages depends on the total amount of the ignitable mixture and its temperature. At low temperatures the combustion reactions might not be fast enough to release energy while the piston is close to top dead center. As the expansion process proceeds the gas temperatures may drop, and slow the combustion reactions. Eventually combustion may fail in spite of the formation of the ignition nuclei.

In this analysis the fuel is considered to be volatile enough and the injection rate and timing are adjusted to produce an enough amount of the ignitable mixture for combustion to be completed.

The above analysis indicate that the dependency of the diesel cold startability on the different parameters is very complicated. Detailed computer programs can be developed to simulate the engine dynamics and combustion (3). However, a simplified description of the interrelationships between the major parameters which affect starting can give more insight and a better understanding of the starting process.

The goal of this paper is to describe in a graphic way a phenomenological model for engine startability. The model is developed in two step. The first is for a frictionless engine and the second is for engines with friction.

SIMPLIFIED STARTABILITY DIAGRAM FOR A FRICTIONLESS ENGINE:

Fig. (1) shows a startability diagram developed for a frictionless engine. The diagram is divided into four quadrants. The first relates the rotational speed to the net torque on the crankshaft. The second relates the ignition delay period to rotational speed. The third relates the gas torque to the ignition delay period. Point O represents the condition where the net gas torque is equal to zero. A point between O′ and O indicates a negative torque because the work during the expansion stroke is less than the compression work and the pumping losses. The fourth quadrant relates the net driving torque on the crankshaft to the starter torque, if it is still engaged, and the gas torque.

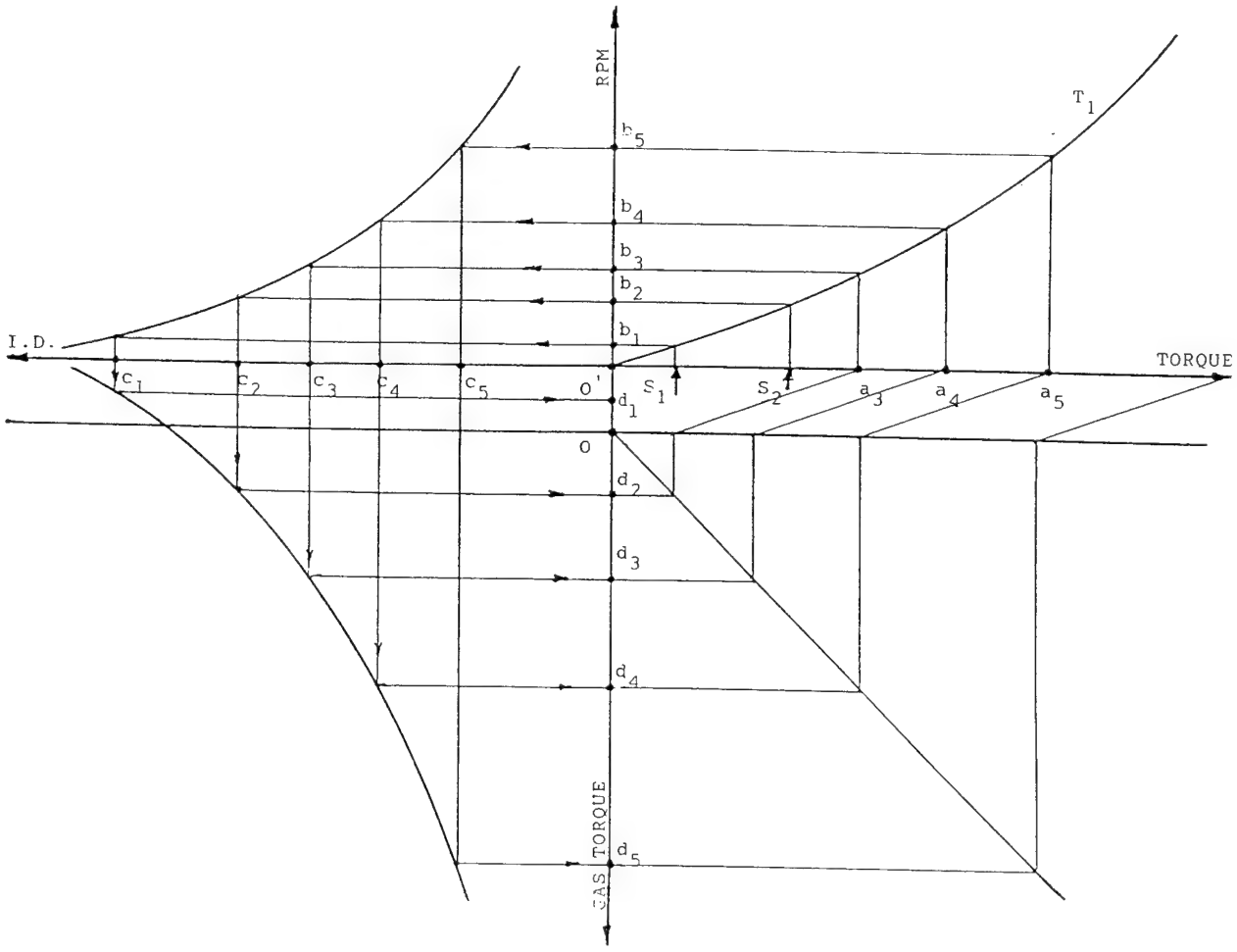

Fig.(1): Startability Diagram for a Frictionless Single Cylinder Engine

The use of this diagram can be explained as follows:

1- Points S_1 and S_2 represent two different starter cranking torques which rotate the engine at cranking speeds represented by points b_1 and b_2.

2- The rotation at speeds b_1 and b_2 produce ignition delays represented by c_1 and c_2.

3- The ignition delays c_1 and c_2 result in gas torques d_1 and d_2 respectively. The gas torque represented by d_1 is a negative torque. The gas torque represented by d_2 is transmitted to the crankshaft without frictional loss, according to the assumption made for this diagram. Here we have two possibilities. The first is for the starter being turned off. The result is that the engine fails to start. The second possibility is for the starter being kept on, and the gas torque is added to the starter torque. Under this condition the total torque acting on the crankshaft, represented by a_3, causes the engine to accelerate to a rotating speed b_3. The ignition delay is c_3 and gas torque is d_3. If the starter is turned

off the engine will stop because e_3 is less than s_2. If the starter is kept on, the total torque would be a_4, and the engine will accelerate to b_4, resulting in I.D. c_4 and a gas torque d_4. It is noticed that e_4 is more than the starting torque s_2, which means that the engine will keep rotating even if the starter is turned off. If the starter is turned off the engine will decelerate momentarily and then accelerate again. But if the starter is kept on, the engine will accelerate to b_5, produce I.D. c_5, and a gas torque d_5 and will probably start successfully.

EFFECT OF AMBIENT TEMPERATURE ON STARTABILITY:

Lowering the ambient temperature affects the actual engine startability in many ways. It results in the following:

a- lower cranking speeds because of the lower battery discharge rate and the higher oil viscosity,

b- longer ignition delays because of the lower compression temperatures,

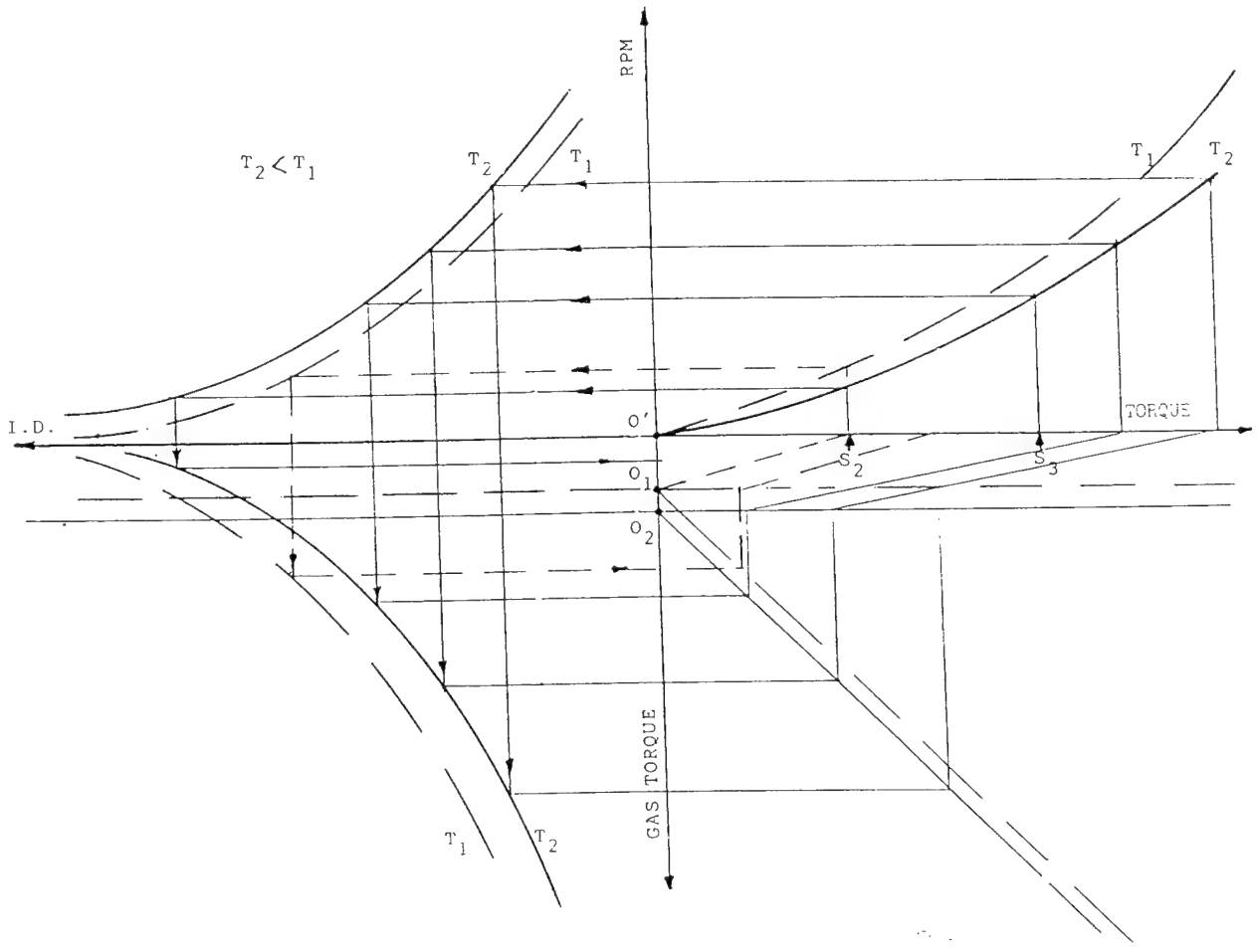

Fig. (2): Effect of Ambient Temperature on Starting

c- lower gas torques because of the higher heat losses and the slower evaporation and combustion reactions.

In this simplified case the engine is considered frictionless and lowering the ambient temperature affects only the I.D. and indicated work. Fig. (2) illustrates the effect of lowering the ambient temperature from T_1 to T_2 on the startability of the frictionless engine. The dashed lines are for T_1 and the solid lines are for T_2. For the same starting torque the cranking speed at T_2 is less than at T_1. Following the lines for each temperature shows that a torque s_2 produced a successful starting at T_1 but failed to start the engine at T_2. Even if the engine was cranked at the same RPM, the ignition delay at T_2 would have been longer than that at T_1. The negative indicated work at T_2, O_2 is more than O_1 at T_1, because of the higher rates of heat transfer losses at the lower temperature. While a starting torque S_2 failed to start the engine, a torque S_3 which is twice S_2 would successfully start the engine.

The above analysis indicates that there is a critical starting torque which should be exceeded before the engine starts. The critical S_c is illustrated in Figure (3). Sc_2 for T_2 is higher than Sc_1 for T_1.

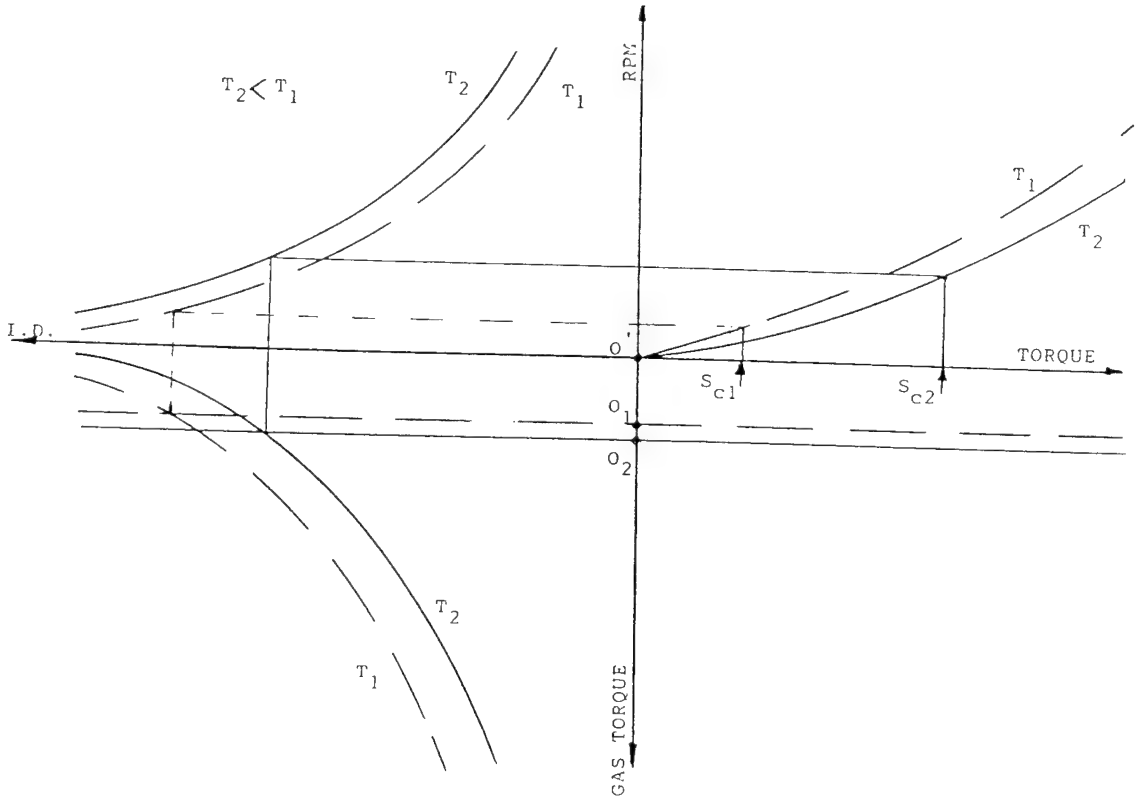

Fig. (3): Effect of Ambient Temperature on the Critical Starting Torque

EFFECT OF THE CETANE NUMBER ON STARTABILITY

The effect of Cetane Number of the fuel is illustrated in Figure (4). The starting of the engine with fuel of a lower cetane number will be more difficult. This requires a higher starting torque than the fuel of higher cetane number. Figure (5) indicates that the critical starting torque increases with the drop in cetane number.

STARTABILITY DIAGRAM FOR ENGINES WITH FRICTION

Two types of engines are considered: a single cylinder engine and a multiple cylinders engine.

1- Single Cylinder Engine:

The effect of engine friction is accounted for in the fourth quadrant of the startability diagram as shown in Fig. (6). The torque produced by the engine is related to the gas torque by lines N_1, N_g and N_2. The frictional torque increases with engine speed and load.

To illustrate the use of the diagram consider the case when the starting torque cranks the engine at rotating speed b_1. This produces ignition delay C_1 and a gas indicated torque at d_1. The gas brake torque is represented by distance $d_1 e_1$. If the starter is turned off the engine will not accelerate, and will stop. If the starter is kept on, the

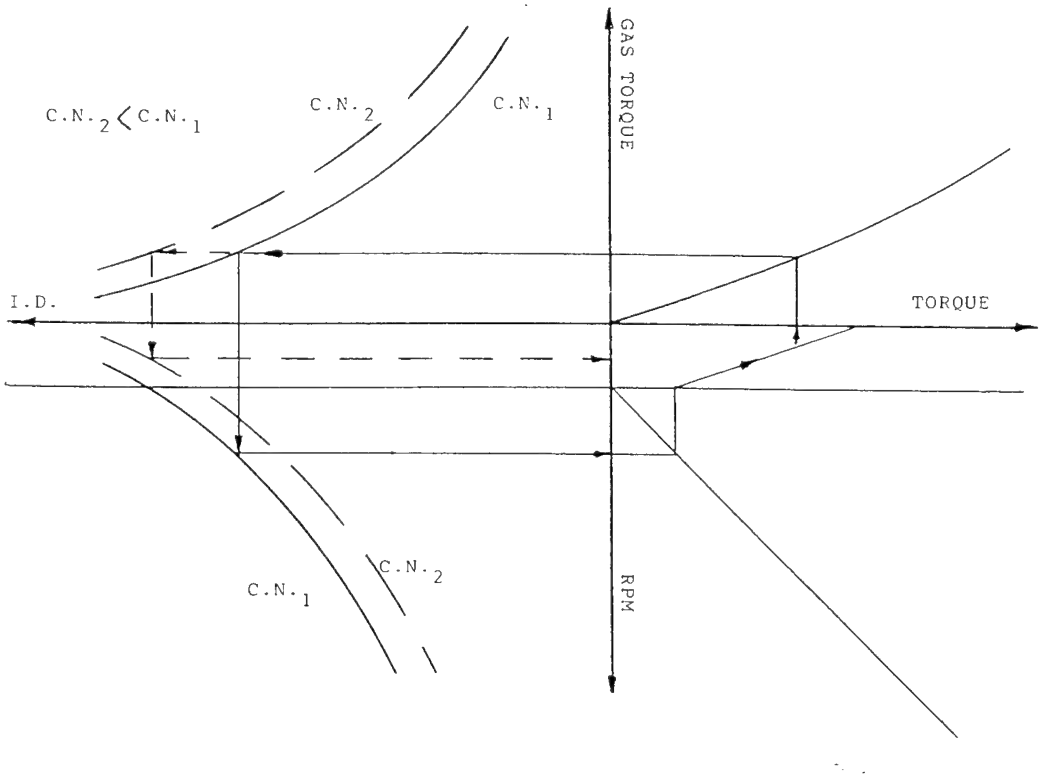

Fig. (4): Effect of Cetane Number on Engine Startability

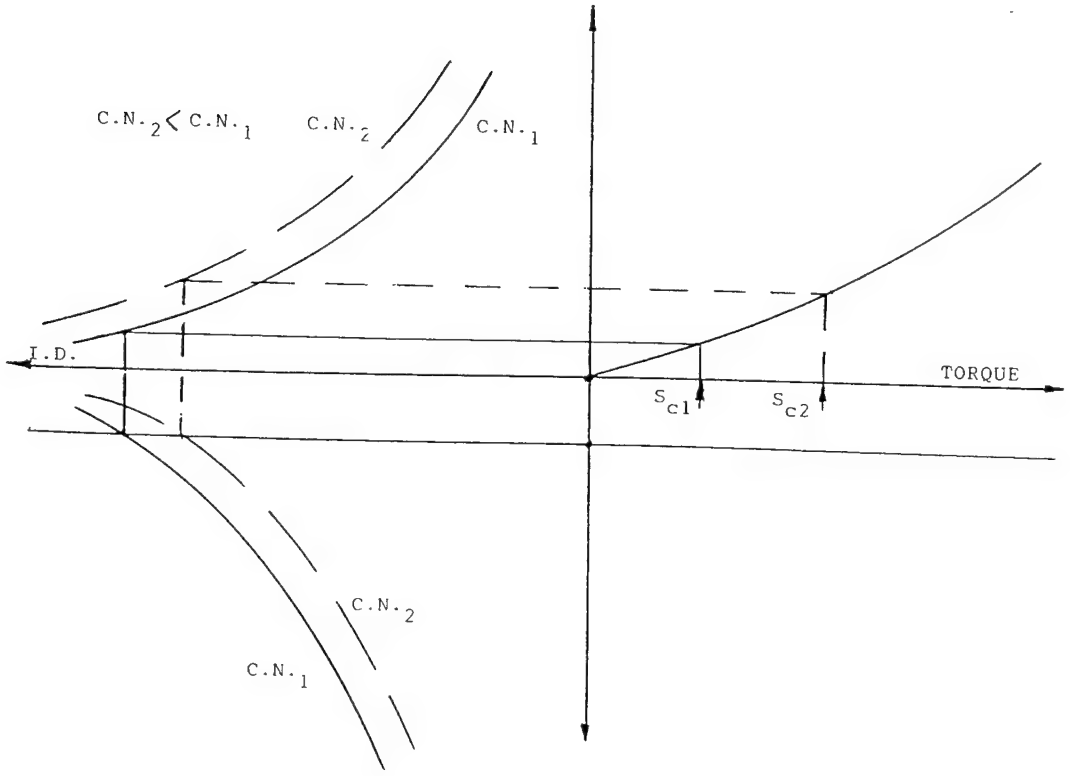

Fig.(5): Effect of Cetane Number on the Critical Startability Torque

gas torque d_1e_1 will be added to the starter torque and produces a torque a_2. The engine accelerates to b_2 and b_3. At this speed the governor will control the fuel flow to m_s and if the starter is turned off the engine decelerates to speed N_s.

2- Multicylinder Engine

Figure (7) is the startability diagram for a six cylinder engine. The engine is cranked at N_1. If the first cylinder fires the engine speed increases to N_2. If the next cylinder fires the speed increases to N_3. The same routine is followed in the rest of the cylinders till the governor is activated and

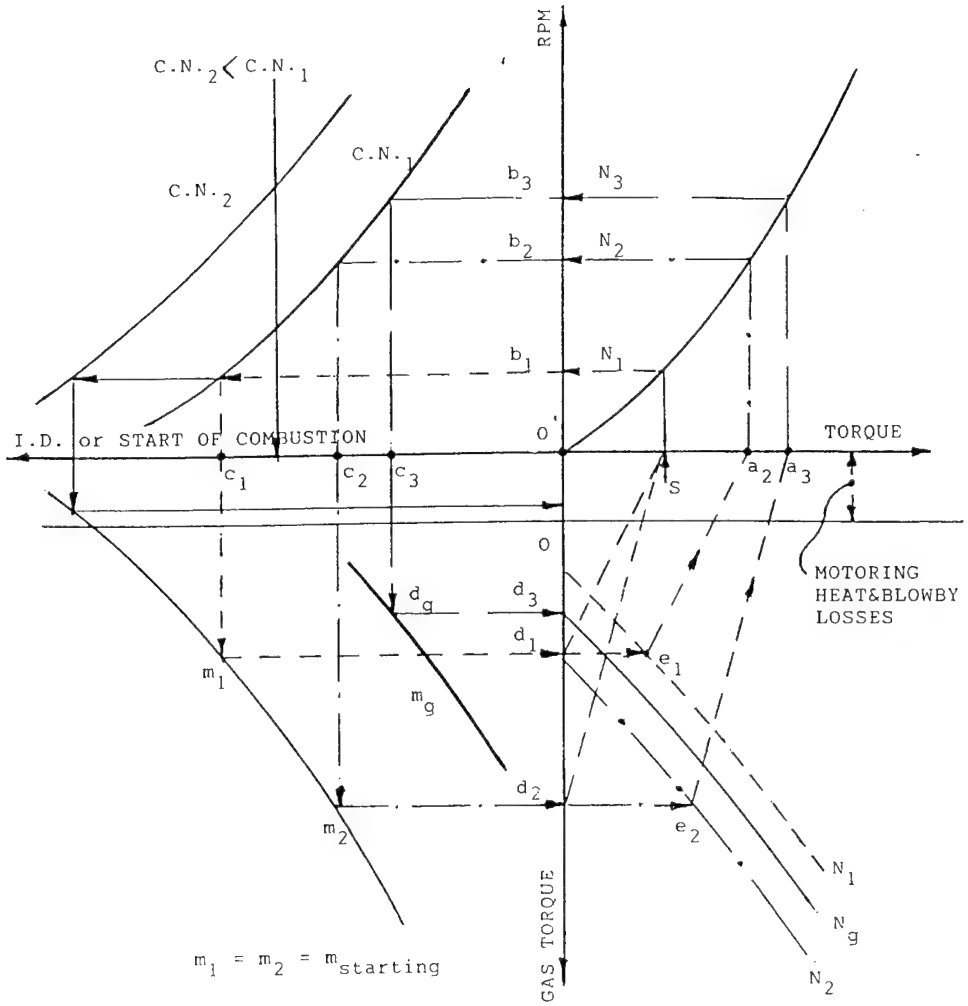

Fig.(6): Startability Diagram for a Single Cylinder Engine with Governor

reduces the amount of fuel to m_g. This brings the speed to the governed speed N_g. It is clear that the most difficult cylinder to start is the first cylinder to come in the firing order after the start of cranking.

CONCLUSIONS

1- A phenomenological model has been developed for the starting of diesel engines. The model is explained graphically in terms of startability diagrams which relate many parameters which affect engine starting.

2- The startability diagram can explain the effects of ambient temperature and cetane number of the fuel on engine starting.

3- The startability diagram explains the starting of single cylinder as well as multicylinder engines.

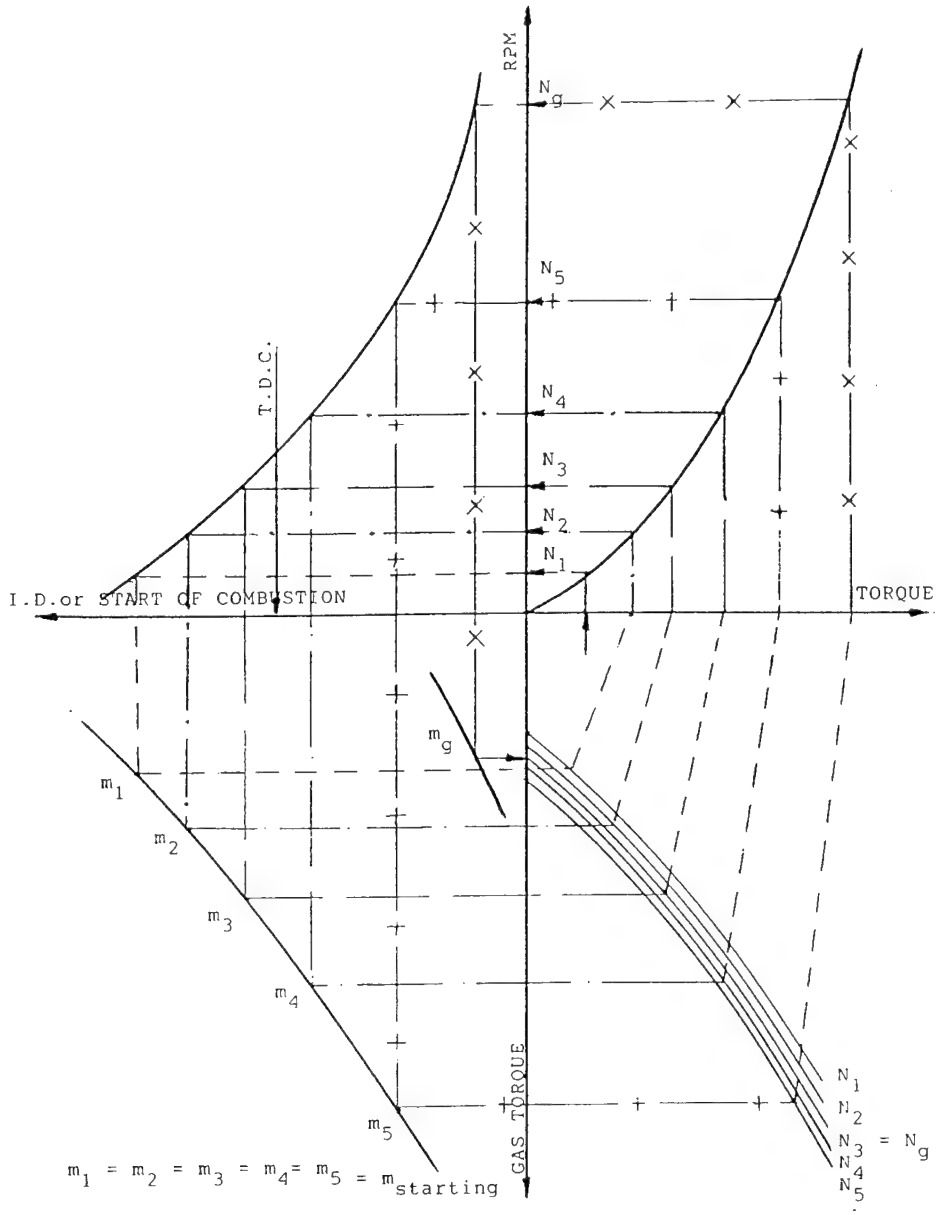

Fig.(7): Startability Diagram for a Six Cylinder Engine with Governor

4- The startability diagram indicated the need for basic information and expressions for the following:

i- The thermodynamic processes in the engine under the cranking and cold starting conditions.

ii- The autoignition and combustion processes of different fuels under the cranking and cold starting conditions.

iii- the instantaneous frictional torque under the transient conditions of cranking and cold starting.

LIST OF SYMBOLS

A = constant
C.N. = cetane number
t = time
T = torque
r = crank radius
R = universal gas constant
m = mass of reciprocating parts
(TK) = transformer ratio =

$$\frac{\sin\theta+\frac{r}{l}\sin\theta\cos\theta}{[1+(\frac{r}{l}\sin\theta)^2]^{0.5}}$$

I.D. = Ignition delay
l = length of connecting rod
I_e = inertia of rotating parts
E = global activation energy for the preignition processes
P = pressure
n = constant
N = speed
θ = angle
ω = angular velocity

SUBSCRIPTS

S : starter
g : gas or governor
f : friction
l : load

LIST OF REFERENCES

1. Porblon, M and Patterson, D. J., "Instantaneous Crank Speed Variations as Related to Engine Starting"' SAE Paper No. 850482.

2. Henein, N. A. and Lee, C. S., "Autoignition and Combustion of Fuels in Diesel Engines Under Low Ambient Temperatures", SAE Paper No. 861230, 1986.

3. Gardner, T. P. and Henein, N. A., "Diesel Starting: A Mathematical Model", SAE 1988 Transactions, Journal of Engines, pp.6,728--6,740.

Appendix 2

" Diesel Cold Starting: Actual Cycle Analysis Under Border-Line Conditions," Zahdeh, A. R., Henein, N. A., and Bryzik, W.

SAE paper No. 900441, 1990

The Engineering Society
For Advancing Mobility
Land Sea Air and Space®
INTERNATIONAL

400 COMMONWEALTH DRIVE, WARRENDALE, PA 15096-0001 U.S.A.

SAE Technical Paper Series

900441

Diesel Cold Starting: Actual Cycle Analysis Under Border-Line Conditions

Akram Zahdeh and Naeim Henein
Center for Automotive Research
College of Engineering
Wayne State University
Detroit, MI
Walter Bryzik
U.S. Army Tank Automotive Command
Warren, MI

International Congress and Exposition
Detroit, Michigan
February 26 — March 2, 1990

900441

Diesel Cold Starting: Actual Cycle Analysis Under Border-Line Conditions

Akram Zahdeh and Naeim Henein
Center for Automotive Research
College of Engineering
Wayne State University
Detroit, MI
Walter Bryzik
U.S. Army Tank Automotive Command
Warren, MI

ABSTRACT

Combustion in a diesel engine during cold starting under normal and border-line conditions was investigated. Experiments were conducted on a single cylinder, air-cooled, 4-stroke-cycle engine in a cold room. Tests covered different fuels, injection timings and ambient temperatures. Motoring tests, without fuel injection indicated that the compression pressure and temperature are dependent on the ambient temperature and cranking speeds. The tests with JP-5, with a static injection timing of 23° BTDC indicated that the engine may operate on the regular 4-stroke-cycle at normal operating ambient temperatures or may skip one cycle before each firing at moderately low temperatures, i.e. operate on an 8-stroke-cycle mode. At lower temperatures the engine may skip two cycles before each firing cycle, i.e. operate on a 12-stroke-cycle mode. These modes were reproducible and were found to depend mainly on the ambient temperature. The actual cycle analysis under-border line conditions indicated that the gas compression pressure, temperature, cyclic fuel injection, ignition delay, rate of heat release and cumulative heat release varied from one cycle to another in any set of 8-stroke-cycle or 12-stroke-cycle modes. The mass of fuel burned in each cycle was calculated and compared with the mass of fuel injected.

Many of the difficulties experienced in the cold starting of diesel engines can be attributed to the failure of the combustion process [1,2,3][1]. Combustion in diesel engines is initiated by an autoignition process near the end of the compression stroke in the absence of any ignition source, such as a spark plug or a glow plug. The processes which lead to autoignition and combustion are combinations of many interacting physical and chemical processes [4]. The physical processes include fuel injection, spray penetration, formation of liquid droplets, heat transfer from the air to the liquid, evaporation, mass transfer, mixing of the fuel vapor and air. The chemical processes which result in autoignition include the decomposition reactions of the fuel, formation of preignition radicals at a critical concentration, and formation of ignition nuclei [5,6,11].

After autoignition takes place in one or more locations of the combustion chamber, combustion starts in the premixed part of the charge which has a fuel-vapor-air ratio within the rich, stoichiometric and lean ignition limits [7,8]. The rest of the fuel-air mixture burns, mostly in a diffusion or mixing-controlled combustion mode.

Failure in any of the above physical or chemical processes results in the complete failure of the engine to start or to misfire [9,10]. Combustion failure may occur in the first or later cycles during cranking, and the engine might not start even after fairly long periods of cranking. Combustion may take place after a period of cranking but fails in subsequent cycles. To the knowledge of the authors, the analysis of the phenomena which cause such a behavior have not been reported in the literature.

Many fuels and design and operating parameters which affect autoignition and combustion during starting have been investigated in a program conducted at Wayne State University. The emphasis of this paper is to identify and examine the different phenomena which take place in the diesel engine, during the transient modes of cranking and acceleration to a speed at which the governor kicks in and controls the fuel delivery. A detailed analysis is made on

1 Numbers in parentheses designate references at the end of paper.

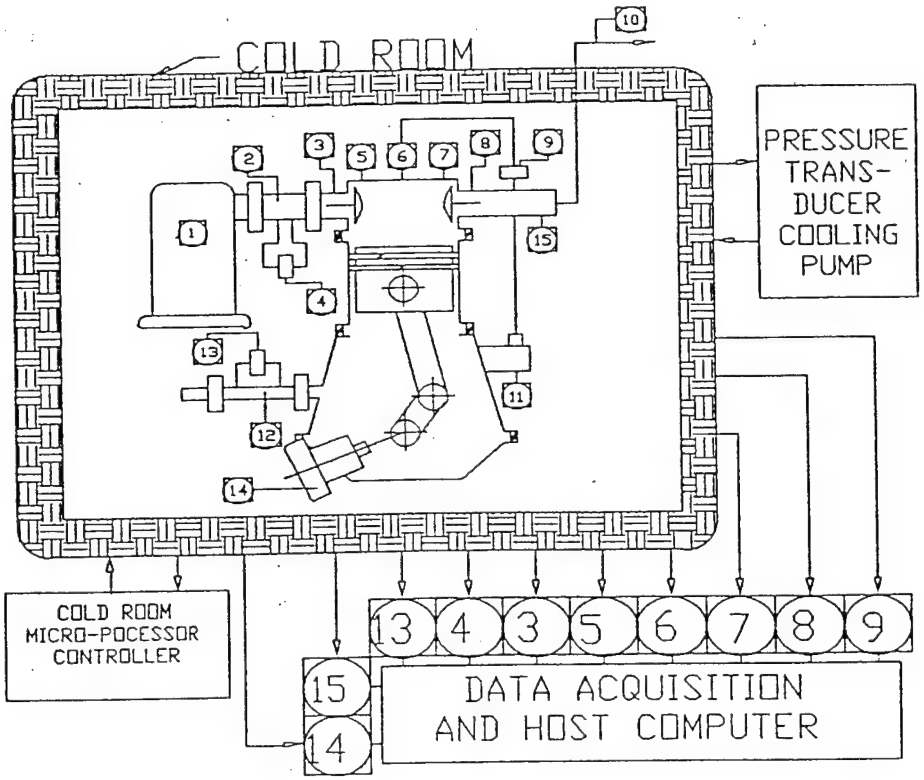

1. Intake Air Filter
2. Laminar Flow Element
3. Intake manifold Pressure Transducer
4. Differential Pressure Transducer
5. Cylinder Pressure Transducer
6. Needle lift Sensor
7. Cylinder-Head Thermocouple
8. Exhaust Fast Response Thermocouple
9. Fuel line Pressure Transducer
10. Laboratory Exhaust Fan
11. Fuel Injection Pump
12. Laminar flow Element
13. Differential Pressure Transducer
14. Optical Shaft Encoder

Fig 1 Experimental Setup Layout

the actual thermodynamic processes while the engine is starting under border-line transient conditions.

EXPERIMENTAL SETUP AND INSTRUMENTATION

Fig (1) shows a layout of the experimental setup inside a cold room. The engine is a Deutz, single cylinder, 4-stroke-cycle, direct injection, air cooled diesel engine. Its specifications are given in appendix A. The engine is instrumented with a cylinder pressure transducer, a needle lift sensor, an intake manifold pressure transducer, an air mass-flow meter, an instantaneous blowby meter and a high response exhaust thermocouple. The sampling of the data is performed using a digital data acquisition system. Data sampling synchronization with the position of the crank shaft rotation is achieved by using an optical shaft encoder which generates a square transistor to transistor logic (TTL) pulse. The TTL signal is used to trigger the data sampling at each crank angle degree during the cycle, and for calculating the angular velocity. The start of the engine cycle is marked by a pulse from the shaft encoder.

The temperature in the cold room is controlled by a micro-processor which provides a wide variety of temperatures and rates of cooling. The room temperature can be varied in a range between 30°C and -50°C within ±1°C. The room temperature was brought down to the desired level and kept for a soaking period of 3 hours. The engine was then started by its own battery which was soaked with engine and continuously charged by a booster. After 70 cycles (140 revolutions) the sampling of the data was terminated. The starting was considered to be successful if the engine fired and accelerated to a speed at which the governor kicked in. Other attempts were made if the engine failed to start. The data for all the attempts were recorded and analyzed. The experiments were repeated four times before the starting was considered to be a complete failure. The experiments covered different ambient temperatures, fuels and fuels injection timings. This paper presents the data for JP-5 at a static injection timing of 23 CA° BTDC. As a base line, experiments were conducted with the engine motored at different ambient temperatures, without fuel injection.

EFFECT OF MOTORING WITHOUT FUEL INJECTION

The cranking speed of the engine depends on many factors including the starter torque, the thermodynamic losses and the mechanical losses. Many of these factors are dependent on the ambient temperature. Fig (2a) shows the ($P-\theta$) and ($\omega-\theta$) traces for the first seventy cycles of the motored engine without fuel injection. The engine accelerated during the first five cycles and reached the steady cranking speed. The angular velocity reached a minimum at the end of the compression stroke of each cycle. Fig (2b) gives more detailed traces for the first ten cycles. Fig (3) shows the effect of the ambient temperature on the maximum, minimum and the average angular velocity in the cycle, compression pressure and compression temperature. Fig (4) shows the effect of ambient temperature on IMEP.

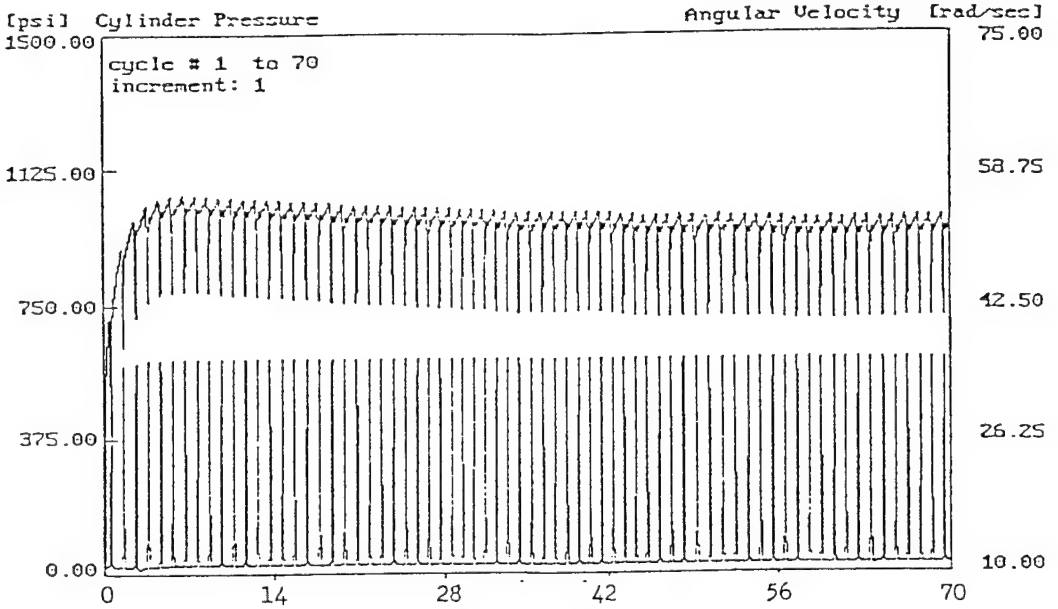

Fig (2,a) $T_{ambient}$=20°C Type = Motoring First

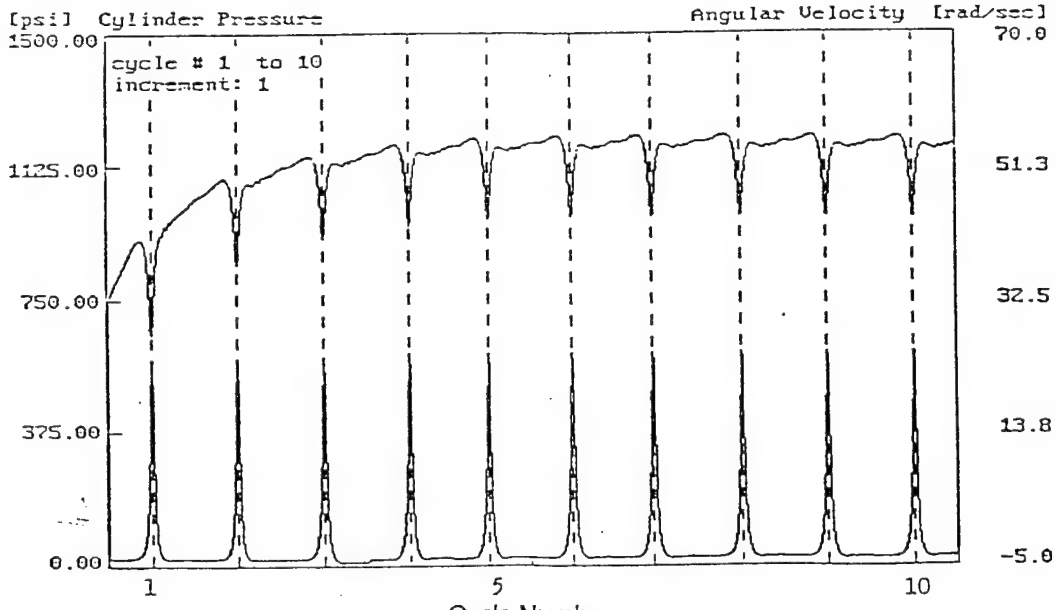

Fig (2,b) $T_{ambient}$=20°C Type = Motoring First

Fig 2: Pressure and Angular Velocity Traces During Motoring Without Fuel Injection

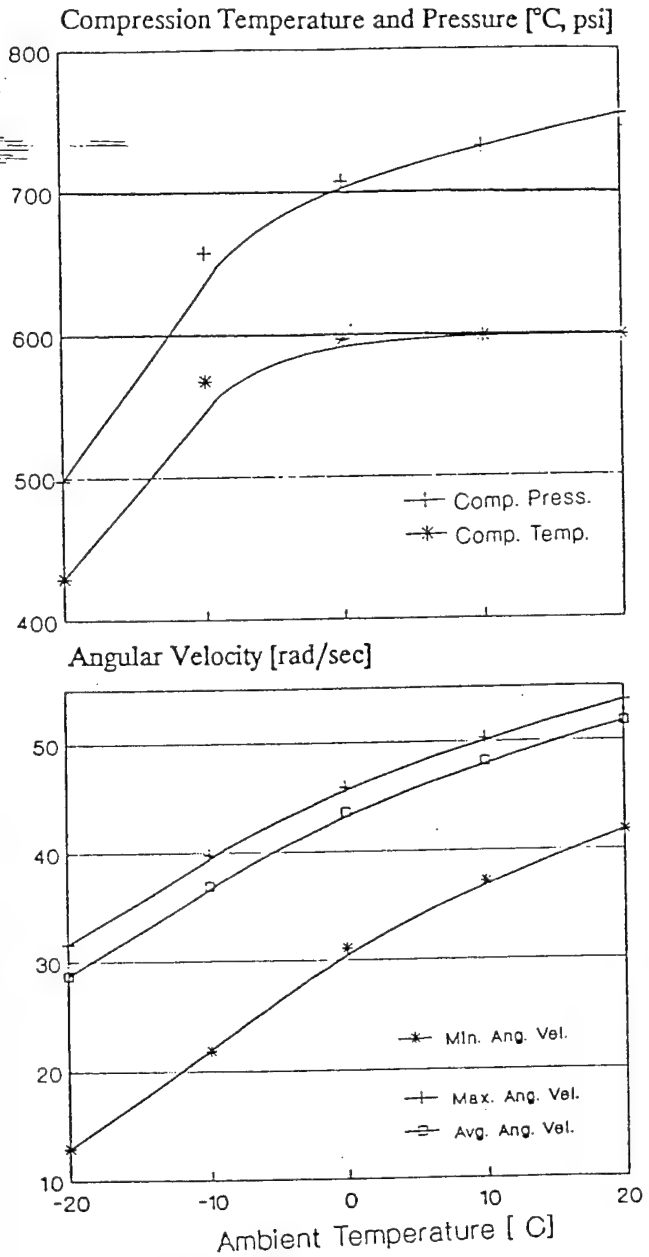

Fig 3: Effect of Ambient Temperature on Motoring Angular Velocity, Compression Pressure and Temperature Without Fuel Injection

A drop of 40°C in the ambient temperature caused at a drop of 23.3 rad/sec (222 RPM) in the average speed, a drop in IMEP from -0.97 to -1.37 bars, a drop in compression pressure from 597 Psi to 428 Psi, and a drop in compression temperature from 752°K to 498°K, or 254°C. The rate of drop in the compression pressure and temperature was higher as the ambient temperature dropped below -10°C. The compression temperature dropped at a rate of 2.1°C per degree, from T_a = 20 °C to T_a = 0. This rate was 4.8°C per degree from T_a = 0

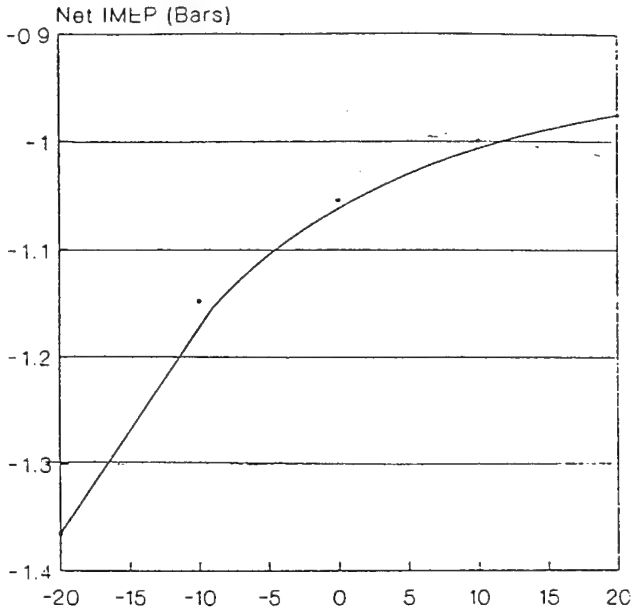

Fig 4: Effect of Ambient Temperature on IMEP.

to T_a = 0. This rate was 4.8°C per degree from T_a = 0 to T_a = -10°C. The sharpest drop was between T_a = -10°C and T_a = -20°C where it reached 16.1°C per degree. The drop in the compression pressure followed the same pattern as the drop in the compression temperature. The main reasons for the drop in compression temperature are:

1- the drop in the temperature of the charge at the start of compression.
2- the increase in the heat losses, because of the lower wall temperatures and cranking speeds.
3- the increase in the blowby losses because of the lower cranking speeds, allowing more time for gas flow from the combustion chamber to the crankcase.

EFFECT OF LOWERING THE AMBIENT TEMPERATURE ON STARTABILITY

Fig (5) gives the (P - θ) and (ω - θ) traces for the first seventy engine cycles during cranking with fuel injection at ambient temperatures of 25°C, 0°C and -10°C. Two attempts were made to start the engine at 0°C and -10°C. At 25°C, Fig (5,a) shows that the engine started in the first cycle where the cylinder pressure reached 1173 psia and the engine accelerated to 75 rad/sec (715 RPM). The governor kicked in at 97.2 rad/s after 9 cycles. The two attempts to start the engine at 0°C are shown in fig (5,b) and (5,c) respectively. The results of the first attempt shows that the engine fired in the first cycle, and misfired in the following few cycles. The combustion in the first

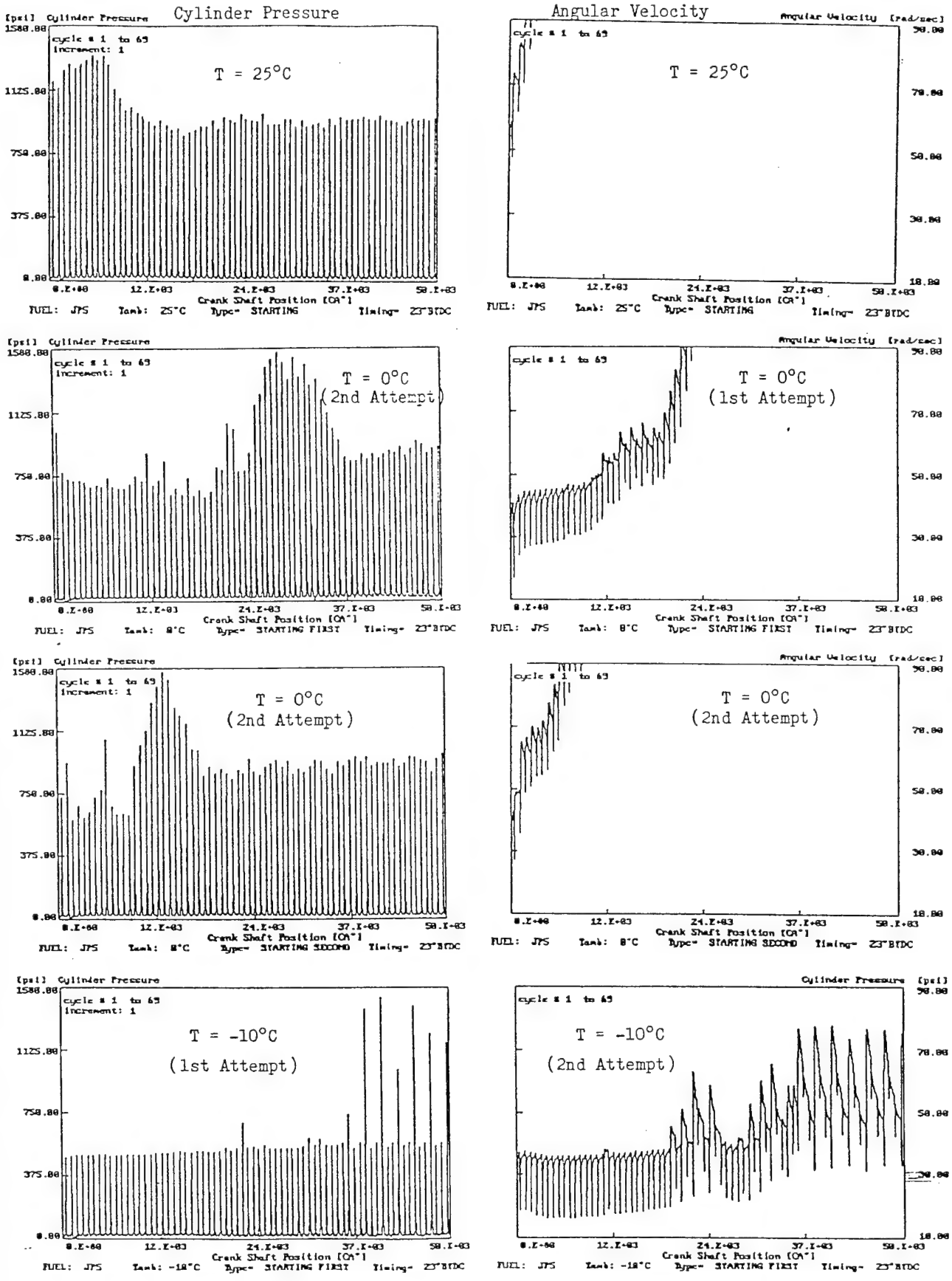

Fig 5: Effect of Ambient Temperature on Angualr Velocity and Cylinder Pressure during Starting, JP5 and 23°CA BTDC

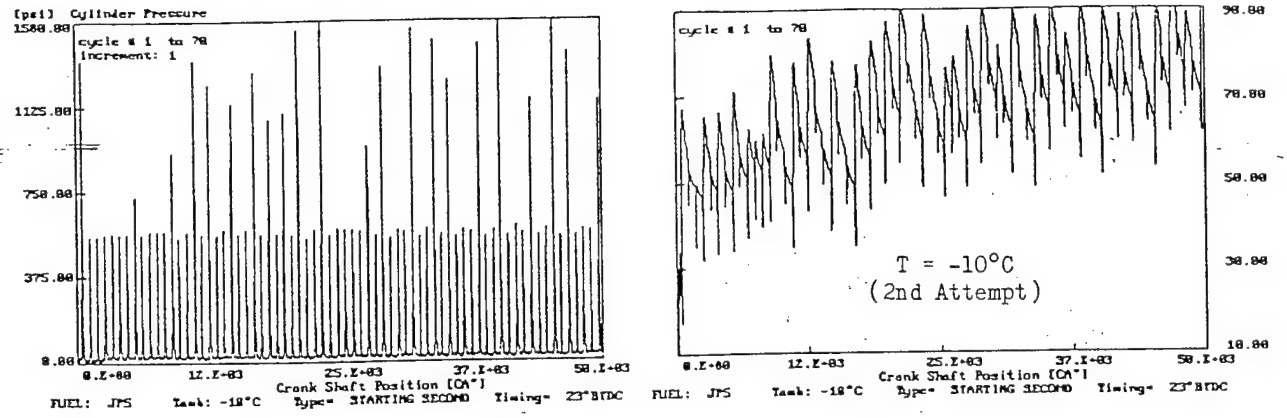

Fig 5: Effect of Ambient Temperature on Angualr Velocity and Cylinder Pressure during Starting, JP5 and 23°CA BTDC

cycle is believed to be caused by the fuel which was accumulated in the cylinder during previous runs. The analysis of the data indicated that the amount of fuel injected in the following few cycles was small and increased as cranking progressed. The pressure and heat release traces indicate that some weak exothermic reactions took place, but they were not strong enough to cause any appreciable pressure rise in the cylinder. Starting from cycle 17 the engine fired every other cycle or operated on an eight-stroke-cycle, after which it accelerated to 97.2 rad/sec, when the governor kicked in. Fig (5,c) for the second attempt at 0°C, shows that the engine fired from the first cycle and accelerated to the governed speed.

The main differences between the second and first attempts are: (i) The cranking speed was higher, (ii) the heat losses were lower because of the hotter cylinder walls and, (iii) the residual gases from the first attempt helped the combustion process, (vi) the blowby losses were lower due to the higher cranking speed, the reduction of the ring gaps and the sealing effect of the lubricating oil film.

At an ambient temperature of -10°C two attempts were made to start the engine, as shown in Fig (5,d) and (5,e) respectively. In the first attempt the engine was motored for 27 cycles after which it fired and partially fired every other cycle or every third or fourth cycle. In the second attempt the engine fired in the first cycle and misfired or partially fired every other cycle or every third cycle.

The ($P - \theta$) traces near TDC for the seventy cycles in the first starting attempt are superimposed in Fig (6). The compression pressure increased from 482 psi in the first cycle to 574 psia in 70th cycle. In some of these cycles there were no signs of exothermic reactions. Many of these traces indicate the existence of cool flames before the pressure rise due to combustion. The pressure traces for the expansion stroke of some cycles showed fairly late low rates of heat release. As cranking progressed the heat release rate increased and occurred closer to TDC. A study of these traces indicated different modes of operation, which consisted, mainly, of 2 skip cycles followed by a firing cycle referred to by a 12-stroke-cycle.

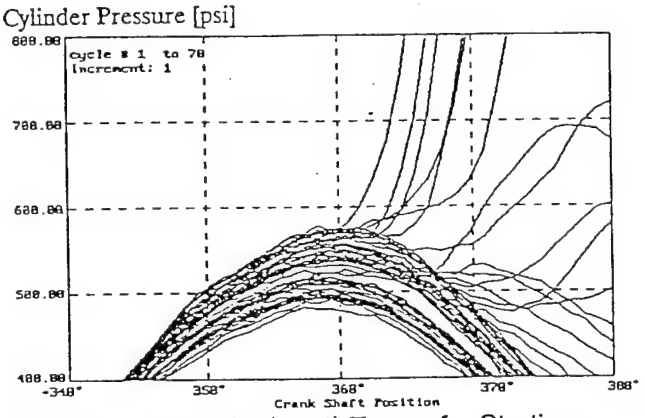

Fig 6: Composite ($P - \theta$) Traces for Starting First Attempt, JP5, -10°C, 23 CA° BTDC

12-STROKE-CYCLE OPERATION

Fig (7,a) to (7,f), for the ($p - \theta$) and ($\omega - \theta$) traces for cycles 51 to 68 of Fig (6), show a consistency of misfiring for two cycles before a firing cycle. The two misfiring cycles produced deceleration in the engine as the speed dropped about 21 rad/sec (200 RPM). The increase in engine speed during the firing cycle amounted to 29 rad/sec (276 RMP). The pressure rise due to combustion in the firing cycle amounted to 810 psi. The amount of fuel burned in this cycle was 39 mg, while the fuel injected was 10 mg. It is clear that some of the fuel burned was from the previous two cycles.

Figs (8,a) to (8,h) are detailed cylinder pressure traces superimposed for each of the two misfiring cycles which follow each of the firing cycles, Cycle No. 48 had a reaction which started early in the compression stroke, resulted in an increase of the peak pressure in the compression

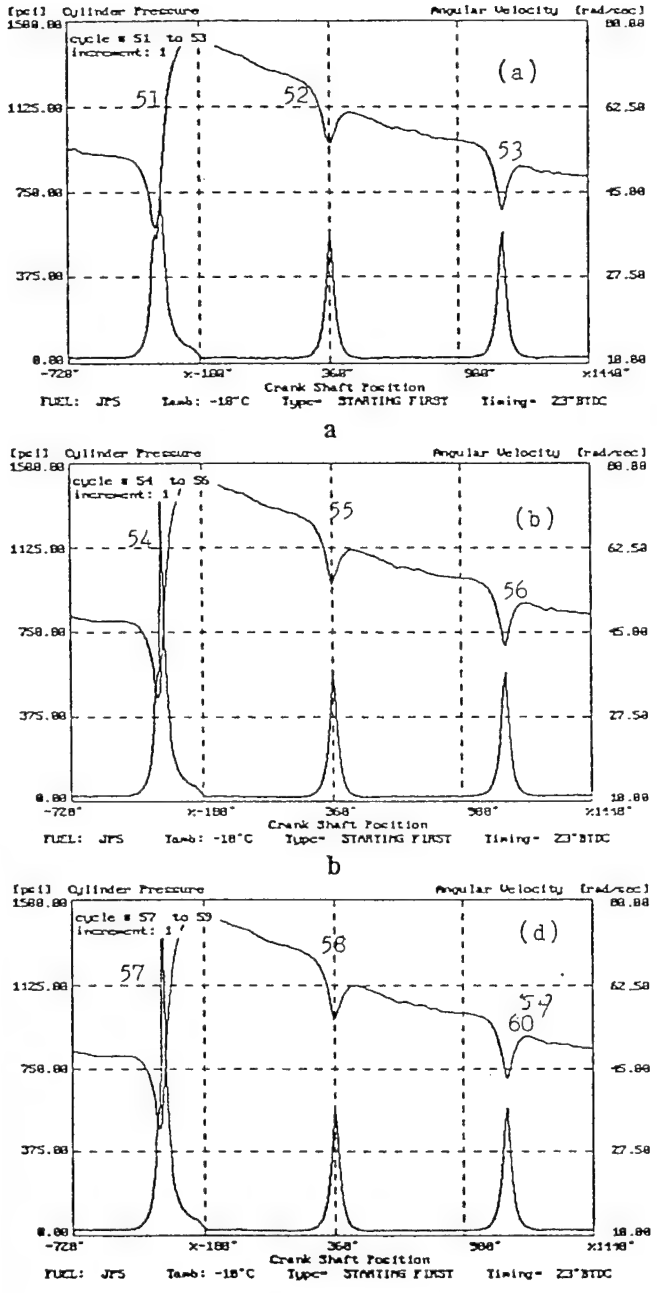

Fig 7: Composite ($P - \theta$) Traces for Starting, First Attempt, JP5, -10°C, 23 CA° BTDC (a-c)

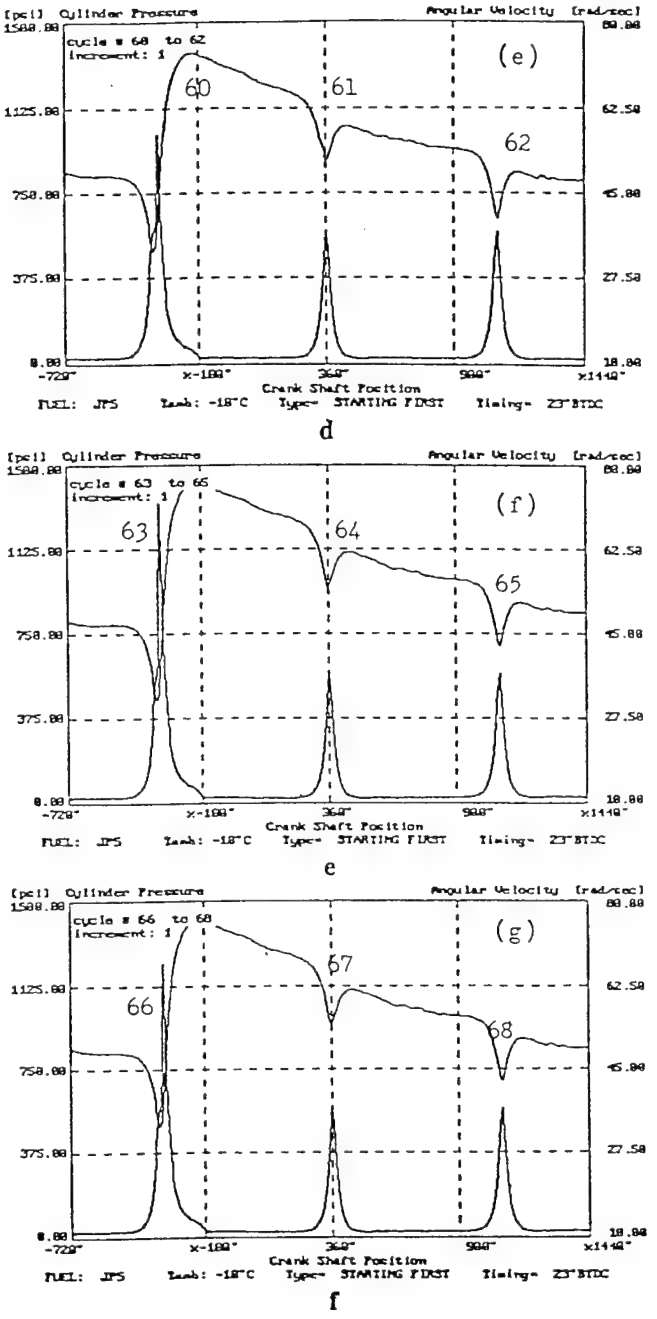

Fig 7: Composite ($P - \theta$) Traces for Starting, First Attempt, JP5, -10°C, 23 CA° BTDC (d-f)

pressure, and a very late release of the chemical energy of reaction. This did not cause any positive pressure slope. The cumulative amount of energy released in this cycle was 72 Joules. This is an equivalent to 1 mg of fuel. The cycles No. 49 and 50 showed a near complete failure of the combustion process. The following cycle, No. 51, showed no sign of energy release in the compression stroke, but the existence of a cool flame before active combustion. Combustion took place after a long ignition delay of 23 CA° and resulted in a clear increase in pressure and a positive pressure slope. The cumulative energy released in cycle 51 was 1083 Joules, equivalent to 39 mg of fuel. Cycle 52 had higher compression pressures than cycle 51 indicating higher gas temperatures, due to the higher angular speed, mixing with the hot residual gases, a very weak exothermic reaction taking place before the fuel was injected and lower heat losses. This indicates that cycle 51 did not burn all the fuel, probably leaving some chemical products in the cylinder to react during the compression of cycle 52. The cumulative energy released

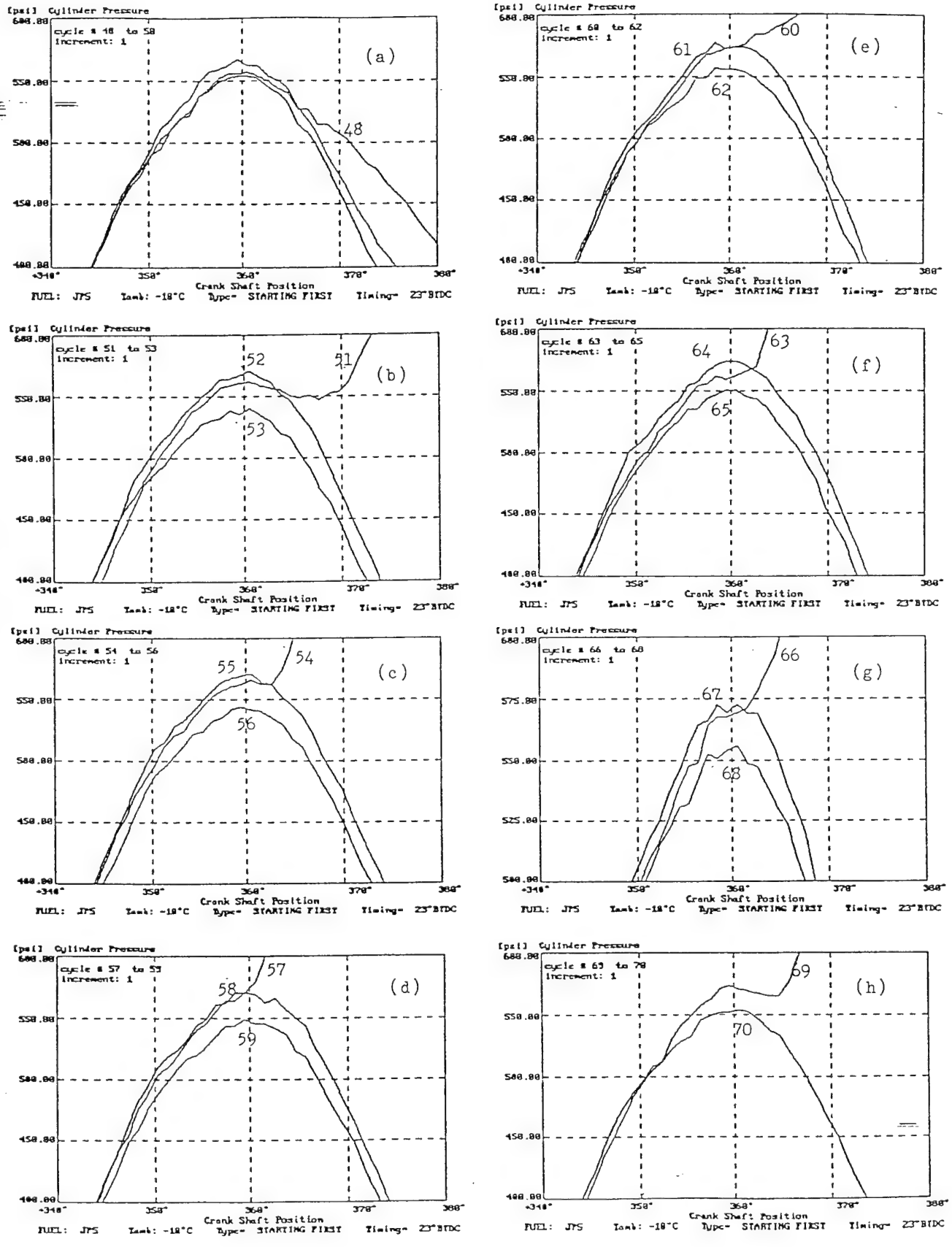

Fig 8: Detailed ($P-\theta$) Traces for the 12-Stroke-Cycle Operation

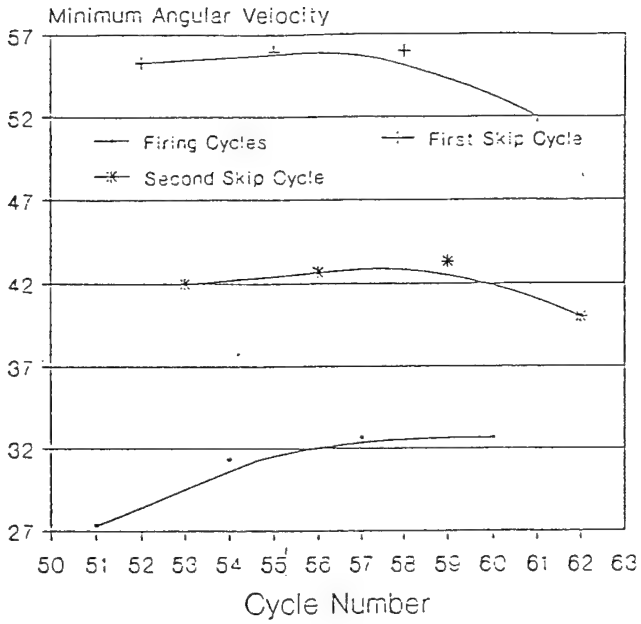

Fig 9: Minimum Angular Velocity During 12-Stroke-Cycle Operattion

in cycle 52 was almost 0 joules. Cycle 53 appeared to have some energy release during the early compression stroke, but produced a noticeable drop in pressure after the start of fuel injection. This might indicate that some exothermic reactions were taking place before injection and where chilled by fuel injection. Cycle 54 had combustion with a shorter ignition delay and a higher rate of pressure rise, than the previous firing cycle no. 51. A cool flame preceded the high rate of heat release. Cycle 55 followed the same pattern of cycle 52 showing higher gas pressures during the compression stroke. Cycle 56 showed the chilling effect of fuel injection. Cycle 57 followed the pattern of the previous firing cycles 54 and 51 but had a shorter ignition delay and a higher rate of pressure rise. Cycles 58 and 59 show the same pattern as the previous misfiring cycle. Fig (8,e) to (8,h) show that the 12-stroke mode of operation continued till cycle 70 when the data acquisition was terminated.

Fig (9) shows the minimum instantaneous angular velocity for the sets of three cycles which form the 12-stroke-cycle operation. The top trace is for the first skip cycles after the acceleration in the firing cycles. The middle trace is for the second skip cycles. The bottom trace is for the firing cycles.

Fig (10) shows the CHR and cyclic fuel injected for the first attempt at -10°C. The CHR explains the observation made in Fig (9). The cyclic fuel injected varied according to the instantaneous angular velocity during the fuel injection process. The first skip cycles had the highest cyclic fuel injection. The second skip cycle had lower cyclic fuel injected than the first skip cycle. The firing cycle has the lowest cyclic fuel injection.

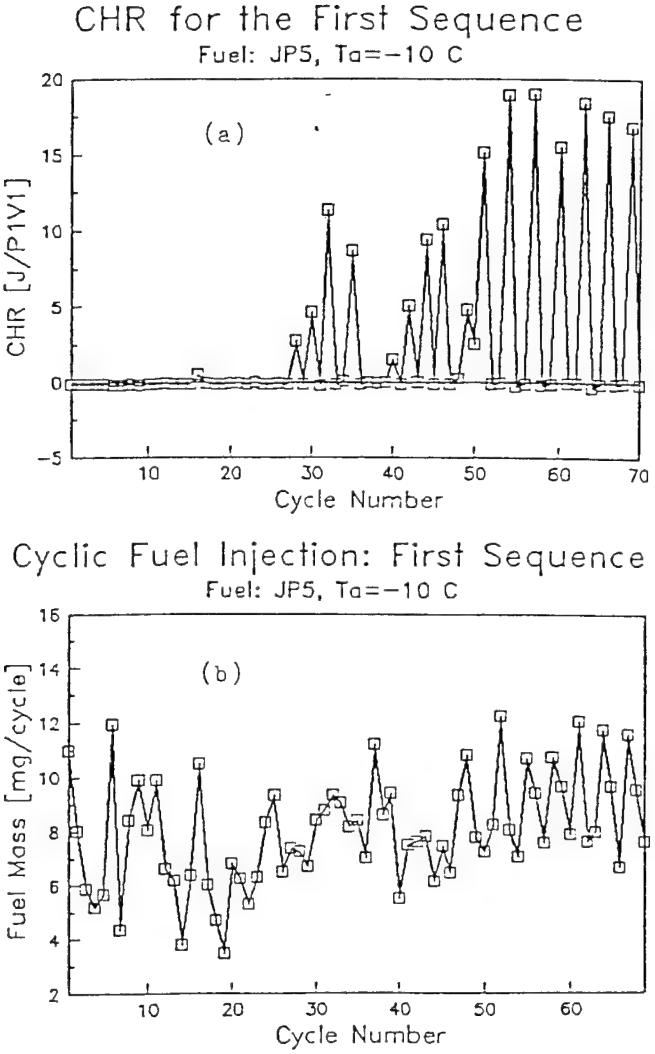

Fig 10: CHR and Cyclic Fuel Injection for the First Attempt

Fig (11) shows a comparison of the normalized cylinder gas pressure, mass averaged cylinder gas temperature, cumulative heat release for one set of the three cycles which compose the 12-stroke-cycle operation. The compression gas temperature in the first skip cycle No. 55 was slightly higher than the other two cycles. The rate of heat release for the firing cycle No. 54 shows the drop due to fuel evaporation and endothermic reactions before the heat release due to premixed combustion. The CHR traces show that the first skip cycle No. 55 had less losses than the second skip cycle No. 56 as explained earlier.

The operation of the engine on the 12-stroke-cycle mode can be summarized as follows:

1- After a firing cycle the engine skipped two consecutive cycles before another firing. In the first skip cycle the compression pressures, even before fuel injection, were close, or in the majority

of the cases are higher than those of the firing cycle. In the second skip cycle the compression pressures as well as the expansion pressures were lower than those of the firing and the first skip cycle.

2- The ignition delay of the firing cycles decreased with the progression of the cranking process.

3- The rate of release of the chemical energy of combustion reactions increased with the progression of the cranking process.

4- The energy released in the firing cycle was more than the energy of the injected fuel in the cycle. Obviously, some of the carried-over fuel or its derivatives from the skipped cycles were burned.

5- Cool flames precede combustion in the firing cycles.

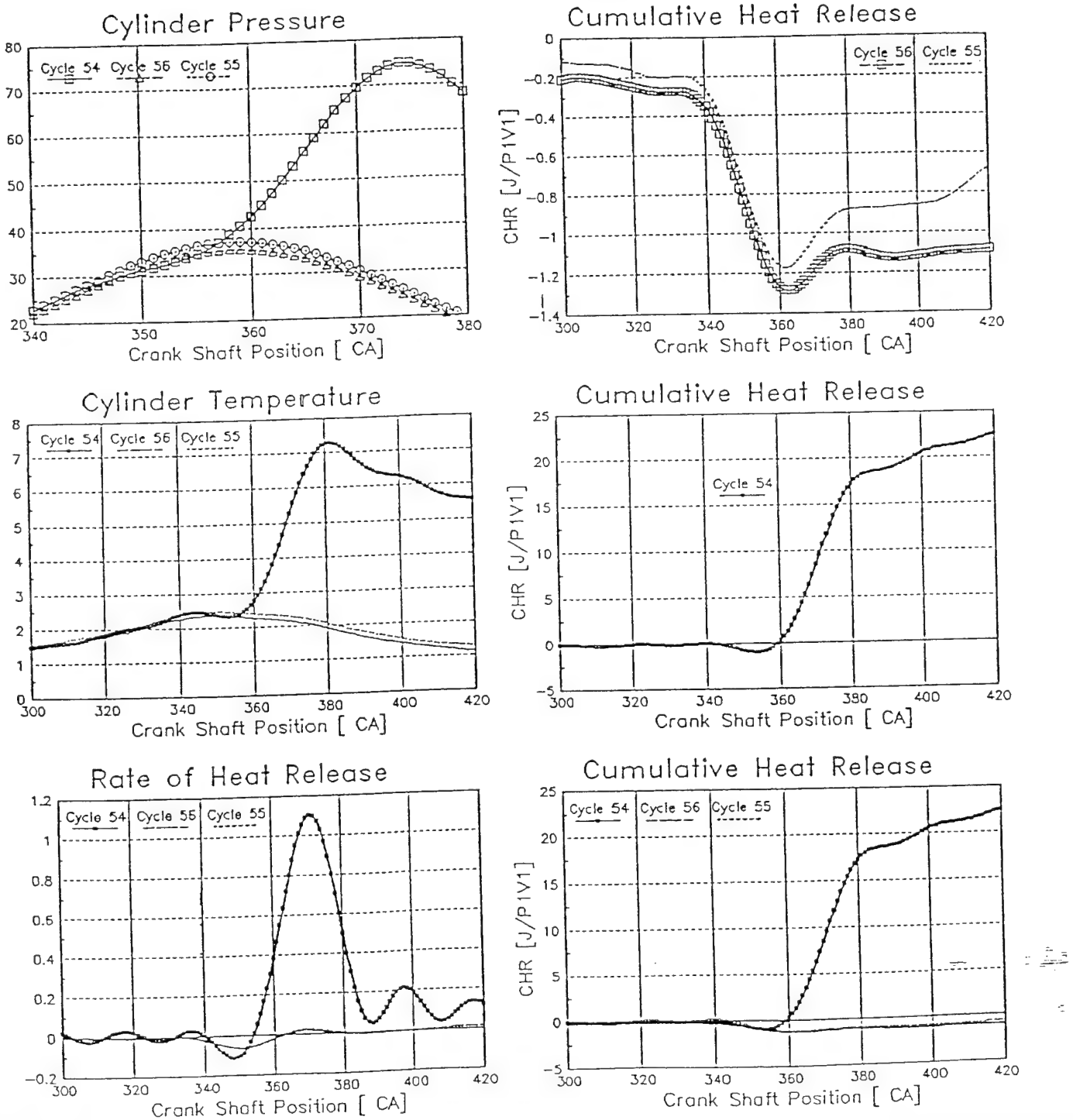

Fig 11: Heat Release Analysis for the 12-Stroke-Cycle Operating Mode

The fuel which was injected in the skipped cycle and not burned in the firing cycle may explain the emission of the high concentrations of hydrocarbon emissions or white smoke during the cold starting of diesel engines.

8-STROKE-CYCLE OPERATION

The operation on the 8-stroke-cycle mode was observed in the second attempt to start the engine at -10°C. The ($P-\theta$) and ($\omega-\theta$) traces for the second attempt are compared with the traces of the first attempt in Fig (8). Fig (12) is for the superimposed ($P-\theta$) traces for the seventy cycles of the second attempt. The pressure at TDC varied from 550 psia to 590 psia. The ignition delay decreased and the rate of pressure rise increased with the increase of the cycle number. Low rates of pressure rise due to cool flames are observed in these traces. The period for cool flames is observed to decrease with the progression of cranking.

Fig (13,a) to (13,h) are for the cylinder pressure and angular velocity for the first nineteen cycles in the second attempt. The details of the pressure development near TDC are given for the same cycles in Figs (14,a) to (14,h). These figures show that combustion in the first cycle accelerated the engine, while it was cranked by the electric starter, to an angular velocity of 68 rad/sec (652 RPM).

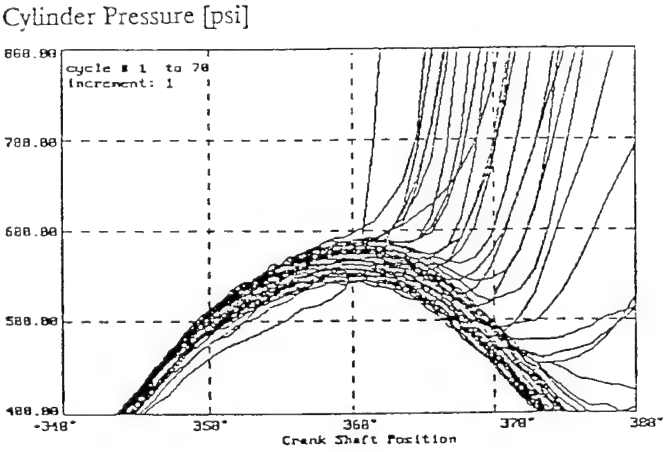

Fig 12: Composite ($P-\theta$) Traces for Starting Second Attempt, JP5, -10°C, 23 CA° BTDC

In the rest of the cycles the engine remained at an average velocity of about 50 rad/sec (477 RPM). The combustion in the first cycle appeared to be the result of fuel accumulated in the cylinder from the first starting-attempt, in addition to the fuel injected. The cumulative energy released in the first cycle accounts for the energy of combustion of 30 mg of fuel, while the fuel injected in this cycle was 19.8 mg. This means that the equivalent of an additional 11.2 mg of fuel was burned in cycle 1. This behavior is similar to the first cycle in the 12-stroke-cycle operation explained earlier. Cycle 2 misfired. Cycle 3 fired with a fairly long ignition delay period of 20 CA°. Pressure rise due to cool flames preceded the high rate of pressure rise due to combustion. In cycle 3 the angular velocity after expansion was equal to that at the beginning of compression, indicating the work done was just enough to overcome the frictional losses. Cycle 4 fired late and accelerated the engine from 50 rad/s (477 RPM) to 67 rad/s (640 RPM). Fig (13) and (14) show that the 8-stroke-cycle operating mode was followed in all the subsequent cycles, except for cycle 11 which showed low energy release.

Fig (15,a) shows the normalized cumulative heat release for 70 cycles from which the previous phenomenon of 8-stroke-cycle operation was demonstrated. In fig (15,b) the cyclic fuel injection for the 70 cycles is presented. During this operation the fuel injection in the skipped cycles was higher than that of the firing ones due to the increase of the angular velocity.

Fig (16,a) shows the net (integrated) cumulative energy released for 70 cycles for both the first and second attempts at -10°C. In the first attempt the release of the energy started at cycle 30 and increased at a slow rate until cycle 48 after which the rate of energy released became much faster. It should be noted that this is the same cycle number after which the engine operated at 12-stroke-cycle consistently. Fig (16,b) shows the net cyclic fuel injection for the 70 cycles. In the first sequence, the net cyclic fuel injection was lower than that of the second sequence.

The details of the pressure traces in Fig (12) indicate the following:

1- The compression pressure in the misfiring cycle was higher than the corresponding pressure in the firing cycle. This trend is similar to the first skip in the 12-stroke-cycle operation.

2- The injection of fuel in the misfiring cycle results in a chilling effect and reduces the compression pressure.

3- The ignition delay of the firing cycles decrease with the progression of cranking process.

4- Cool flames precede combustion in the firing cycles.

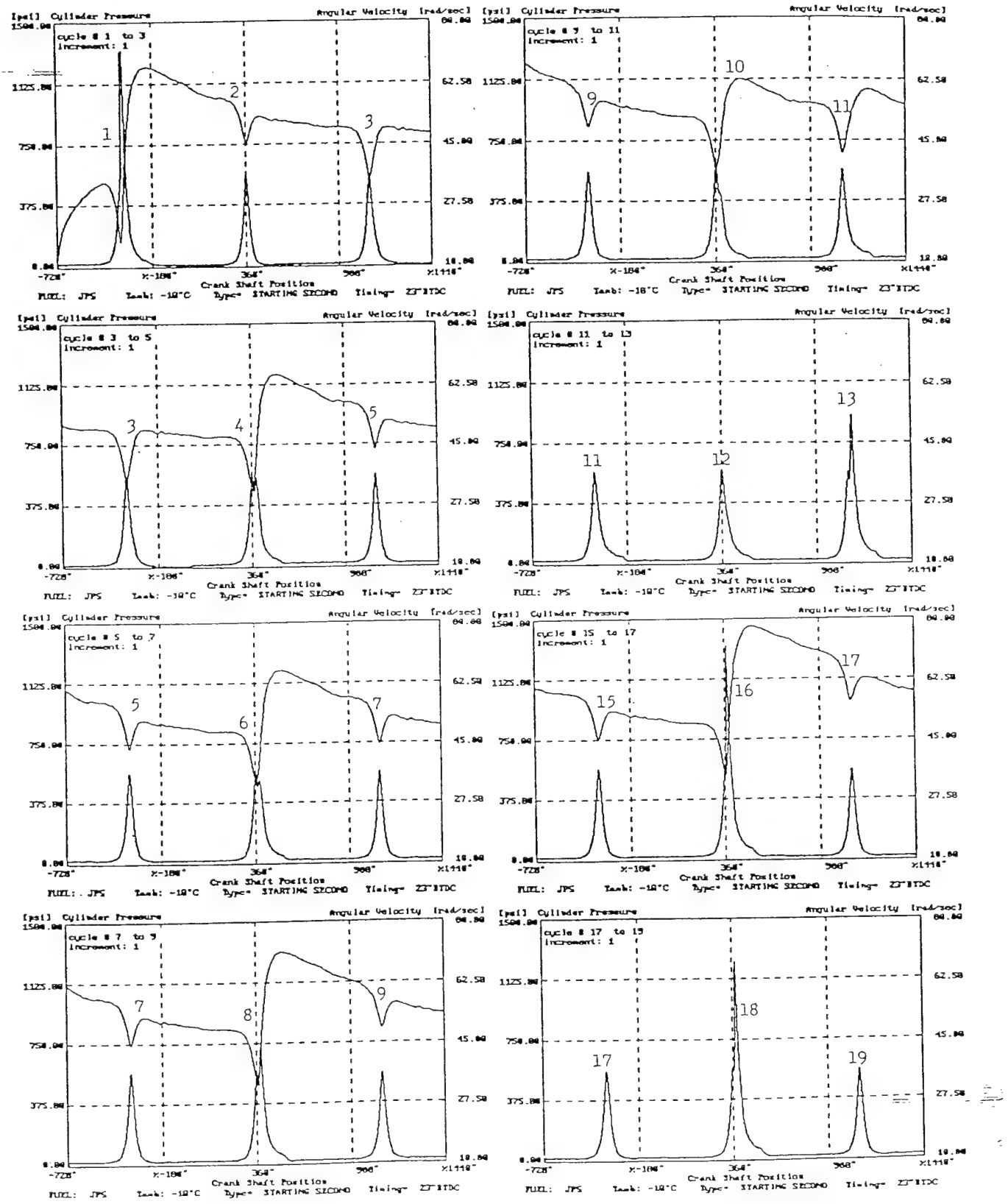

Fig 13: $(P-\theta)$ and $(P-\omega)$ Traces for the Engine While Operating on 8-Stroke-Cycle

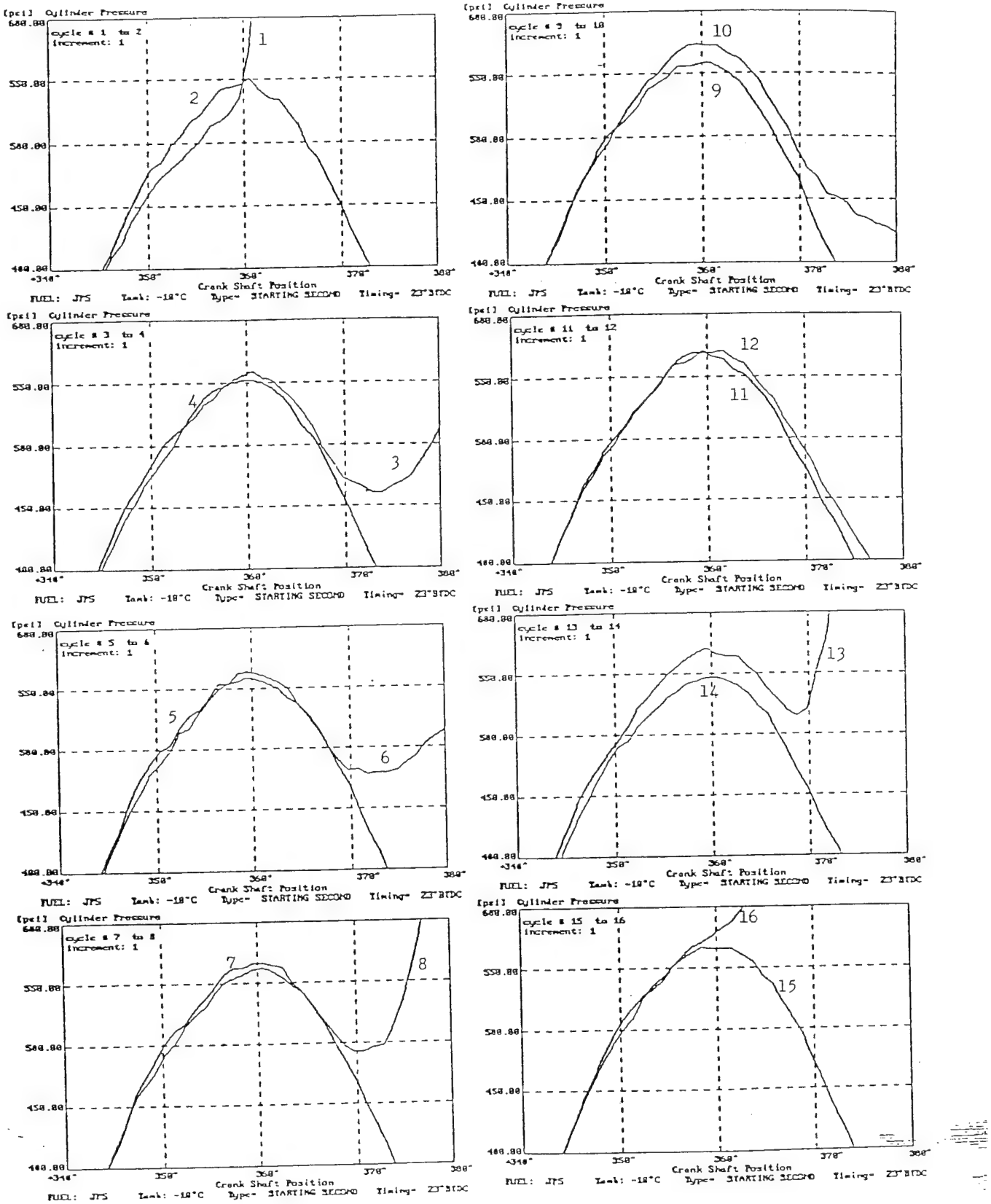

Fig 14: Detailed ($P-\theta$) Traces for the 8-Stroke-cycle Operation

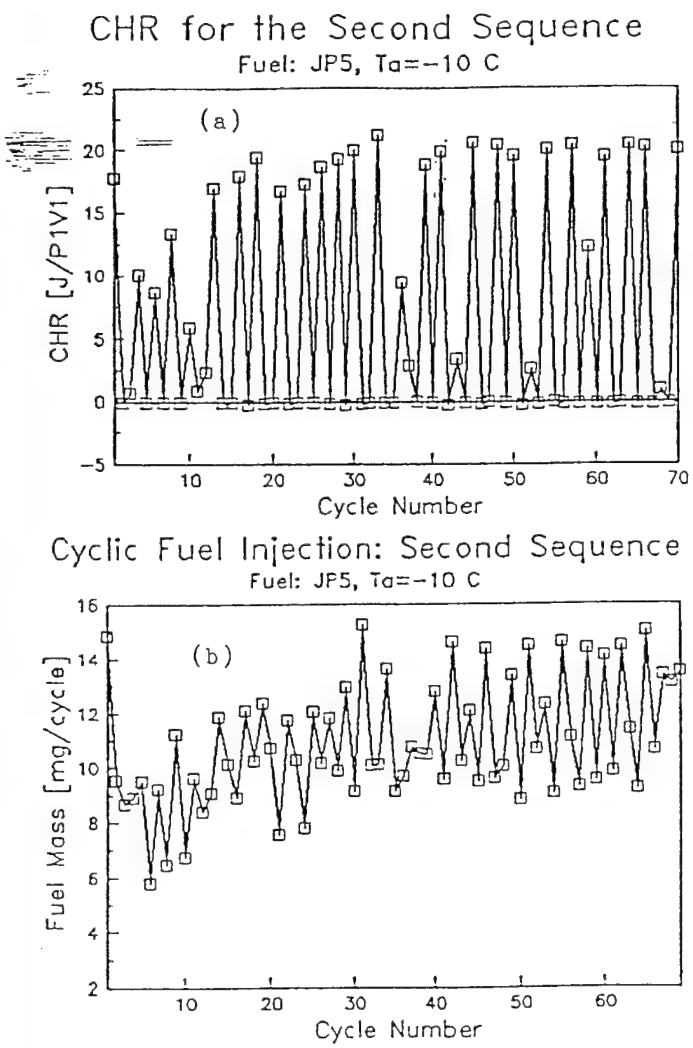

Fig 15: CHR and Cyclic Fuel Injection for the Second Attempt

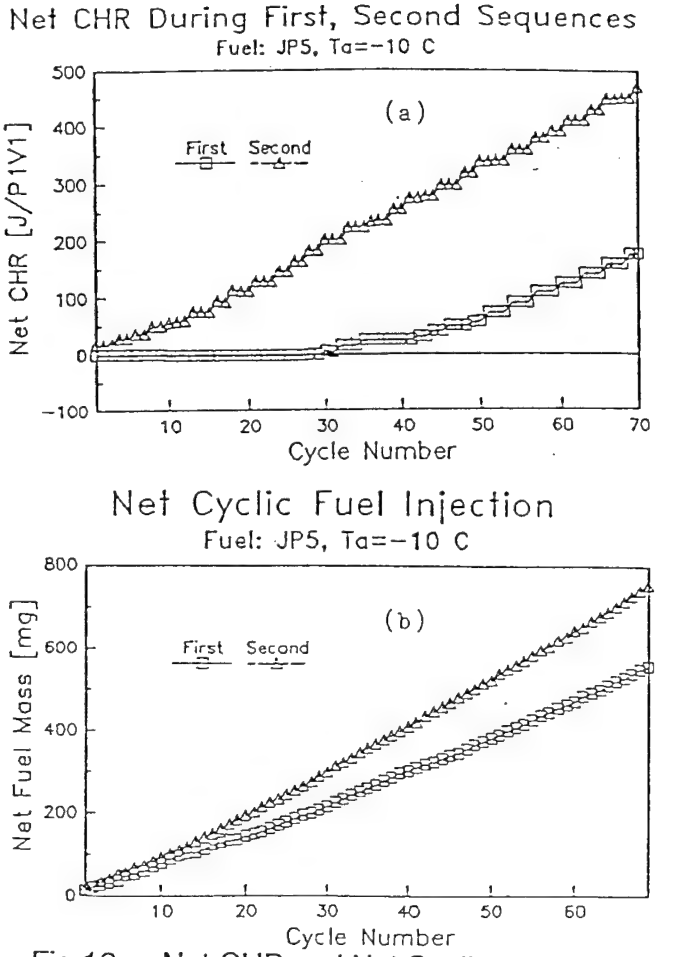

Fig 16: Net CHR and Net Cyclic Fuel Injection During First and Second Attempts

CONCLUSIONS

The following conclusions are based on an experimental investigation on the cold startability of a single cylinder, air cooled, direct injection, four-stroke-cycle diesel engine. The study covered a wide range of fuels and injection timings. The conclusions are based on the analysis of the results obtained on JP-5 fuel only with a static injection timing of 23° BTDC. Attempts to start the engine were made for 70 consecutive cycles (140 revolutions). If the engine failed to accelerate to the governed speed, other attempts, up to four, were made.

1- The cranking speed, without fuel injection, was dependent on the ambient temperature, while all the other starter parameters were kept constant. Lowering the ambient temperature caused an increase in frictional torque and a drop in cranking speed.

2- The compression pressure and temperature, without fuel injection, increase with the cranking speed, as a result of the drop in blow-by losses and heat transfer losses.

3- The engine experienced several modes of operation: i- the regular 4-stroke-cycle, ii- a single-skip cycle referred to as an 8-stroke-cycle, iii- a double-skip cycle followed by a firing cycle, referred to as a 12-stroke cycle and iv- a triple or more skip cycles, before a firing. The 4-stroke operation was observed at ambient temperatures above 0 °C. Lowering the ambient temperature resulted in the operating 8-stroke-cycle mode. Lowering the temperature further, resulted in the 12-stroke and 16-stoke-cycle modes of operation. At certain temperatures the engine operated on a combination of the different modes.

4- The 12-stroke-cycle operation was repetitive at an ambient temperature of -10°C during the first attempt to start. The first-skip cycle after a firing cycle had compression pressures higher than the

firing cycle, even before fuel injection. The second skip cycle had a lower compression and expansion pressures than the first skip cycle.

5- The mass of fuel injected in each cycle was proportional to the instantaneous angular velocity of the engine during the injection process. The first-skip cycle had the largest amount of fuel, followed by the second-skip cycle. The firing cycle, had the smallest amount of fuel, because the angular velocity during injection was the lowest.

6- The 8-stroke-cycle operation was observed at an ambient temperature of -10°C during the second attempt. The skip cycle followed the same trend as the first skip cycle in the 12-stroke-cycle, operating mode.

7- Some of the misfiring in the early cycles of cranking may be partially contributed to the small needle lift and the small amounts of fuel injected.

8- Cool flames were observed before the sharp pressure rise in the firing cycle. Cool flames were also observed in the first skip cycle.

RECOMMENDATIONS

1. Investigate the factors which contribute to combustion failure during the skip cycles.
2. Investigate the effect of fuel properties and injection timing on combustion during starting.
3. Investigate the cause of cool flames and their contribution in the firing cycle and in the skip-cycles.

ACKNOWLEDGEMENT

The authors acknowledge the support of the U.S. Army Tank Automotive Command, Warren, Michigan, and the U.S. Army Research Office, Research Triangle, N.C. The help of the students at the Center for Automotive Research, Wayne State University, particularly Mahmoud Yassine, Deepinder Singh and Minghui Li are greatly appreciated. The support of Mr. Fred Pompei of the Machine Shop in designing and machining some of the equipment is acknowledged with thanks.

APPENDIX A
Engine Specifications

Engine type	F1L 210 D
Total Piston Displacement (cm^3)	673
Working Cycle	Four stroke Diesel
Combustion System	Direct Injection
Bore (mm)	95
Stroke (mm)	95
Direction of Rotation	When Facing Flywheel Left Counterclockwise
Rated Speed (max) (rev/min)	3000
Compression Ratio	17:1
Compression Pressure (bars)	19-21
Needle Opening Pressure (bars)	190-200
Injection Timing (without advance unit) (CA°)	23±1
Inlet Valve Opening (degree)	23°
Inlet Valve Closing (degree)	63°
Exhaust Valve Opening (degree)	63°
Exhaust Valve Closing (degree)	23°

REFERENCES

1. A.E.W. Austen & W.T. Lyn, "Some Investigation on cold-Starting Phenomena in Diesel Engines". Gas and Oil Power, Annual Technical Review Number, 1959.
2. T.W. Biddulph, W.T. Lyn, "Unaided Starting of Diesel Engines". Proc. Insn Mech Engrs 1966-67.
3. H.P. Lenz, G.Akiskalos, W. Zeiner, "Behaviour of the Diesel Engines in the Warming-up Phase", CIMAC, Session A6, D71, 13th International congress on Combustion Engines.
4. M.Brunnèr, H.Ruf, "Contribution of Problem of Starting and Operating Diesel Vehicles at Low Temperature", Proc Instn Mech Engrs No 5 1959-60.
5. W.T.Lyn, E. Valdmanis, "The Effect of Physical Factors on Ignition Delay", Proc Instn Mech Engrs Vol 181 Pt 2A No 1, 1966-67.
6. A. Andree, S.J. Pachernegg, "Ignition Conditions in Diesel Engines", SAE 690253.

7. Ramkrishna Phatak & Tadoa Nakamura, "Cold Startability of Open-Chamber Direct-Injection Diesel Engines-Part 1: Measurement Technique and Effects of Compression Ratio", SAE paper 831335.
8. Ramkrishna Phatak & Tadoa Makamura, "Cold Startability of Open-Chamber Direct-Injection Diesel Engines-Part 2: Combustion Chamber Design and Fuel Spray Geometry and Additional Air and Glow Plug as a Starting Aid", SAE paper 831396.
9. Kobayashi A, Suzuki T. Nakajima M., "Combustion Analysis of the Vehicular Diesel Engine in Cold Starting Condition Via High Speed Photography", ASME paper n 80-DGP-7 for Meet Feb 3-7 1980 7 p.
10. Komiyama K. & Okazaki T., "Cold Start Mechanism of Diesel Engines: Computer Simulation and Experiments", ASME paper n 80-DGP-45 for Meeting Feb. 3-7 1980 6 p.
11. N.A. Henein, "Analysis of Pollutant Formation and control and Fuel Economy in Diesel Engines", Progress in Energy and Combustion Science, Vol. 1, pp. 165-207, Pergamon Press, 1976.

Appendix 3

"Diesel Engine Cold Starting: Combustion Instability," Henein, N. A., Zahdeh, A. R., Yassine, M. K., and Bryzik, W.

SAE paper No. 92005,1992

920005

Diesel Engine Cold Starting: Combustion Instability

Naeim A. Henein, Akram R. Zahdeh, and Mahmoud K. Yassine
Wayne State University

Walter Bryzik
U.S. Army Tank Automotive Command

ABSTRACT

Combustion instability is investigated during the cold starting of a single cylinder, direct injection, 4-stroke-cycle, air-cooled diesel engine. The experiments covered fuels of different properties at different ambient air temperatures and injection timings. The analysis showed that the pattern of misfiring (skipping) is not random but repeatable. The engine may skip once (8-stroke-cycle operation) or twice (12-stroke-cycle operation) or more times. The engine may shift from one mode of operation to another and finally run steadily on the 4-stroke cycle. All the fuels tested produced this type of operation at different degrees. The reasons for the combustion instability were analyzed and found to be related to speed, residual gas temperature and composition, accumulated fuel and ambient air temperature.

INTRODUCTION

The difficulty of starting diesel engines at low ambient temperatures represents a major problem facing the engine designer. In many cases the compression ratio of the engine is made higher than that required for best brake thermal efficiency in order to facilitate the cold startability. Contrary to the diesel engine, the starting of the spark ignition (gasoline) engine is easier because of the high volatility of the fuel and the use of an electric spark to ignite the charge. In the diesel engine, the fuel is much less volatile than gasoline, and the start of combustion is by an autoignition process. Here the compressed air temperature and pressure play a major role in the evaporation of the fuel, in the formation of an ignitable mixture, in the autoignition chemical reactions and finally in the combustion of the fuel-vapor-air charge. The air temperature and pressure at the start of fuel injection depend on many factors such as the ambient temperature, cranking speed and injection timing. The rate of the autoignition reactions depends on the molecular structure of the fuel in addition to the air temperature and pressure. Volatile fuels are easier to evaporate, but might be more difficult to autoignite.

Many of the processes of spray formation, evaporation, autoignition and combustion in diesel engines are not well understood even under warmed-up steady state conditions for single compound fuels. The analysis of the different physical and chemical processes under cold starting

conditions is more difficult because of the relatively lower compression air temperature and the transient operation of the engine. Also, diesel fuels are blends of many compounds of different volatilities and molecular structures.

The goal of this paper is to present some observations made in a research program on combustion instability during the cold starting of a direct injection, 4-stroke-cycle diesel engine. One of the issues we would like to address is whether combustion instability during cold starting is a random or a repeatable phenomena. The probable causes for combustion instability and the effect of ambient air temperature are discussed.

COMBUSTION INSTABILITY

The instability of combustion during cold starting is caused mainly by the failure of combustion in one or more cycles. Combustion failure may be complete or partial. Complete combustion failure may be due to lack of autoignition caused by very slow preignition reactions rates. During the compression stroke, after fuel injection, heat is transferred from the air to the liquid fuel spray, supplying its sensible heat and latent heat of evaporation. This in turn causes a drop in the local air temperature. The resulting charge of fuel-vapor and air undergoes preignition reactions which are not well defined. These reactions may be divided into decomposition and oxidation reactions. The decomposition reactions lead to the formation of intermediate radicals. Some of the radicals combine in exothermic reactions forming combustion products and release the chemical energy of the reaction. In diesel combustion, the processes of injection, liquid heating and evaporation, vapor diffusion and mixing with hot air, preignition decomposition reactions and exothermic reactions occur simultaneously. All these processes take place while the piston is moving. If these processes occur during the compression stroke, energy is added to the charge and their rates increase. If one or more of these processes occur during the expansion stroke, energy is taken from the charge and their rates decrease. Meanwhile, heat transfer and blowby losses reduce the internal energy and the temperature of the charge. The balance between the energies of all these processes determines the final temperature of the charge and the overall rate of preignition reactions. If these reactions produce radicals at a critical concentration in some localities in the spray, autoignition takes place.

Combustion failure can be also caused by the inability of the autoignition sources to burn the surrounding mixture. This may be caused by the lack of formation of a combustible mixture or its formation at low temperatures.

Combustion is also considered to fail during starting if the reactions do not result in enough net energy capable of overcoming the frictional losses, and supplying the energy required to accelerate the engine to the idle speed. If the frictional losses exceed the work done by the gases on the piston, the engine decelerates and vice versa.

The effective time interval for the combustion reactions to take place is when the piston is close to TDC. At lower speeds, the interval of time available for mixture formation, preignition and combustion reactions increases proportionally to the drop in speed. However, the heat transfer and blowby losses increase as the speed decreases.

Combustion instability during cold starting depends on many factors, some of which will be investigated in this paper.

EXPERIMENTAL PROCEDURES AND INSTRUMENTATION

Experiments were conducted on a single cylinder, 4-stroke, air-cooled, direct injection diesel engine. The engine specifications are listed in Appendix (A). The engine was equipped with a starting motor, and a battery. A battery booster was used in all the tests to compensate for the loss of battery power due to the cold ambient temperatures.

The engine (with its fuel tank, battery and starter) was placed in a cold room equipped with a microprocessor to control the ambient temperature. The engine was soaked for 3 hours at the desired temperature before the start of the test. The fuel rack was set at its maximum position. Three attempts were made to start the engine. All the data reported in this paper are for the first attempt. Four different fuels were used in the experiments. These are DF2, Ref1, Ref2 and JP5. The fuel specifications are given in Appendix (B). Experiments were conducted with three injection timings: 23°BTDC, 16°BTDC and 10°BTDC. The ambient temperatures varied from 30°C to -20°C.

The engine was instrumented with an AVL water-cooled, shielded, platinum-plated quartz pressure transducer, flush mounted in the cylinder head. The angular velocity was measured by a shaft encoder with a resolution of one crank angle degree. A Bently Nevada needle lift sensor was used to measure the start, duration and magnitude of the needle lift. An AVL transducer was used to measure the fuel line pressure just before the injector. A fast response K-type thermocouple with a wire of 0.002 inch (0.05/mm) diameter was used to measure the exhaust temperature.

A data acquisition system was used to collect the data, every crank angle degree of the first 70 cycles. The details of the experimental work, instrumentation and analysis are given by Zahdeh, 1990.

EXPERIMENTAL RESULTS

Figure (1) shows the cylinder pressure and instantaneous angular velocity for the first 70 cycles of the engine. The fuel used was DF-2, the ambient temperature was -5°C and the injection timing was 23°BTDC. The angular velocity traces show that the engine accelerated (due to combustion) in cycles no. 1, 4, 6, 7, 10, 13, 18, 21, 24, 27, 30, 32, 35 to 39, 41, 43 to 47, 50 and 52. During the cycles in between the above cycles, the engine either stayed at the same speed or decelerated. After cycle no. 52, the engine accelerated steadily. The starter was disconnected at cycle no. 57. The pressure traces show the peak pressures and do not give the details

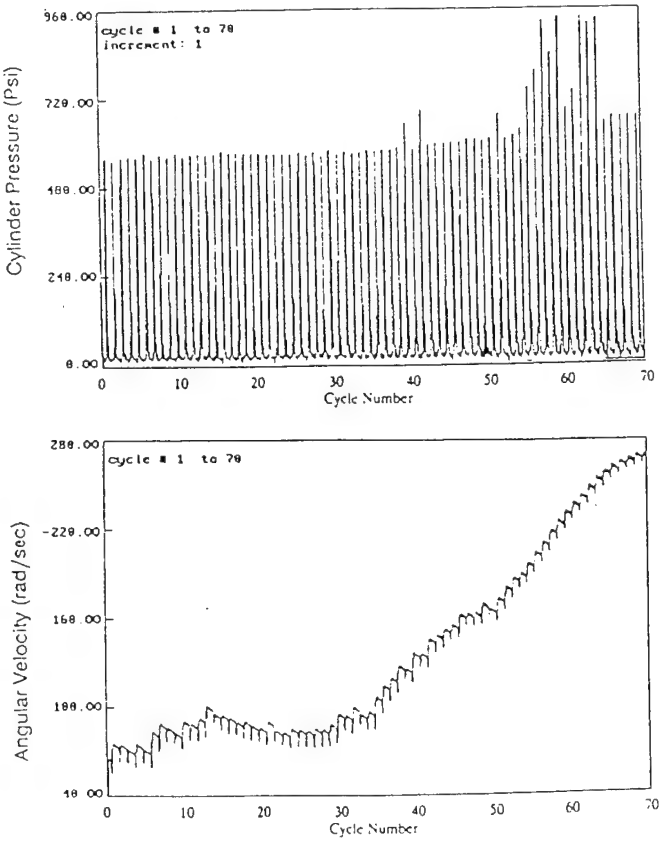

$T_{ambient}$ = -5°C, Fuel = DF2, Timing = 23°BTDC

Figure 1: Cylinder Pressure and Angular Velocity Traces during Starting

of the expansion stroke where late combustion might have taken place. The pattern of the engine operation indicates that the engine misfired (skipped) once or more after firing during the first 52 cycles.

Similar combustion instabilities and engine decelerations after firing were reported by other investigators (Photak et al., 1983, Kobayashi et al., 1984 and Gardiner et al., 1991).

STARTER DISENGAGEMENT

One of the factors which might haved caused deceleration after firing is the disengagement of the starter. Gardiner et al., 1991 reported that the deceleration was caused by the drop in cranking power. They investigated the behavior of a gasoline engine, motored by an electric dynamometer, during starting. In their tests, the firing cycles produced substantial cranking speed accelerations. The increased cranking speeds triggered the electric dynamometer controls and cut its motoring power, causing its speed to drop to near zero during the following cycle. This was not the case in our present work because the engine was cranked by its electric starter and battery system. The current and voltage consumed by the starter were measured, together with the cylinder gas pressure and instantaneous angular velocity. The voltage was observed to remain constant because the battery was always connected to the charger. Figure (2) shows that the current drawn by the starter was high during the whole cranking period. The sharp increase in the current during each cycle occurred during the compression stroke. The current dropped to zero when the starter was turned off after cycle no. 57. After cycle 57, the starter pinion gear disengaged from the flywheel gear teeth. No disengagement occurred before cycle 57, when the engine repeatedly accelerated after firing. Accordingly, deceleration of the engine was caused by autoignition and/or combustion failure rather than by the disengagement of the starter.

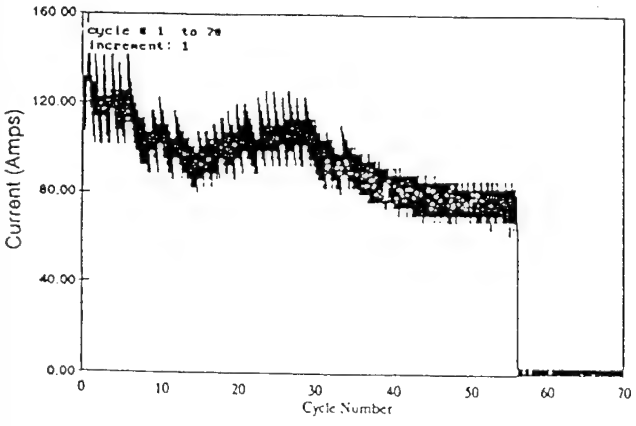

$T_{ambient}$ = -5°C, Fuel = DF2, Timing = 23°BTDC

Figure 2: Starter Current

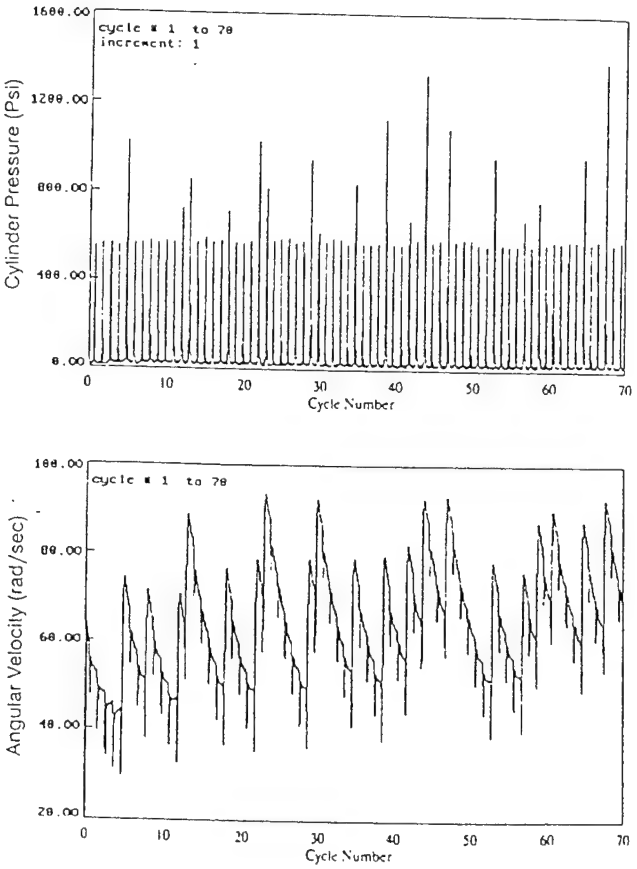

$T_{ambient}$ = 0°C, Fuel = Ref1, Timing = 23°BTDC

Figure 3: Cylinder Pressure and Angular Velocity Traces during Starting

CYCLIC VARIATIONS DURING STARTING

Figure (3) shows the cylinder gas pressure and instantaneous angular velocity for the first 70 cycles of the engine at an ambient temperature of 0°C, injection timing at 23°BTDC, for Ref1 fuel. Figure (4) shows a composite of all the pressure traces. The engine fired and misfired in a repeated manner. The engine skipped once, twice, three times or more cycles after acceleration due to firing. This type of operation is referred to as 8-stroke, 12-stroke and 16-stroke cycle operation. Figure (5) shows the details of the angular velocities for cycles 11 to 29. It is clear that the firing and misfiring patterns are generally reproducible. Cycles 22 to 29 are analyzed in detail. The minimum instantaneous angular velocity in any cycle occurred at TDC at the end of the compression stroke. In cycle 22, the minimum angular velocity was 35.5 rad/sec (339 RPM). During the expansion stroke, the engine accelerated to 78.4 rad/sec (750 RPM). In cycle 23, the minimum angular velocity was 58 rad/sec (551 RPM) and the engine accelerated to 93.5 rad/sec (893 RPM). In cycles 24, 25, 26, 27 and 28, the engine misfired.

The following is a discussion of the autoignition and combustion processes, and the different ignition delay periods. The probable causes of misfiring after acceleration are analyzed to determine the effect of engine speed, residual gases, fuel accumulation and ambient temperature.

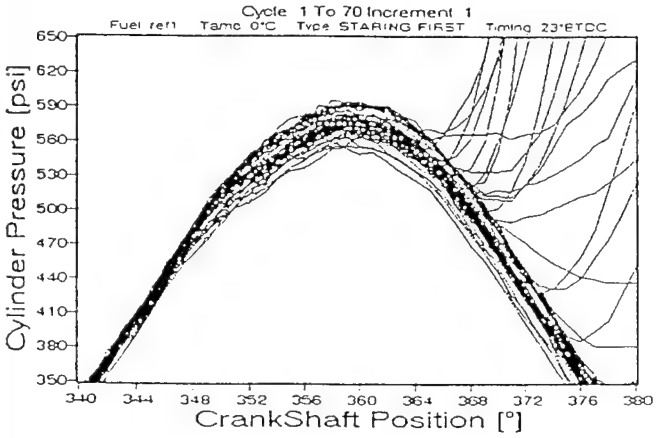

$T_{ambient}$ = 0°C, Fuel = Ref1, Timing = 23°BTDC

Figure 4: Superimposed Cylinder Pressure Traces for All 70 Cycles

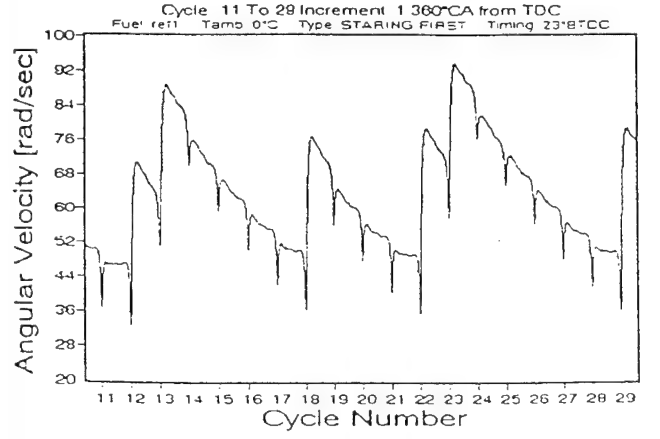

$T_{ambient}$ = 0°C, Fuel = Ref1, Timing = 23°BTDC

Figure 5: Instantaneous Angular Velocity for Cycles 11 to 29

AUTOIGNITION

The autoignition reactions in diesel engines may be considered to take place in two stages. First, slow reactions occur and form intermediate radical compounds such as peroxides and aldehydes (Garner et al., 1961). Second, once a critical concentration of these intermediate compounds has been reached, very fast chain reactions occur and lead to the formation of autoignition nuclei. If the critical concentration is not reached in any part of the spray, the autoignition reactions will fail to form ignition nuclei and the whole combustion process will fail. The autoignition delay $I.D._i$ may be considered to end once the critical concentrations for the intermediate compounds are reached. If we deal with the autoignition reactions as one lumped reaction between the fuel and oxygen, the following relation applies.

$$[F] + [O_2] \rightarrow [I.C.] \rightarrow ignition\ nuclei \quad (1)$$

Hence, the rate of formation of the intermediate compounds can be given by an Arrhenius-type relationship in terms of the fuel and oxygen concentrations

$$\frac{d[I.C.]}{dt} = k[F]^{n}[O_2]^{m} \qquad (2)$$

where k = reaction velocity constant, [F] = fuel vapor concentration, $[O_2]$ = oxygen concentration, [I.C.] = intermediate compounds concentration, n and m = order of the reaction with respect to the fuel and oxygen, respectively, t = time. K can be expressed as:

$$k = c_1 e^{\frac{-E_i}{\bar{R}T}} \qquad (3)$$

where c_1 = constant, E_i = apparent or global activation energy for the autoignition reactions, $\bar{R}$ = universal gas constant, T = absolute temperature.

The ratio of the oxygen to fuel vapor concentrations can be given in terms of the fuel-air ratio or the equivalence ratio, ϕ, and equation (2) can be reduced to

$$\frac{d[I.C.]}{dt} = C_2 e^{\frac{-E_i}{\bar{R}T}} [F]^{n_1} \phi^{-n_2} \qquad (4)$$

where ϕ = equivalence ratio, and c_2, n_1 and n_2 = constants.

The critical concentration of the intermediate compounds which is enough to produce the ignition nuclei, and start the combustion process may be considered constant for any fuel. The time taken to form the ignition nuclei or the ignition delay $I.D._i$ can be expressed as follows:

$$I.D._i = A_1 e^{\frac{E_i}{\bar{R}T}} [F]^{-n_1} \phi^{n_2} \qquad (5)$$

where A_1 = constant which depends on the state of the combustion system.

COMBUSTION

Once ignition takes place, a flame propagates in the surrounding combustible mixture releasing the energy of combustion. Part of the fuel burns in a premixed mode and the rest is burned in diffusion controlled mode. The cylinder gas pressure increases if the rate of energy released from the premixed combustion exceeds the sum of the rates of energy consumed in fuel evaporation, endothermic reactions, heat transfer and blowby losses. In addition, the work due to the change in the gas volume should be accounted for. This work will add energy to the gases during compression and consume energy from the gases during expansion.

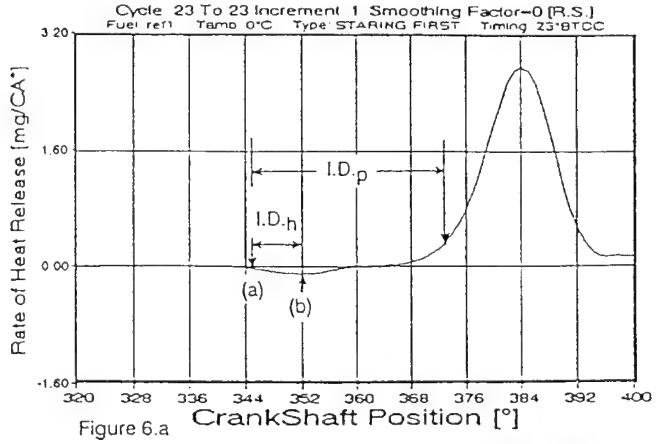

Figure 6.a

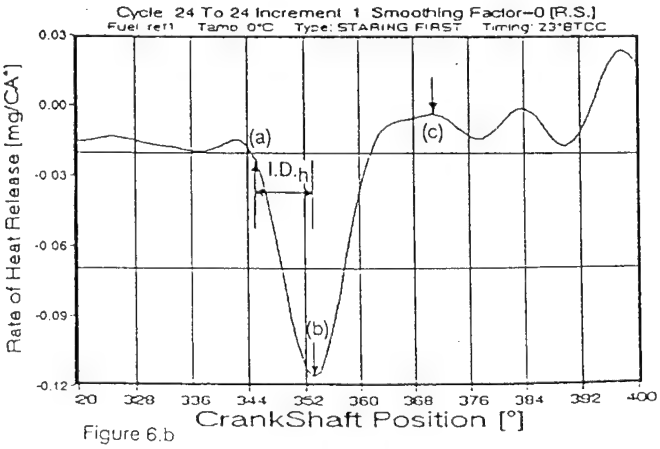

Figure 6.b

Figure 6: Rate of Heat Release for Cycles 23 and 24

Figure (6a) shows the rate of heat release in cycle 23 where combustion took place. The rate of heat release is shown in terms of the equivalent mass of fuel burned in mg per crank angle degree. Injection started at 345° or 15°BTDC. At 352°, the sum of the energy production rates from combustion and the compression work was equal to the sum of the rates of all other losses. After 352°, the rate of the energy released by combustion exceeded that of the other losses. At 373°, the pressure rise due to combustion was detected.

The energy released after ignition depends on the amount of the premixed, fuel-vapor and air available for combustion. If the fuel evaporation or mixing was not fast enough, autoignition may occur but combustion would fail.

Figure (6b) shows the rate of heat release in cycle 24 when combustion failed. Fuel injection started at point (a). Point (b) shows the point at which the rate of energy released by premixed combustion was equal to the rate of the losses. The period between the start of fuel injection and point (b) will be referred to as $I.D._h$ (Itoh, 1991). After point (b), the energy produced from the premixed combustion started to exceed the other losses. After point (c), the combustion process failed to produce energy in excess of the energy consumed in the other process. While ignition took place in cycle 24, the expansion work and the other losses chilled the reactions.

Figure (7) shows the ignition delay $I.D._h$ for cycles 13 to 35. The cycles with successful combustion (firing) are designated with letter F. It is observed that $I.D._h$ for the misfiring cycles was always shorter than $I.D._h$ for the firing cycles. This might indicate that longer $I.D._h$ was caused by more fuel evaporation and mixing.

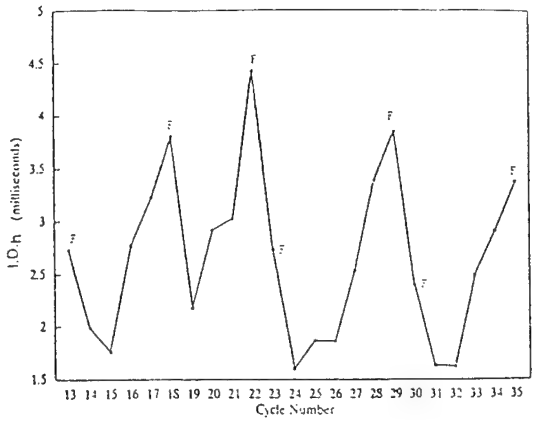

Figure 7: Ignition Delay $I.D._h$ for Cycles 13 to 35

PRESSURE RISE DELAY, $I.D._p$

The period of time between the start of fuel injection, and the start of pressure rise due to combustion is known as $I.D._p$.

In direct injection diesel engines, $I.D._p$ may be correlated to the gas temperature and pressure by equation (6)

$$I.D._p = \frac{Ae^{\frac{E_o}{RT_m}}}{P_m^n} \qquad (6)$$

where A = a constant, E_o = the apparent activation energy for the global autoignition and premixed combustion reactions, n = an exponent, P_m = the integrated mean air pressure during the ignition delay period, T_m = the integrated mean air temperature during the ignition delay period.

EFFECT OF SPEED

Figure (8) shows the minimum instantaneous angular velocity for the first 70 cycles of figure (3). It is noticed that, on the average, the minimum angular velocity occurred in the firing cycle following the skip

cycles. The increase in engine speed after a firing cycle is expected to increase the compression temperature of the first skip cycle as a result of the reduced blowby and heat transfer losses (Henein, 1986). The mass average gas temperature was calculated for all the cycles at every crank angle degree.

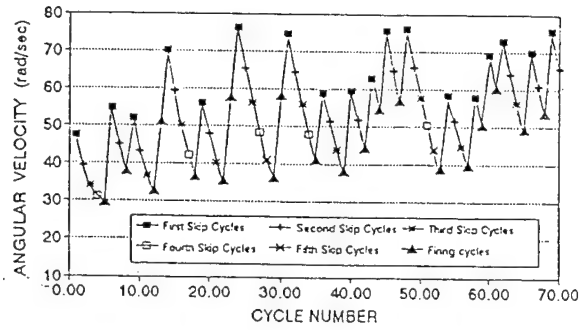

$T_{ambient}$ = 0°C, Fuel = Ref1, Timing = 23°BTDC
Figure 8: Minimum Instantaneous Angular Velocity for All 70 Cycles

The calculations took into consideration the heat losses and the blowby losses (Zahdeh, 1990). Figure (9) shows the mass average cylinder gas temperature at the start of injection in cycles 22 to 29. The temperature increased from 660°K in cycle 22 and 23 to 670°K in cycles 24 and 25 and dropped progressively in the following cycles and reached 650°K in cycle 29 when the engine fired. The increase in temperature and pressure in cycle 24 and 25 should have increased the rate preignition reactions, shortened the ignition delay period, and enhanced combustion. However, combustion failed in cycle 24.

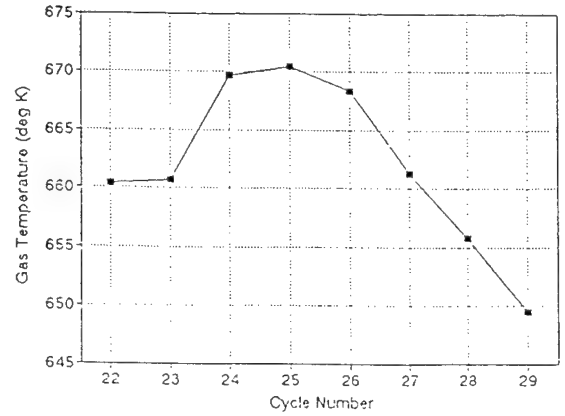

$T_{ambient}$ = 0°C, Fuel = Ref1, Timing = 23°BTDC
Figure 9. Cylinder Gas Temperature at Start of Injection for Cycles 22 to 29

The increase in engine speed also affected the number of crank angle degrees for the exothermic reactions to be completed near top dead center before the gases cooled during the expansion stroke.

The relative effects of shortening the I.D. period, caused by the increase in temperature and pressure and the reduction of the available time near top dead center, caused by the increased engine speed, will be evaluated.

Equation (6) is used in the following analysis. The activation energy, E_o, for Ref1 fuel was calculated from correlations developed for fuels of different cetane numbers at different pressures (Birdi, 1979). E_o, for Ref1 fuel is equal to 28 KJ/g.mol. (12,050 BTU/Mol).

The ratio between $I.D._p$ in any cycle and another cycle may be given by equation (7).

$$\frac{I.D._{p_1}}{I.D._{p_2}} = \left(\frac{P_{m_2}}{P_{m_1}}\right)^n e^{\frac{E_o}{R}\left(\frac{1}{T_{m_1}} - \frac{1}{T_{m_2}}\right)} \quad (7)$$

$I.D._p$ for cycle 22 and 23 were measured from Figure (10) and found to be equal to 9.70 ms and 8.42 ms respectively. I.D. in cycle 23 is 1.28 ms shorter than that in cycle 22

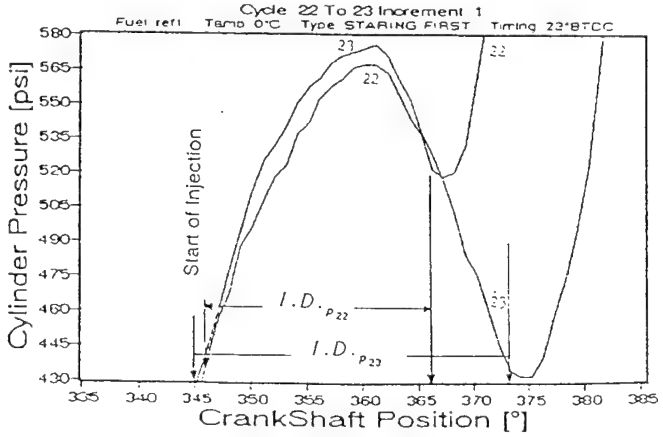

$T_{ambient}$ = 0°C, Fuel = Ref1, Timing = 23°BTDC
Figure 10: Cylinder Pressure for Cycles 22 to 23, 25° from TDC

because of the higher gas temperature and pressure as shown in figure (9, 10). However, in terms of crank angle degrees, the I.D. occupied 20 CAD in cycle 22 compared to 28 CAD in cycle 23.

Applying equation (7), the $I.D._p$ for cycle 24 was calculated and found to be equal to 21 ms. In terms of CAD this is equal to 92°. This means that the pressure rise due to combustion would have started at 437 CAD. This is too late in the expansion stroke.

While the increase in the temperature and pressure from cycle to cycle resulted in a drop in ignition delay, the increase in engine speed resulted in a drop of the available time for the premixed combustion reactions to produce enough energy to accelerate the engine.

EFFECT OF RESIDUAL GASES TEMPERATURE

Residual gases from any cycle mix with the fresh charge of the following cycle and affect both the temperature and composition of the gases during the preignition reactions and combustion periods. The conditions in cycles 24 to 29 are expected to be as follows: The products of combustion of cycle 23, which were at a high temperature, mixed with the fresh charge and contributed to its higher temperature at the start of injection, as indicated in figure (9). The misfiring, as explained earlier, was mainly the result of the sudden acceleration to a higher speed. The situation in cycles 25 to 28 was different than in cycle 24. Figure (11) is for the mass average cylinder gas temperature for cycle 25. At the opening of the exhaust valve the gas temperature was 297°K, compared to 318°K at inlet valve closing. This means that the residual gases of cycle 25 to 28 had a chilling effect on the following cycles. Cycle 29 is expected to have the greatest chilling effect. However, firing took place in cycle 29. Therefore the main cause of misfiring was not the drop in the gas temperature during the compression stroke.

Figure (12) shows the instantaneous exhaust gas temperature during starting on JP5 at 0°C ambient temperature. The temperature dropped to -10°C in the first cycle, -16°C in the second cycle and kept dropping and reached -20°C in cycle 15. The engine fired in cycle no. 16. The autoignition and combustion in cycle 16 occured in spite of the drop in the charge temperature. Therefore, factors other than the charge temperature contributed in enhancing the combustion process.

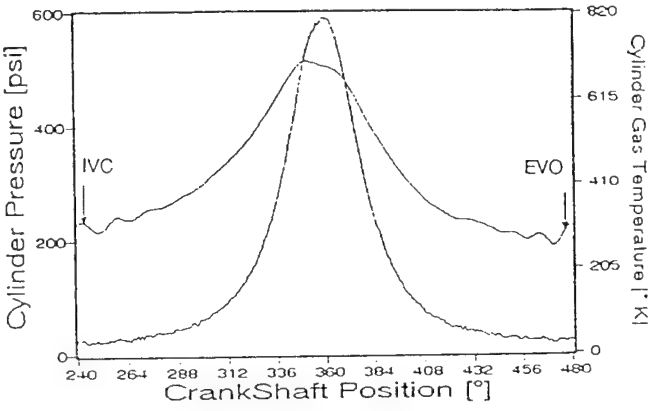

$T_{ambient}$ = 0°C, Fuel = Ref1, Timing = 23°BTDC

Figure 11: Cylinder Gas Pressure and Temperature for Cycle 25

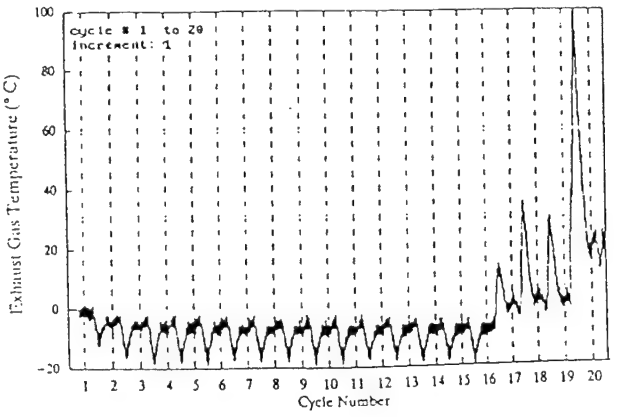

$T_{ambient}$ = 0°C, Fuel = JP5, Timing = 23°BTDC

Figure 12: Exhaust Gas Temperature for the First 20 Cycles

EFFECT OF RESIDUAL GAS COMPOSITION

The exhaust gases, recirculated from one cycle to the next cycle, affect the composition during the compression stroke. It is not clear at the time of writing this paper if this factor played a major role in the failure or success of the autoignition and combustion processes. However, the present analysis might shed some light on this issue. The failure of combustion in cycle 24 of Figures (3), (4) and (5), might be explained in terms of the dilution of the charge by the combustion products of cycle 23. If this was the case, the dilution would have been maximum in the first skip cycle and would have decreased in the following skip cycles. Dilution reached a minimum in cycle 29 when the engine fired. Galliot et al. reported that in a gasoline engine, it required a significant number of cycles, once ignition was turned off, to flush residual gas from the cylinder. If this is the case, in the present work, it took five cycles to flush the residuals of cycle 23.

The recirculated gases from the fired cycles are expected to contain components of fuel and partial oxidation products. If these components exhibited a negative temperature coefficient (negative E in equation (6)) under the higher temperatures and pressures of the first skip cycle, the ignition delay would have increased and resulted in the start of ignition late in the expansion stroke. The negative temperature coefficient behavior for many hydrocarbons was investigated by Lappard, 1990.

EFFECT OF FUEL ACCUMULATION IN THE CYLINDER

Figure (13) shows the cyclic fuel injection during the starting process. The fuel injection per cycle was calculated from the needle lift and the fuel pressure in the high pressure line directly before the injector. The cyclic fuel injection varied from one cycle to the other. The cause of this variation may be attributed to the combined effects of speed and fuel viscosity. At higher speeds, the time for filling the pump barrel would be less. This is particularly true for our engine, in which the flow from the tank to the pump is by gravity.

Tests on Ref1 at 10°C showed that the cyclic fuel injection varied from 35.87 mg/cycle to 13.59 mg/cycle. These values are higher than those shown in figure (13) at 0°C. The fuel

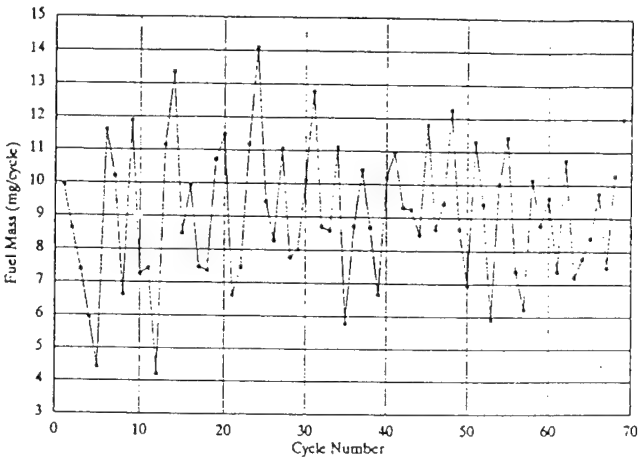

$T_{ambient}$ = 0°C, Fuel = Ref1, Timing = 23°BTDC
Figure 13: Cyclic Fuel Injected for All 70 Cycles

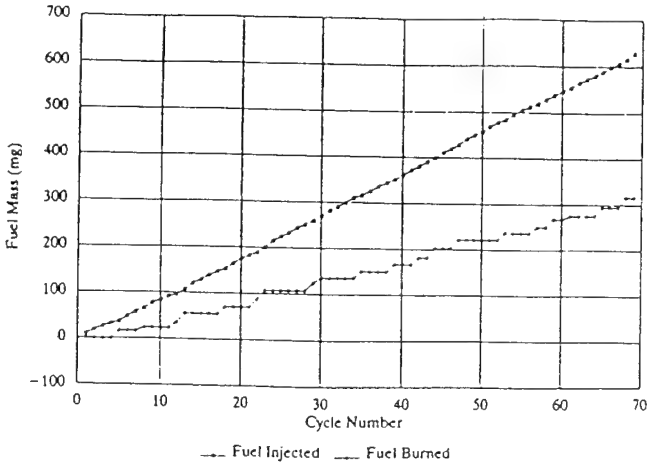

$T_{ambient}$ = 0°C, Fuel = Ref1, Timing = 23°BTDC
Figure 14: Cumulative Fuel Injected and Burned for the First 69 Cycles

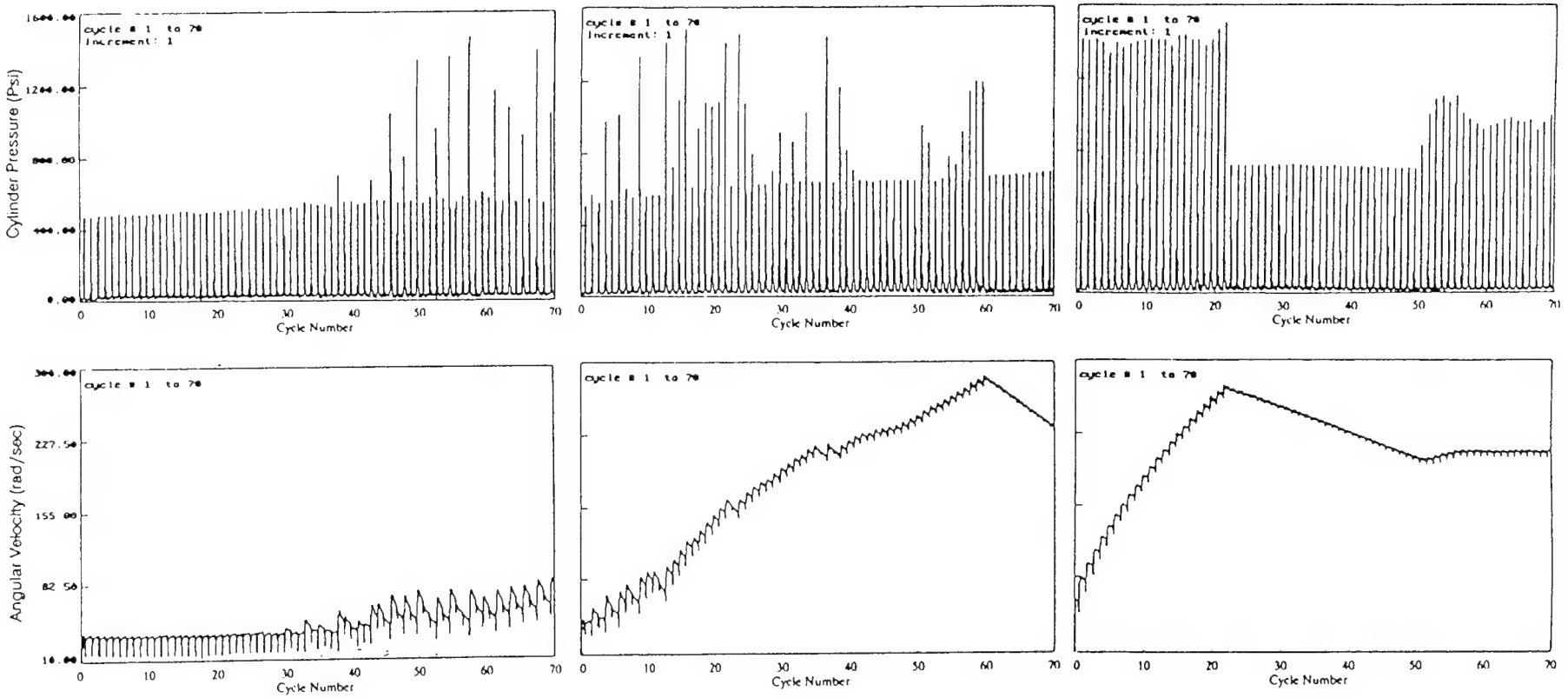

Fuel : DF2
Temp. : -10°C
Timing : 23°BTDC

Fuel : DF2
Temp. : 0°C
Timing : 23°BTDC

Fuel : DF2
Temp. : 30°C
Timing : 23°BTDC

Figure 15: Cylinder Pressure and Angular Velocity Traces under Different Ambient Temperatures

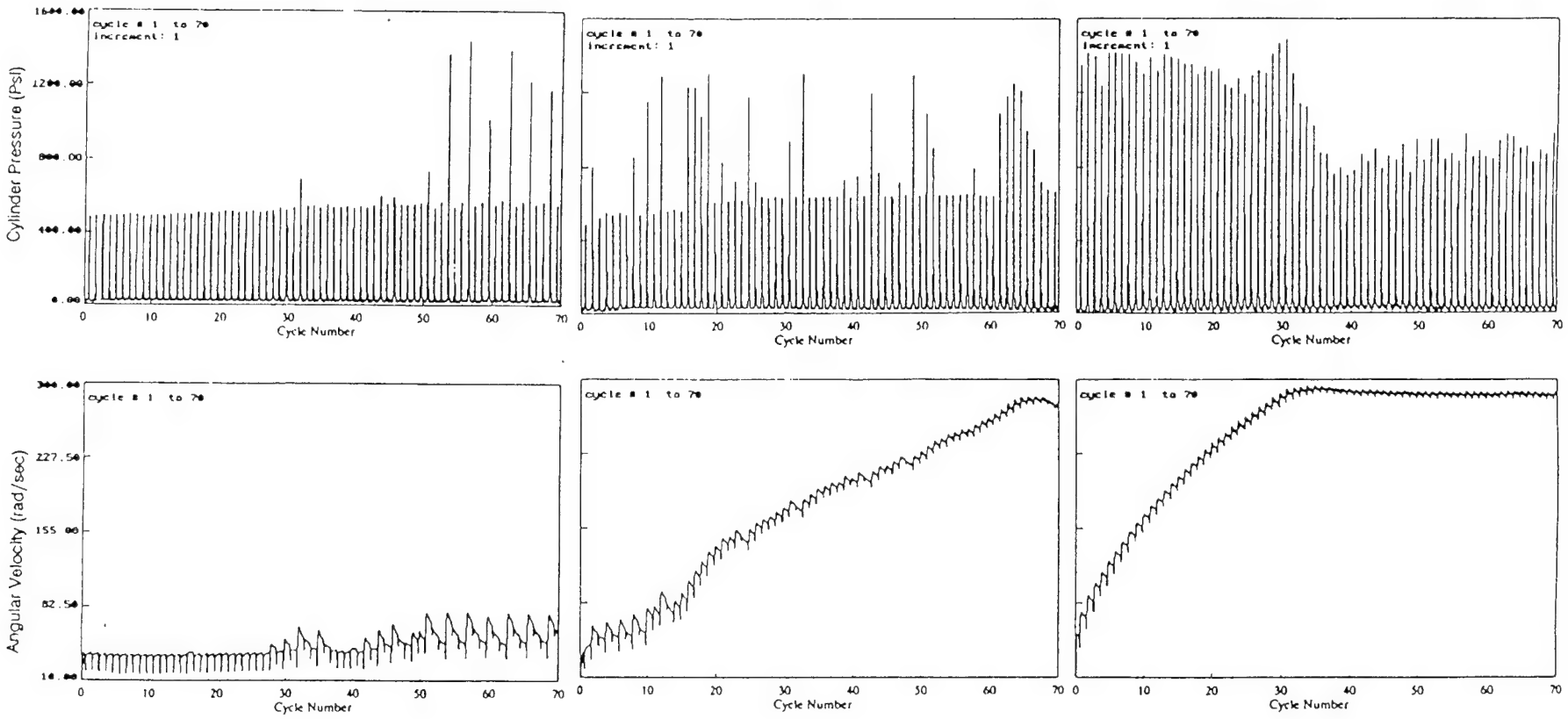

Fuel : JP5
Temp. : -10°C
Timing : 23°BTDC

Fuel : JP5
Temp. : 0°C
Timing : 23°BTDC

Fuel : JP5
Temp. : 10°C
Timing : 23°BTDC

Figure 16: Cylinder Pressure and Augular Velocity Traces under Different Ambient Temperatures

accumulation or the concentration of the fuel vapor in the cylinder during compression is expected to have played a role in the success of the combustion reactions. It is estimated that the fuel accumulated in the cylinder during cycle 29, as a result of the misfiring in cycles 24 to 28, amounted to 58 mgs. Figure (14) shows the cumulative fuel injection and the cumulative fuel burned. The cumulative fuel burned was calculated form the cumulative heat release.

EFFECT OF AMBIENT AIR TEMPERATURE

Figure (15) shows the cylinder pressure and corresponding angular velocity of the engine during the first 70 cycles following turning on the electric starter. The fuel used was DF2. At -10°C, the engine was cranked for 29 cycles and showed signs of very weak combustion in cycle number 30. The engine operated on 12-stroke-cycle till cycle 70. At 0°C, the engine was cranked for one cycle, after which it fired with occasional misfiring, and accelerated at a faster rate to cycle 60, when the governor controlled the fuel. At 30°C, the engine fired in the first cycle and accelerated at a faster rate to cycle 23, when the governor controlled the fuel. The increase in the ambient temperature resulted in shorter cranking (without firing) periods and a higher acceleration to the governed speed.

Figure (16) is for JP5 at -10°C, 0°C and 10°C, injection at 23°BTDC. At -10°C, the engine misfired completely till cycle no. 28, after which the engine operated on 8-stroke-cycle and 12-stroke-cycle operation. At 0°, the engine operated on the 8-stroke-cycle during the first thirteen cycles and shifted to 4-stroke-cycle operation. At 10°C, the engine started on the 4-stroke-cycle without any misfiring.

Figure (17) shows the gas temperature at the start of injection for the three ambient temperatures. As the temperature exceeded 640°K, the operation was on the 4-stroke-cycle. Between 620°K and 640°K, the operation was on 8-stroke-cycle till the temperature reached 640°K. Below 620°K, the engine misfired completely till cycle no. 28. In the following cycles, the temperature increased above 620°K and the engine operated on 12-stroke-cycle and 8-stroke-cycle.

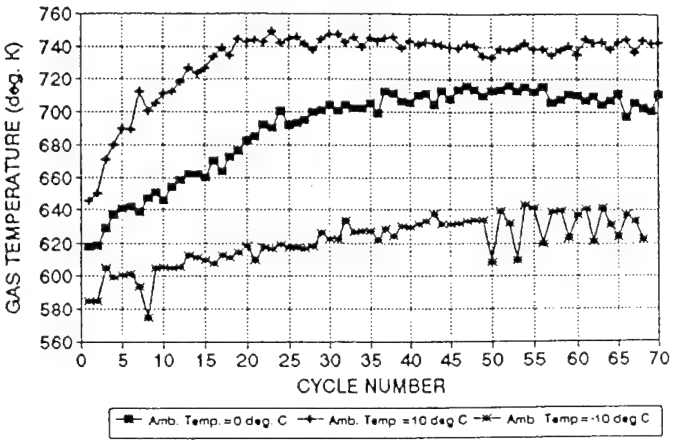

Fuel = JP5, Timing = 23°BTDC

Figure 17: Cylinder Gas Temperature at Start of Injection under Different Ambient Temperatures

CONCLUSION

The following conclusions are based on cold startability tests conducted on a single cylinder air-cooled, 4-stroke-cycle, direct injection diesel engine.

1-Combustion instability during cold starting is not a random process. It follows a repeated pattern where the engine may skip one cycle (8-stroke-cycle mode) or skip two cycles (12-stroke-cycle mode) or skip more cycles. The engine shifts from one mode to another with less skip cycles. Finally it runs on a 4-stroke-cycle mode.

2-All the hydrocarbon fuels, having different volatility, cetane number and specific gravity, experienced combustion instability at low ambient temperatures. Combustion instability caused partial or complete misfiring. This resulted in engine deceleration after the cycle following a firing cycle.

3-Engine deceleration was not caused by the disengagement of the starter after acceleration. It was rather caused by the failure of the combustion process.

4-The number of skip-cycles increased with the drop in the ambient temperature.

5-The causes of misfiring after acceleration appears to be a combination of the following factors:

a- the period of time available for the autoignition and combustion reactions near top dead center, where the gas temperatures are high. When the engine accelerated, autoignition took place, and the pressure rise delay $I.D._{\rho}$ decreased in terms of milliseconds but occupied more crank angle degrees and ended very late in the expansion stroke.

b- the dilution of the charge with the residuals from the firing cycles.

c- the lack of fuel vapor, mixed with oxygen, ready to carry on the combustion process after autoignition. This is related to the fuel present in the cylinder, its volatility and the gas temperature and pressure.

Appendix A

Engine Specifications for
Deutz FIL 210D MAG

Working Cycle	Four Stroke Diesel
Combustion System	Direct Injection
No. of Cylinder	1
Bore & Stroke (mm)	95 x 95
Displacement (cc)	673
Compression Ratio	17:1
Injection Timing (without Advance Unit, CA°)	23 ± 1 BTDC
Inlet Valve Opening (degree)	23°
Inlet Valve Closing (degree)	63°
Exhaust Valve Opening (degree)	63°
Exhaust Valve Closing (degree)	23°
Needle Opening Pressure (bars)	190-200
Rated Speed (max) (rev/min)	3000

Appendix B

Properties of Fuels

Fuels		DF2	JP5	Ref1	Ref2
Specific Gravity		0.8547	0.80908	0.7882	0.9296
Kinematic Viscocity (40°C)		2.7050	1.3621	0.7797	3.7909
Flash Point (0°C)		58.33	60.00	-6.00	58.88
Cetane No.		45	37	25	35
Cloud Point (°C)		-17	-48	-61	-2
Calorific Value (Kcal/kg)		10701.5	11030.0	10904.0	10238.0
Pour Point (°C)		-21	-49	-61	-4
Sulfur Content		0.262 ± 0.010	0.012 ± 0.004	0.010 ± 0.005	0.951 ± 0.051
Aniline Point (°C)		55.20	58.02	38.80	*
Distillation Range (°C)	5%	201.0	194.0	99.0	246.0
	15%	217.5	197.0	118.0	265.0
	25%	228.0	200.0	132.0	274.0
	35%	239.5	203.0	147.0	283.0
	45%	251.0	206.0	162.0	291.0
	55%	262.0	209.0	173.0	299.0
	65%	274.0	214.0	184.0	307.0
	75%	286.0	220.0	199.0	313.0
	85%	302.0	229.0	221.0	344.0
	95%	336.0	244.0	250.0	**

* not transparent.
** 87% maximum recovered only.

REFERENCES

Birdi, P.S., "General Correlation of the Ignition Delay Period in Diesel Engines," Ph.D. dissertation, Wayne State University, Detroit, Michigan, 1971.

Galliot, F., Cheng, W.K., Cheng, C., Sztenderowicz, M., Heywood, J.B. and Collings, N., "In-cylinder Measurement of Residual Gas Concentration in a Spark Ignition Engine," SAE paper no. 900485, 1990.

Gardiner, D.P., Rao, V.K., Bardon, M.F. and Battista, V., "Improving the Cold Start Combustion in Methanol Fueled Spark Ignition Engines by Means of Prompt EGR," SAE paper no. 910377, 1991.

Garner, F.H., Morton, F. and Saundy, J.B., J. Inst. Petrol. 47, pp.175- 183, 1961.

Henein, N.A. and Lee, C-S, "Autoignition and Combustion of Fuels in Diesel Engines under Low Ambient Temperatures," SAE paper no. 861230, 1986.

Itoh, Yasuhiko, "The Characteristics of Diesel Combustion and the Mechanisms of Misfiring under Low Ambient Temperatures," M.S. Thesis, Wayne State University, 1990.

Kobayashi, A., Kurashima, A. and Endo, S., "Analysis of Cold Start Combustion in a Direct Injection Diesel Engine," SAE paper no. 840106, 1984.

Leppard, W.R., "The Chemical Origin of Fuel Octane Sensitivity," SAE paper no. 902137, 1990.

Phatak, R. and Nakamura, "Cold Startability of Open-Chamber Direct- Injection Diesel Engines - Part I: Measurement Technique and Effects of Compression Ratio," SAE paper no. 831335, 1983.

Phatak, R. and Nakamura, "Cold Startability of Open-Chamber Direct- Injection Diesel Engines - Part II: Combustion Chamber Design and Full Spray Geometry and Additional Air and Glow Plug as a Starting Aid," SAE paper no. 831396, 1983.

Zahdeh, Akram R., "Diesel Engine Startability and White Smoke Formation under Cold Temperature Conditions," Ph. D. Thesis, Wayne State University, 1990.

Appendix 4

"Diesel Cold Starting: White Smoke," Zahdeh, A. R., and Henein, N. A.

SAE 920032,1992

920032

Diesel Engine Cold Starting: White Smoke

Akram R. Zahdeh and Naeim Henein
Wayne State University

ABSTRACT

A method to calculate white smoke during starting was developed using a total balance of fuel injected and fuel burned. An accurate needle lift sensor with an in situ calibration was designed and used to measure cyclic fuel injection. The effects of ambient temperature, fuel type, injection timing and the number of repeated starting attempts were studied with regard to white smoke formation, cyclic fuel injection and fuel burned. It was found that the colder the ambient temperature, the less unburned fuel was emitted to the atmosphere due to the decrease in cyclic fuel injection. The more volatile the fuel, the easier it was to start the engine at low temperatures, and the less white smoke was produced. Earlier timing of fuel injection during starting resulted in an increased likelihood of engine starting and less white smoke formation. The experiments were conducted on a single cylinder diesel engine, fully instrumented, and situated in a cold room where temperatures were varied and controlled using a microprocessor.

LITERATURE REVIEW AND BACKGROUND

White smoke formation during engine starting is an extremely complex phenomenon which warrants more attention than it has been given in the literature. To begin the discussion, white smoke will be defined as minute condensed particles of unburned fuel (hydrocarbons) and water vapors which become visible to human eye as white smoke clouds during the cold starting of diesel engines.

So far most of the investigators have used the opacimeter [4,5,6,12][2] to measure the extinction of a pre-known intensity of a light beam passing through a smoke plume. If the initial intensity of light is I_0 and the intensity after passing through the smoke and being measured by a photo detector is I_1, then the smoke opacity is $(1-I_1/I_0)*100$. This method was developed initially to measure the black smoke opacity (black particle concentration).

A brief summary of the work of the previous investigators [4,5,6] will be presented.

Black smoke was measured by installing a photo-detector at an angle 180° from the incident light, while white smoke was measured with another photo-detector at an angle of 36° from the black smoke detectors (the light source, black smoke and white smoke [5] detector are in the same plane). The light reflection from the white smoke plume was measured only by the detector which is located at 36°, while the detector at 180° was used to measure both white and black smoke simultaneously.

The white smoke opacimeter was calibrated using an unfired engine with 9:1 CR. It was noted that the black smoke detector produced a reading even when no combustion was present. Ambient temperature was identified to be the most important factor in engine startability and white smoke formation. Injection timing and nozzle configuration (number of holes and direction of injection) are important factors for starting cold diesel engines, and consequently for white smoke formation. To assure successful starting, the cylinder gas temperature during the compression stroke has to reach a minimum of 419-480°F. Combustion during starting is categorized as an uncontrolled type. It is only by accident that the diesel engine starts under marginal conditions. Continuous fueling during the starting period induces a strong variation of air-fuel-ratio between cycles. Diesel engine starts if the air-fuel-ratio accidentally reaches an optimum value in the combustion chamber. Every cycle that fails to fire will cause the fuel to evaporate and, consequently, produce white smoke. The starting of diesel engines could be improved if control over air-fuel-ratio in the combustion chamber existed. Matching the design of the combustion chamber to the type of injection and spray formation is crucial for the starting of diesel engines. The rate of fuel injection has to be matched for each and every particular type of combustion chamber to assure successful starting and, consequently, the reduction of white smoke formation and emission. Swirl and air movement in the combustion chamber are very important to homogenize the air-fuel-ratio in the combustion chamber.

It is agreed upon among investigators [7,9] that misfiring, low compression temperature and impingement of the fuel particles on the cold walls of the combustion

---

Akram R. Zahdeh is currently with General Motors Corporation
2Numbers in parentheses designate references at the end of the paper

chamber are among the most important factors affecting white smoke[3] formation. A brief summary of these factors will be listed below:

- ***Compression temperature:*** The compression temperature depends on the compression ratio, blowby, cylinder wall temperature (heat transfer) and turbulent intensity in the cylinder. Low compression temperature during starting contributes heavily to misfiring.
- ***Cylinder Wall Temperature:*** This factor includes the coolant temperature (heating elements in the radiator) and the ambient temperature. Cylinder wall temperature could affect both the intensity of heat transfer and the evaporation of impinged fuel particles on the cylinder walls.
- ***Ambient Temperature:*** Low ambient temperature results in low compression pressures and temperature due to the increase of the intensity of heat transfer and the increase of blowby. The increase of blowby could be attributed to the increase in the gaps of the rings at low temperatures.
- ***Fuel Type And Quality:*** Cetane number and fuel volatility are very important factors affecting misfiring during cold starting. Fuel atomization including droplet size, spray shape and nozzle configuration affect the evaporation of the fuel and consequently, self ignition and misfiring.
- ***Combustion Chamber Design:*** This criteria includes the combustion chamber shape (direct injection vs. pre-chamber), intensity of swirl, fuel injector location, crevice volume and the existence of glow plugs. All these factors are tightly interconnected and could have an enormous effect on white smoke formation.
- ***Starting Aid:*** This includes intake manifold heaters, glow plugs and coolant heaters.

ASSESSMENT OF THE USE OF THE LIGHT EXTINCTION METHOD FOR WHITE SMOKE INVESTIGATIONS - Diesel engine exhaust products include carbon particles, unburned fuel, condensed and gaseous hydrocarbons and various organic compounds and sulfates. Smoke measuring instruments are required only to measure aerosols, i.e. solid particles or condensed liquid particles, which are of sufficient size to produce light scattering or absorption detectable by the human eye. Thus it is neither necessary nor desirable for the smoke measuring instrument to respond to the various gaseous components in the exhaust gases.

Potential change in either of these particles will alter comparative smoke measurements. Factors affecting the number density of the particles are:

- Exhaust gas density change due to gas temperature: cooling of the exhaust gases while flowing through a cold piping system.
- Condensation of vaporized components.

Size distribution changes occur as a result of particulate agglomeration or by condensation.

Experiments were conducted in our laboratory to determine the effect of gas temperature on the reading of the opacimeter: a constant fuel rate was injected into the exhaust pipe of an engine during idling condition, but just after the engine was started. The reason that the experiment was conducted while the engine was still warming up was to permit a continuous change of the exhaust gas temperatures during measurements. Both the opacity of the smoke and the temperature of the exhaust gases were measured until the opacimeter reading reached a constant level. Experiments revealed that as the temperature of the exhaust gases increases, the opacimeter reading wanes due to the fuel evaporation. Thus, opacimeter readings are temperature dependent.

COMMENTS ON WHITE SMOKE EXPERIMENT - It is obvious from the literature review that white smoke research is still in its infancy. Until now, the mechanisms of white smoke formation remain unknown. Black smoke opacity meters have been used to measure white smoke concentration during starting, however, no considerations were given to the fact that this device can't differentiate between white and black smoke. Black particles in the exhaust gases were assumed to be totally light absorbent, while liquid particles were assumed to be totally reflective. This assumption is not only unsubstantiated, but with enormous uncertainties due to the following:

Exhaust gases during the starting period consist of:

- ***Black particles***: Mainly agglomerated carbon crystals. These particles are considered to be light absorbent. The size of the particle depends on how far down stream the measurements have been taken. Particle size could change due to particle agglomeration. However, black particles in real life are considered to be not only light absorbers, but random direction light scatterers. Installing a photo-detector in any direction could detect scattered light from black particles.
- ***White smoke particles***: Minute unburned liquid fuel and condensed water vapor. A beam of light passing through these particles could be absorbed (tiny portion), reflected, scattered or refracted from these particles.
- ***Fuel in vapor form***: Light passes through fuel vapors undetected.
- ***Sulfurous and other organic compounds***: These are a very small portion of exhaust gas composition in comparison to other compounds.

From the above information one can see that the exhaust gas during engine cold starting consists of several types of particles with different chemical compounds and complex optical properties. The use of the black smoke detector in such an environment might not be satisfactory.

It is difficult to differentiate between white and black smoke portions of the light reflected, absorbed, refracted or scattered from the particles in the exhaust gases.

The measurement of white smoke is strongly dependent on the exhaust gas temperature: the further the measurement is performed from the exhaust valve, the lower the temperature of the exhaust gases, due to the cooling effect of the exhaust gases in the piping system. A compromise had to be made to choose the place of measurement.

It is difficult to convert the opacity measurement of white or black smoke to a mass flow rate.

---

3 The unburned portion of the fuel will referred to as white smoke, water particles are beyond the scope of this study

Optical methods offer the fastest way to measure smoke density in exhaust gases if only one component is involved (liquid particles or black particles). These methods offer instantaneous measurements of smoke density of the gases passing through the exhaust pipe. To use optical methods for gases with different compounds, very sophisticated analyses have to be performed on the sizes of both black and white particles to determine the contribution of each particle to light reflection, absorption, refraction and scattering in all directions. This information would allow investigators to choose the most relevant optical method. However, this information is very hard to obtain, making the selection and design of measuring instruments difficult.

COMMENTS ON WHITE SMOKE MEASUREMENTS - Based on the above discussion, the following assumptions have to be made before using opacimeters for white smoke measurements:

- The temperature of the exhaust gases has to be constant throughout the entire measurement procedure as: $n \propto \frac{1}{T_t}$.
- The density of the exhaust gases has to remain constant during the experiments.
- The number population of the particles has to remain constant (no agglomeration, vaporization or condensation)

The assumptions are not valid due to the following reasons:

- The temperature of the exhaust gases during the starting period changes continuously as the time progresses; the assumption of constant temperature has to be ruled out.
- Evaporation, condensation and particle agglomeration is present, thus the assumption of constant number population is unjustifiable.
- The density of the exhaust gases during starting is very irregular due to the cooling effect of the exhaust gases as it flows through the piping system.

Opacimeters are devices designed to measure the smoke (black smoke) opacity in the exhaust gases of fully warmed-up engines under steady state conditions. The limitations in the use of opacimeters are due to the assumptions made in the theory based on which the opacimeters operate. The steady state condition is required to satisfy the assumption of constant temperature and number population of the particles, while the fully warmed-up condition is needed to prevent further condensation or evaporation of water or fuel vapors.

Before using opacimeters to measure white smoke the following questions have to be answered:

- What part of the smoke is of interest? (White, black or both)
- What state are these particles in while the measurements are taking place? (Solid, vapor or liquid)
- How does one differentiate between all the particle types and their states? (The exhaust gases contain all of the above simultaneously.)

Based on the little information available about the particle size, distribution, and the mass fraction of their states in the exhaust gases during the starting period, the above questions cannot be made without exhaustive studies and experiments which the present state of technology does not permit.

Opacimeters could be used during the starting period to simulate a human eye looking through a window opening in the exhaust pipe. No intelligent mass breakdown of the exhaust gas content can be made using it's reading due to the uncertainties discussed previously.

EXPERIMENTAL SETUP AND INSTRUMENTATIONS

Fig 1 shows a drawing of the experimental setup used in the investigation of startability and white smoke formation in diesel engines.

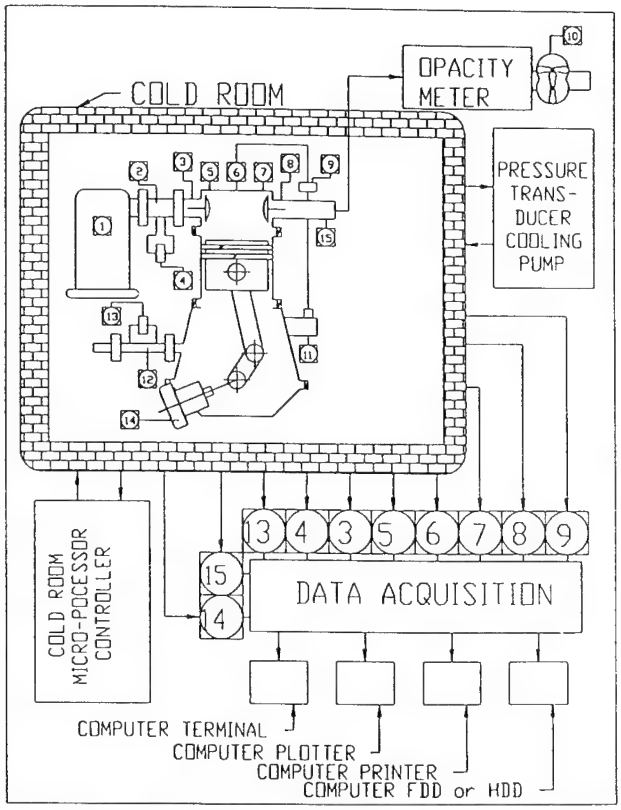

1 *Intake Air Filter*
2 *Laminar Flow Element*
3 *Intake-Manifold Pressure Transducer*
4 *Differential Pressure Transducer*
5 *Cylinder Pressure Transducer*
6 *Needle Lift Sensor*
7 *Cylinder-Head Thermocouple*
8 *Exhaust Fast Response Thermocouple*
9 *Fuel-Line Pressure Transducer*
10 *Laboratory Exhaust Fan*
11 *Fuel Injection Pump*
12 *Laminar Flow Element*
13 *Differential Pressure Transducer*
14 *Optical Shaft Encoder*

Fig 1: Experimental Setup Layout

As shown in the Figure, the engine is located inside a cold room where the temperature can reach -50°F. The engine is instrumented with a cylinder pressure transducer, a needle lift sensor, an intake manifold pressure transducer, intake and blowby mass-flow sensors, and instantaneous cylinder and exhaust thermocouples. The sampling of the data is performed using a digital data acquisition system. Data sampling synchronization with the position of the crank shaft rotation is achieved by using an optical shaft encoder which generates a square pulse (TTL) signal. The TTL signal is used to trigger the start of data sampling and calculation of the angular velocity. The start of the engine cycle is marked by a pulse from the shaft encoder every time the engine reaches the TDC (every 360 CA°).

The temperature in the cold room is controlled precisely by using a micro-processor controller which provides a wide variety of combinations and rates of cooling.

The temperature was brought down to the desired level in a certain soaking time, then the engine was started and the data was recorded using the data acquisition system.

SINGLE CYLINDER DIESEL ENGINE - This is a Deutz general purpose 10 HP engine used for construction purposes. The engine is a direct injection, air cooled type. Table [1] shows the specifications of this engine.

Table 1 Engine Specifications

Specification	Description
Engine Type	F1L 210 D
Total Piston Displacement (cm^3)	673
Working Cycle	Four-stroke diesel
Combustion System	direct injection
Bore (mm)	95
Stroke (mm)	95
Rated Speed (max) (rev/min)	3000
Compression Ratio	17:1
Compression Pressure (bar)	19-21
Needle lift Opening Pressure (bar)	190-200
Injection Timing (without advance unit) (degree)	$23^{\pm 1}$
Dimension of the Injection Pump (mm)	$82.8^{\pm 0.2}$
Inlet Valve Opening (degree)	23°
Inlet Valve Closing (degree)	63°
Exhaust Valve Opening (degree)	63°
Exhaust Valve Closing (degree)	23°

The engine's head had to be modified to accommodate the installation of the fuel injector, the pressure transducer and the thermocouple. A specific holder had to be designed for the modified fuel injector with a needle lift sensor. To accommodate the modified injector, the opening for the fuel injector insertion in the head had to be enlarged. A 1/4 inch from the top of the head was shaved to account for the thickness of the fuel injector holder. The pressure transducer was installed close to the intake-valve to minimize the errors due to thermal shock. The transducer was installed as close as possible to the piston bowl without piercing through the walls of the intake or the exhaust manifolds walls.

PRESSURE TRANSDUCER - In order to choose a piezoelectric pressure transducer, special attention has to be given to the following characteristics:

1) Error compensation for thermal shock, 2) Drift compensation, 3) Heat shielding, 4) IMEP reproducibility during steady state operation of the engine and 5) Frequency response compatibility with data sampling.

A careful screening of the available pressure transducers on the market showed that the AVL golden-plated transducer, type "QC 41 B-E X" produced the most reproducible data. The transducer showed very satisfactory resistance to thermal and long-time drifting under the most adverse engine operating conditions.

The AVL 3057-A01 amplifier with automatic resetting after each cycle produced good pressure data.

NEEDLE LIFT SENSOR - This sensor measures the start and duration of the fuel injection, and the needle lift. The needle lift, fuel line pressure and cylinder pressure were used to calculate the instantaneous mass of the fuel injection into the engine cylinder.

Previously, the position sensors (needle lift sensors) were calibrated on a bench outside of the fuel injectors. The calibration is assumed to remain valid after the installation of the position sensor in the fuel injector. However, it was proven in this work that the above assumption was invalid due to the presence of other magnetic parts like springs, the casing, and the adjusting washers inside the fuel injector. These parts interfere with the magnetic field generated by the sensor. The presence of the fuel could add to the source of uncertainties in the sensor signal calibration. In this work the calibration of the sensor was made while it was installed in the injector. The sensor calibration was found to be nonlinear due to the magnetic interference. Thus, the actual calibration data was fitted to a fourth order polynomial.

Fig 2 shows the needle lift sensor designed and manufactured with an in-situ calibration.

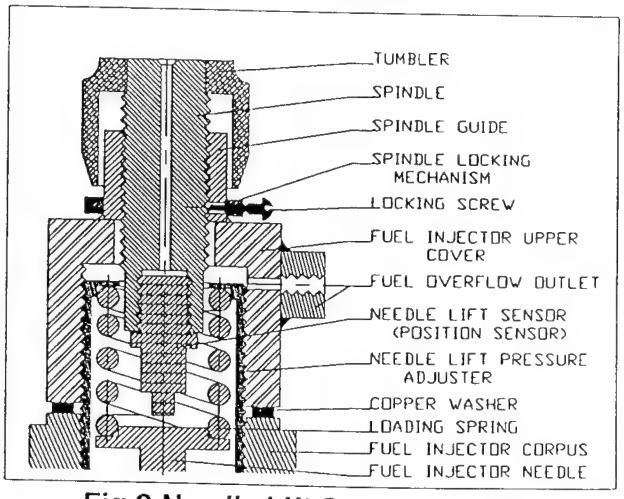

Fig 3 Needle Lift Sensor Design

The figure shows that the position sensor was installed on a spindle and tumbler to accommodate an in-situ calibration.

The original fuel injector of this engine had the high pressure fuel connection located right on the top of it (on the opposite side of the nozzle), which made the installation of the position sensor virtually impossible. A fuel injector casing which was originally used for a Ford diesel passenger car was used instead. In this fuel injector, the high-pressure fuel line connects to the fuel injector corpus at a 30° angle from the injector axis. The back flow which was on top of the fuel injector, was modified and relocated to the side of the injector. The original fuel injector-nozzle from the Duetz engine was used with no modifications to preserve the characteristics of the spray. The needle lift opening pressure (pop pressure) was left unchanged at 3000 psi. 1/1000 inch marks were ingrained on the tumbler to provide an in-situ calibration of the sensor. After the injector was filled with fuel (the engine was operated for about an hour), the voltage was measured for every 1/1000 inch of needle displacement. Fig 3 shows the needle lift sensor calibration.

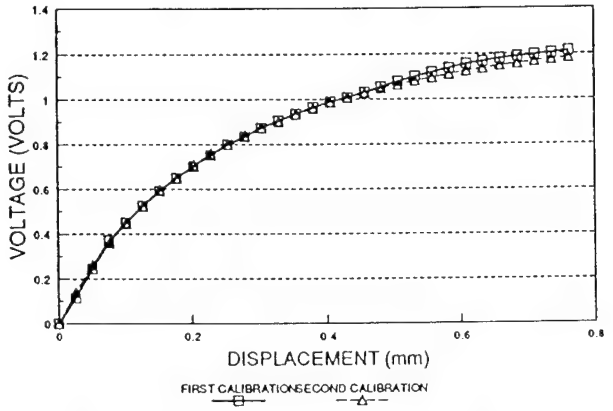

Fig 3 Needle Lift Calibration

DATA ACQUISITION - A four channel data acquisition system was used. The data was saved in a binary format. Further analysis and graphic displays of the data were made possible using special software written specifically for this purpose.

COLD ROOM - The cold room is controlled by a programmable microprocessor controller to provide a variety of cooling cycles with any cooling rates and time intervals within the limitations of the refrigeration unit. The cooling cycle adapted in our experiment was such that the desired temperature could be reached in less than 10 minutes. The cold room temperature was held for a soaking period of 3 hours to ensure homogeneous cooling of all the parts of the engine.

EXPERIMENTAL PROCEDURE

Data from all our sensors were collected simultaneously using the 4 channel data acquisition system. The data collection was triggered from a shaft encoder mounted on the crank shaft of the engine. Collection of data could begin from the time of starter motor engagement. The system was capable of collecting up to 70 cycles, with a resolution of 1 crank angle degree.

The data collected was analyzed as follows:

- Cylinder pressure, intake air mass flow rate and angular velocity were used to calculate the heat release [3,1], from which the rate of burned mass of fuel is determined.
- Needle lift and fuel injection pressure data were used to determine the mass flow rate of fuel injection into the engine.
- The difference between the mass flow rate of the fuel injected into the engine and the mass flow rate of burned fuel gives the mass flow rate of the fuel emitted to the atmosphere.
- The data from the differential pressure transducers, which are connected to the laminar flow elements, were used to calculate the instantaneous intake air flow and blowby rates[1].
- The start of the fuel admission to the combustion chamber was obtained from the needle lift signal.
- The gas exhaust temperature was conditioned using special software which was written especially for the temperature calibration and the reference junction compensation. The software was written due to the unavailability of commercial amplifiers and signal conditioners capable of handling the response needed for our research.
- The signals from the pressure transducer and the angular velocity were used to analyze engine combustion, starting and white smoke formation.
- The data was saved in unformatted binary in files. A postprocessor program was developed to handle the data conversion, graphics, analyses and signal manipulations.

RESULTS AND DISCUSSIONS

NEEDLE LIFT SIGNAL AND FUEL LINE PRESSURE - Knowing the needle lift and the fuel line pressure, the rate of fuel injection can be calculated as follows:

$$\frac{dQ_f}{dt} = A_e C_d (2(P_2 - P_1)\rho)^{0.5} \qquad (1)$$

$$= \pi d L_n C_d (2g(P_2 - P_1)\rho)^{0.5}$$

where:

$A_e = \pi d L_n$ effective area of the orifice
d diameter of the nozzle
L_n needle lift
C_d discharge coefficient
P_2 fuel line pressure
P_1 cylinder pressure at corresponding crank angle
dt crank angle increment
ρ density of the fuel

To find cyclic fuel injection equation 1 becomes:

$$Q_f = \int_{\tau_1}^{\tau_2} \pi d L_n C_d (2g(P_2 - P_1)\rho)^{0.5} dt \qquad (2)$$

where:

τ_1 needle lift opening time [sec]
τ_2 needle lift closing time [sec]

The opening duration of the needle lift was measured using two clocks driven by the TTL signal of the shaft encoder. The extraction of the time interval for every crank angle degree (Δt), which is needed for the integration, was part of the post processor where all the analyses were performed. Fig 4 show a typical signal of the fuel line pressure superimposed on the cylinder pressure during cold starting attempt. Fig 5 shows the needle lift signal of the same cycle superimposed on cylinder pressure.

FUEL INJECTION: CYCLIC AND CUMULATIVE - Fig 6 shows the effect of timing on cyclic fuel injection. At a timing of 23 CA° BTDC the cyclic fuel injection was started at about 18 mgs/cycle until the governor kicked in at cycle 20 when the cyclic fuel injection dropped to 10 mgs/cycle and stayed constant until the end of the run. At a timing of 15 CA° BTDC the cyclic fuel injection started at the same level as the previous timing except that the governor kicked in at cycle 44. For the 10 CA° BTDC timing the cyclic fuel injection was started at the same level as the previous runs and kept increasing until it reached 28 mgs at cycle 58 where the governor kicked in and almost shut off the fuel injection completely. This behavior of high cyclic fuel injection at late timing is not completely understood at this point.

Fig 7 shows the total net fuel injection. From this figure it can be observed that at late timing the net total fuel injection was 1600 mgs while at an earlier timing it reached a maximum of 900 mgs. One further observation is that the net fuel injection showed a trend of leveling off at late fuel injection timing while a steady increase in the fuel injection was observed at an earlier timing.

Fig 8 shows that at low temperature (-10°C) the cyclic fuel injected was only about 8 mg/cycle, while the rack was at its maximum fuel delivery position. This is extremely low compared to the cyclic fuel injected at higher ambient temperatures. At 0°C, the maximum fuel injection was 16 mg/cycle while at +10°C, the maximum cyclic fuel injection was 36 mg/cycle. This observation can lead to the following conclusions: First, the cyclic fuel injection increased with increasing ambient temperature due to the decrease of fuel viscosity where the more viscid the fuel, the more difficult the filling of the fuel injection plunger cavity becomes. The usual plugging of the fuel filter at low temperatures was not a factor in these tests because the filter was removed. Second, the needle opening had a shorter duration of opening and smaller maximum lift. The same conclusions can be drawn from the same graphs with net fuel injection.

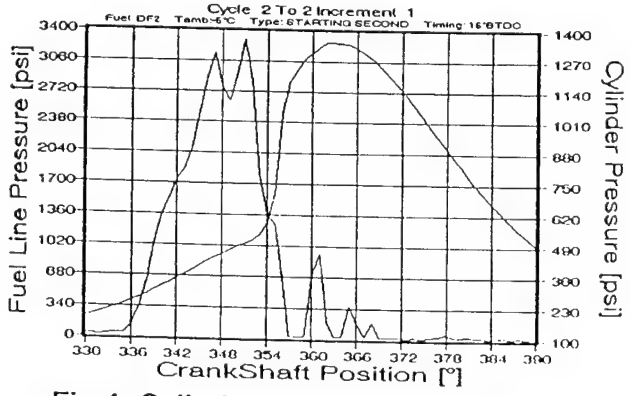

Fig 4: Cylinder and Fuel line Pressure

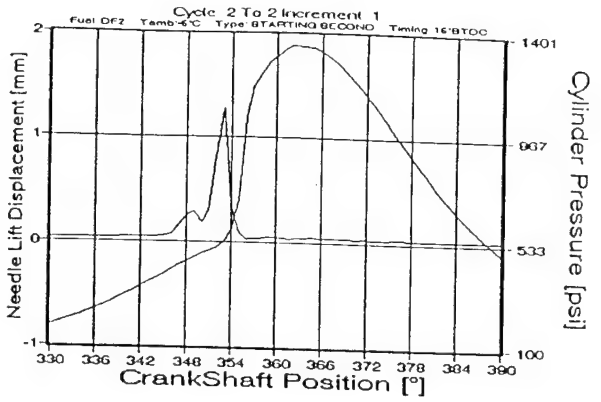

Fig 5: Cylinder Pressure and Needle Lift Signal

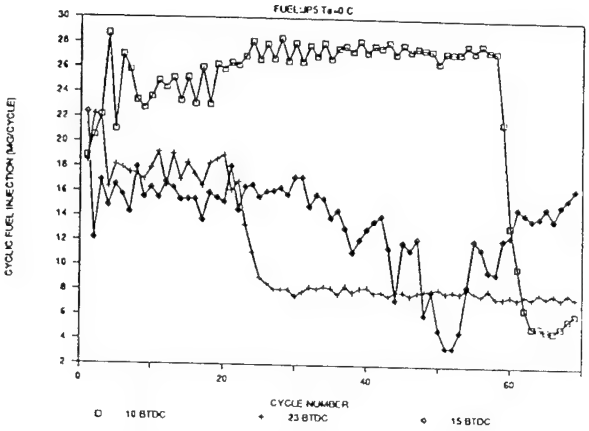

Fig 6: Cyclic Fuel Injection: Effect of Timing

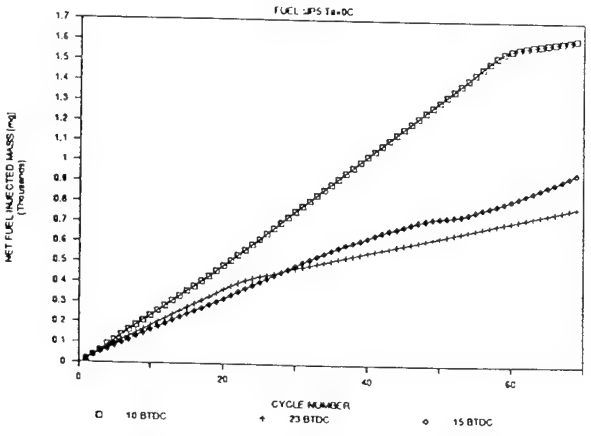

Fig 7: Net Fuel Injection: Effect of Timing

Fig 9 shows the effect of ambient temperature on the net total fuel injection. From figure 9 the following conclusion can be drawn: the total net fuel injection decreased due to increased fuel viscosity.

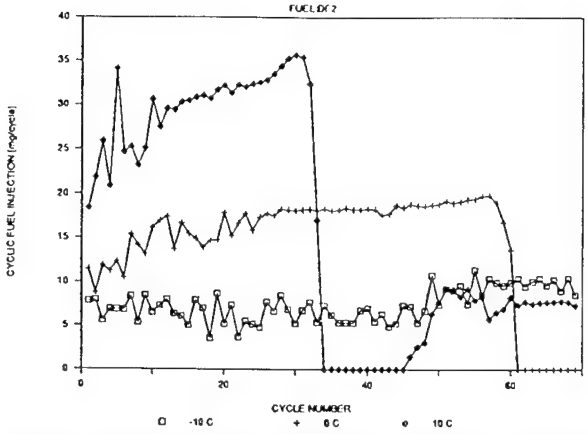

Fig 8: Cyclic Fuel Injection: Effect of Ambient Temperature

Fig 10 and 11 show that fuel JP5 was the quickest to start and it took the governor the shortest period of time to kick in with this fuel. DF2 fuel injection started at the same level as JP5 except that it stayed at the same level much longer than JP5. REF2 and REF1 showed high cyclic fuel injection throughout the 70 cycles. REF2 was lower by about 4% due to its high viscosity which results in poor filling of the cavity. The net fuel injection graphs showed that REF1 had the highest amount of fuel injection while DF2 had the next highest amount, REF2 was third and JP5 had the lowest amount of fuel injected.

FUEL BURNED: CYCLIC AND CUMULATIVE - Figs 12, 13 show that a 23 CA° BTDC fuel injection timing proved again to be the optimum timing for starting as the burned fuel consistently increased its value to reach about 16 mg/cycle and then dropped to 8 mg/cycle after the governor kicked in. 15 CA° BTDC fuel injection timing showed a steady but slow increase of the burned fuel to finally reach 8 mg/cycle. The late injection of fuel produced an erratic 8 and 12 stroke cycle operation [2].

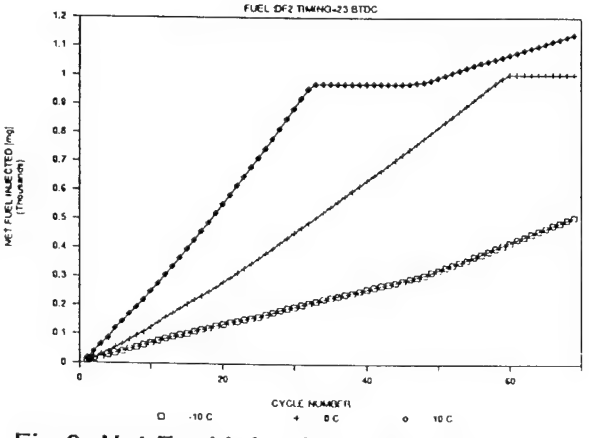

Fig 9: Net Fuel Injection: Effect of Ambient Temperature

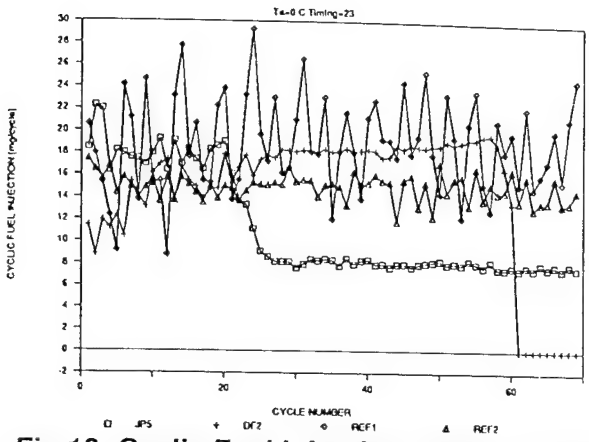

Fig 10: Cyclic Fuel Injection: Effect of Fuel Type

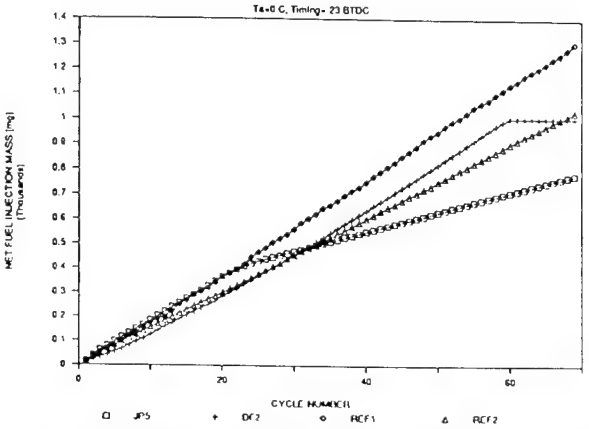

Fig 11: Net Fuel Injection: Effect of Fuel Type

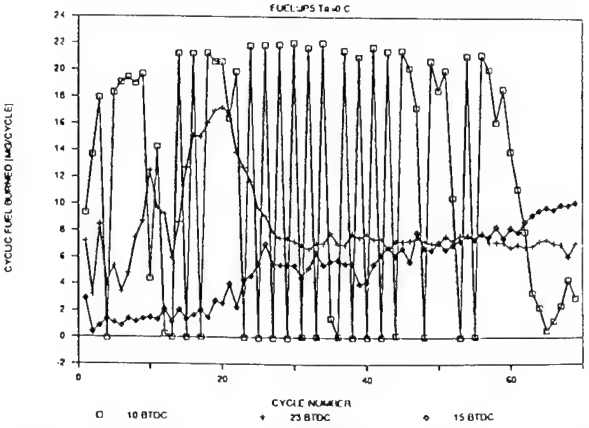

Fig 12: Cyclic Fuel Burned: Effect of Timing

Figs 14, 15 show the ambient temperature had a very important effect on the amount of fuel burned. At +10°C, the engine started very quickly to reach a maximum of 20 mg/cycle of cyclic fuel injection and then dropped down after the governor kicked in. At a low temperature (-10°C)

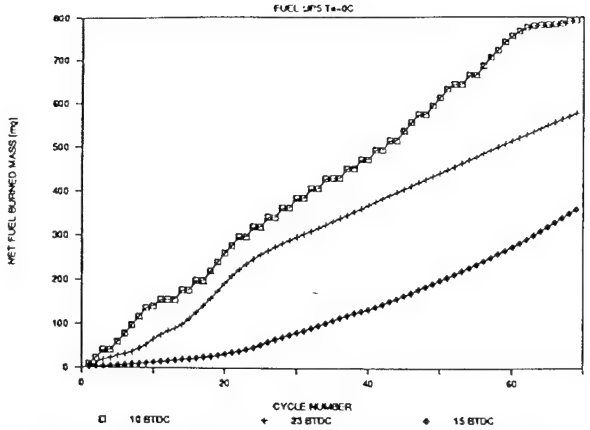

Fig 13: Net Fuel Burned: Effect of Timing

the engine misfired until cycle 45 where a small combustion of 10 mg/cycle took place. At 0°C, DF2 was operating at 8 and 12 stroke cycles.

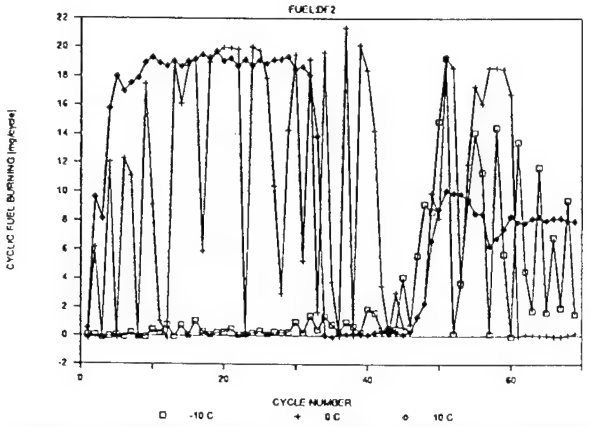

Fig 14: Cyclic Fuel Burned: Effect of Ambient Temperature

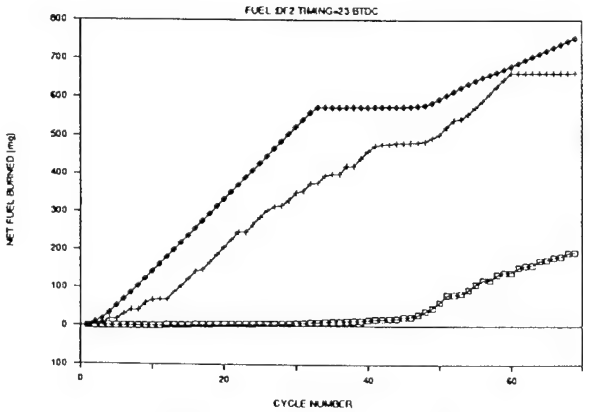

Fig 15: Net Fuel Burned: Effect of Ambient Temperature

Figs 16, 17 show the effect of fuel type on the amount of fuel burned at 0°C and fuel injection timing of 23°BTDC . It was found that of all the fuels, REF2 misfired throughout the starting procedure. JP5 started very smoothly and DF2 and REF1 started with 8 and 12 stroke cycles. Heavy fuels were found to be hard to burn under cold temperature conditions. DF2 and JP5 produced almost the same net fuel injection at the end of the 70 cycles except in the case of JP5 where the governor intervened in a shorter period of time.

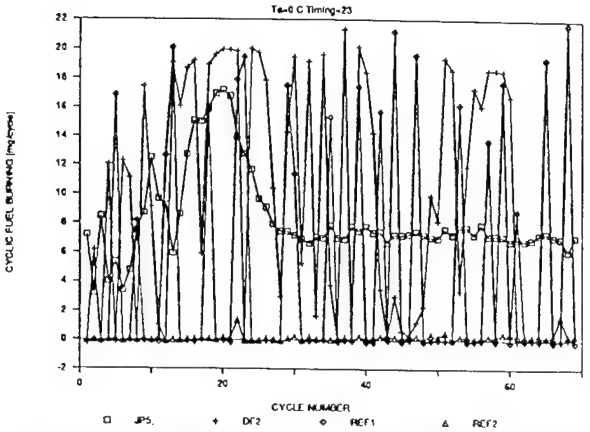

Fig 16: Cyclic Fuel Burned: Effect of Fuel Type

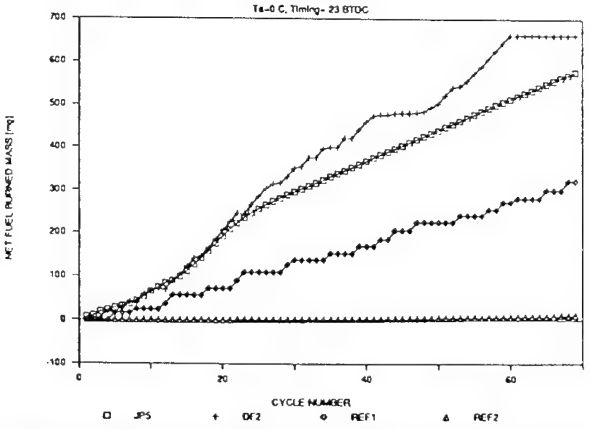

Fig 17: Net Fuel Burned: Effect of Fuel Type

WHITE SMOKE: CYCLIC AND CUMULATIVE - White smoke was calculated from the difference between the fuel injected into the cylinder and the fuel burned. The injected fuel was calculated using the measured instantaneous needle lift, cylinder pressure and fuel line pressure. The fuel burned was calculated by from the heat release using the measured pressure and considering all the losses of heat transfer and blowby. Fig 18 shows the cyclic mass of fuel emitted to the atmosphere. Fig 19 shows the same results as in the previous figure, except that the fuel was calculated cumulatively to give the net fuel emitted to the atmosphere at any cycle during the starting period.

A timing of 23 CA° BTDC produced 11 mg of white smoke in the first cycle, 19 mg in the second cycle, and dropped down to almost zero when the governor kicked in at cycle 20. White smoke at this timing stayed almost constant (1 mg/cycle) for the rest of the 70 cycles. A timing of 15 CA° BTDC produced the same level of white smoke during the first cycle and decreased when the governor controlled the flow of fuel injected into the cylinder starting from cycle 46. The rate of decrease was much slower than that of the previous timing. This is believed to be due to the lower mass average gas temperature reached in the cylinder as shown in Fig 18. A timing of 10 CA° BTDC showed a large variation of white smoke emission due to misfiring of the engine as shown in Fig 18. White smoke was low when the engine fired and high when it misfired. The engine operated at an 8 stroke cycle.

From this graph the following conclusion can be drawn: A timing of 10 CA° BTDC resulted in misfiring and consequently large amounts of cyclic white smoke, while low amounts of white smoke or even negative white smoke resulted when the engine fired. The negative white smoke means an accumulation of the fuel in the cylinder from previous cycles was used in the combustion of the firing cycle. This phenomenon was also observed at a timing of 15 CA° BTDC starting from cycle 52.

Fig 19 shows the total cumulative white smoke shows more clearly the above mentioned points. From this graph the following conclusions can be drawn:

1- On the average, white smoke emissions increased by retarding the timing from 23 CA° BTDC to 10 CA° BTDC. The steady state total cumulative white smoke reached a value of 200 mg at cycle 70 with a timing of 23 CA° BTDC, while it reached a value of 800 mg at a timing of 10 CA° BTDC.

2- The residence time of the fuel in the chamber could be attributed to the decrease of white smoke during early fuel injection as more time available for fuel evaporation.

Fig 20 shows the effect of the ambient temperature. The cyclic white smoke emission at an ambient temperature of 10°C continuously increased until the governor kicked in to indicate that the engine started. At 0°C, white smoke decreased at a slow rate. At a low temperature (-10°C), the cyclic white smoke emission was high when the engine missed and was negative when it fired. This is for operation on an 8 stroke cycle. This might indicate that occurrence of 8 stroke operation is due to the unavailability of sufficient amounts of fuel or its decomposition products, or partial oxidation products. It took two or three consecutive injections for enough fuel or its derivatives to accumulate for firing during the cycle.

Fig 21 shows that 400 mgs was the maximum total amount of white smoke during the run conducted at 10°C. At lower temperatures the maximum total reached about 300 mgs. This can be attributed to the inhibition of the filling of the plunger cavity due to increased fuel viscosity at lower temperatures.

Fig 22 shows that of all the fuels, JP5 produced the least white smoke. All the REF2 fuel injected in the engine was emitted to the atmosphere as white smoke. REF1 and DF2 emitted large amounts of white smoke during misfiring while operating on an 8 stroke cycle.

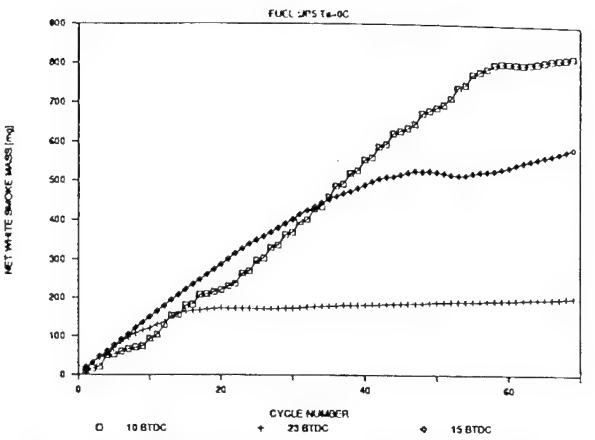

Fig 18: Effect of Timing on White Smoke: Net

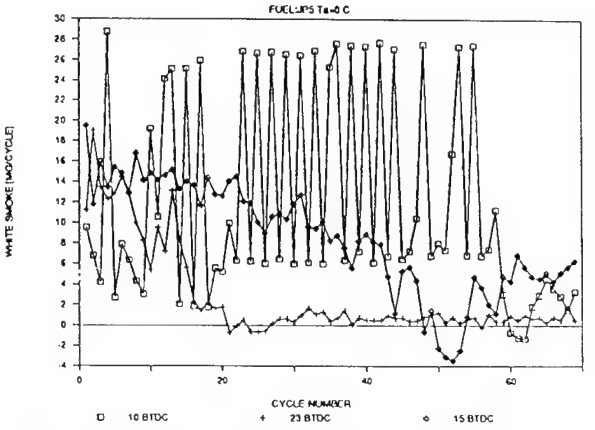

Fig 19: Effect of Timing on White Smoke: Cyclic

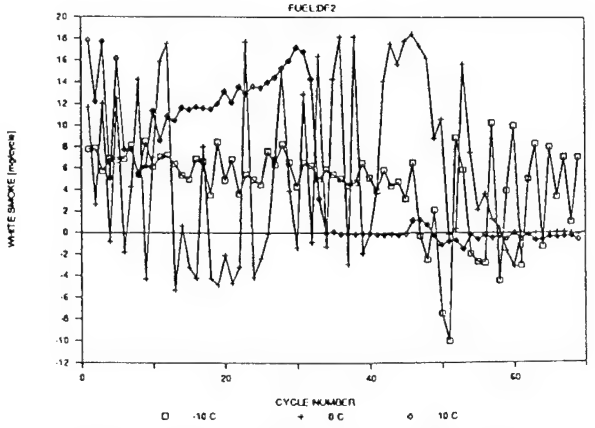

Fig 20: Effect of Ambient Temperature on White Smoke: Cyclic

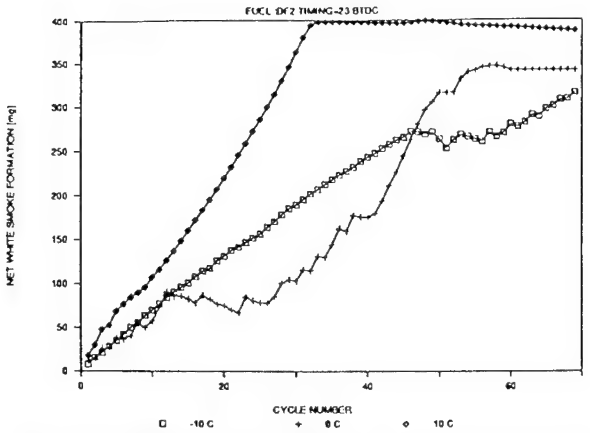

Fig 21: Effect of Ambient Temperature on White Smoke: Net

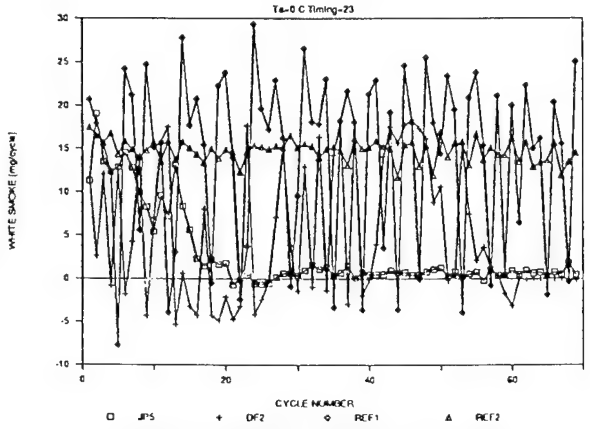

Fig 22: White Smoke: Cyclic

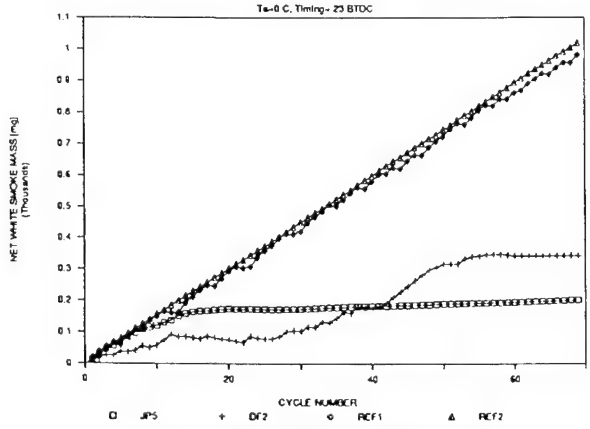

Fig 23: White Smoke: Net

Fig 23 shows that JP5 and DF2 fuels produced the least amount white smoke since the governor kicked in after about 15 to 20 cycles. With DF2 white smoke emission to the atmosphere was greater at higher ambient temperatures, since the viscosity of the fuel decreases allowing better filling of the fuel pump plunger cavity (the Deutz engine has no low pressure fuel pump and the fuel flows to the engine by gravity). This problem might be encountered in larger engines with a low pressure fuel pump since the engine speed might be too low to produce a substantial positive pressure to force the filling of the plunger cavity. REF1 and REF2 fuels produced almost the same amount of white smoke (REF1 produced a slightly lower amount) even though the engine totally misfired throughout the 70 cycles with REF2 fuel (less so with REF1). It seems that REF2 was accumulated mostly as a liquid in the combustion chamber. The part of the fuel which evaporated appeared in the exhaust as white smoke. For REF1, combustion took place in some cycles and the exhaust gases carried some of the unburned fuel which appeared as white smoke.

WHITE SMOKE: MULTIPLE STARTING ATTEMPTS - Fig 24 shows the cyclic fuel injection during four attempts of starting the engine with JP5 fuel at -5°C and a fuel injection timing of 16°CA BTDC. Fig 25 shows the net fuel injected during the same four staring attempts. The total mass of fuel injected decreased after each starting attempt as the battery was getting depleated and consequently decreasing the angular velocity.

Fig 26 and 27 show the cyclic fuel burned and the net mass of the fuel burned during the four starting attempts. The first attempt showed no fuel burned in both cyclic and cumulative, while the second attempt showed little fuel burned at the end of the starting attempt. The third attempt showed some sporadic combustion, but the engine still failed to start. The fourth cycle showed a clear tendency for starting by the steady increase of the mass of the fuel burned.

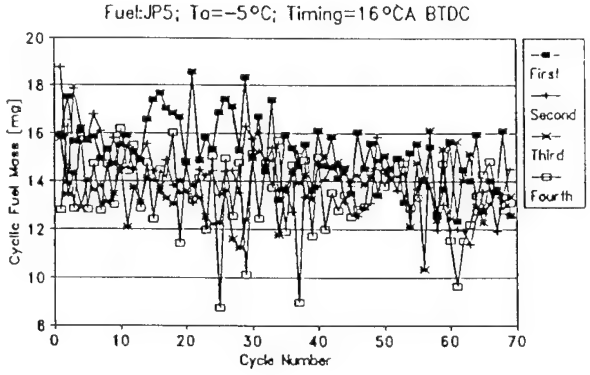

Fig 24: Cyclic Fuel Injection Mass During Four Starting Attempts

Fig 28 and 29 show the cyclic and net mass of white smoke during the four starting attempts. While all the fuel injected during the first and the second attempts ended up being emitted to the atmosphere as white smoke, some of the fuel in attempts three and four was burned. In attempt number four, white smoke dropped to a negative level to show that some of the fuel injected in the engine in previous cycles was accumulated to be burned in the subsequent cycles. This trend was consistent for all starting attempts at low temperatures. One can conclude from the above discussion that repeated starting attempts lead to a reduction of emitted fuel to the atmosphere due to: 1) the decrease of the amount of fuel injected after each attempt, and 2) increase of fuel burned due to the heating of the walls and residual gases in the cylinder after each attempt.

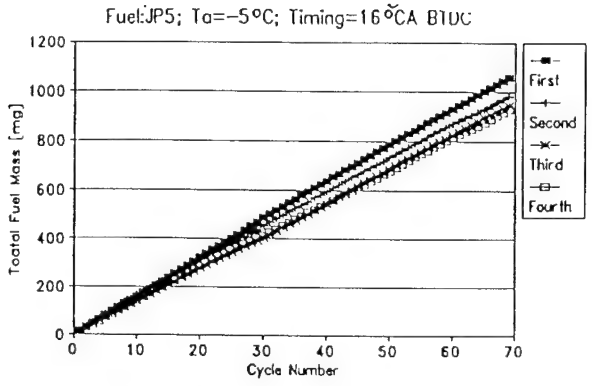

Fig 25: Total Fuel Mass Injected During Four Starting Attempts

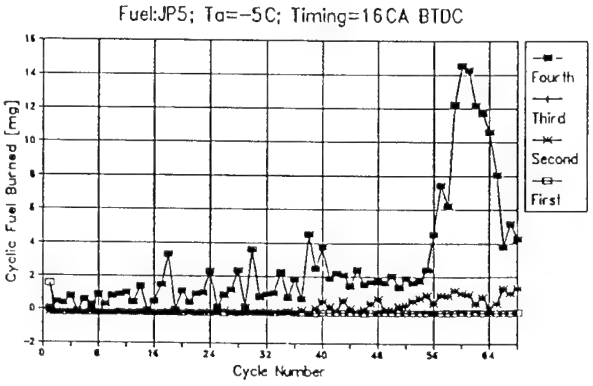

Fig 26: Cyclic Fuel Injection Mass During Four Starting Attempts

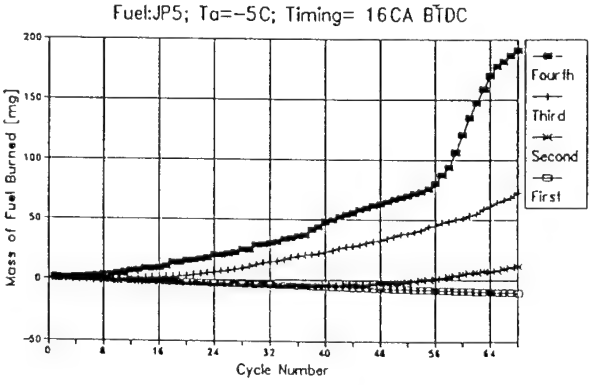

Fig 27: Total Fuel Mass Burned During Four Starting Attempts

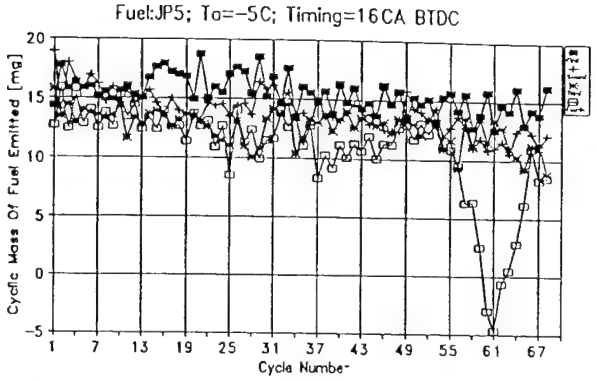

Fig 28: Cyclic White Smoke Emitted During Four Starting Attempts

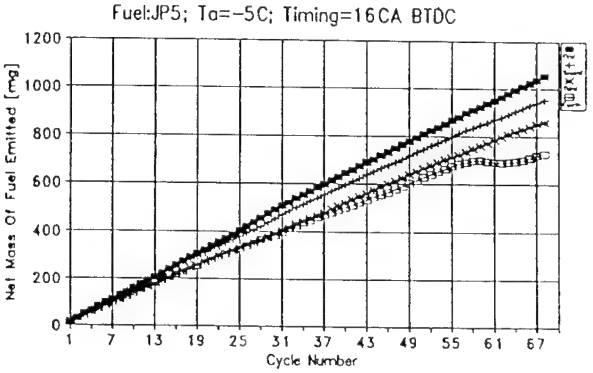

Fig 29: Net Mass of White Smoke During Four Starting Attempts

CONCLUSIONS

1. A method to measure unburned fuel emission during cold starting was developed. The method is very promising due to the fact of the agreement of the calculation of the fuel burned and fuel injected. To have obtained the same quantity of the fuel burned and fuel injected during both the steady state and the warmed-up operation of the engine proves the validity of the methodology.
2. The new design for the needle lift measurements with in situ calibrations produced very reliable and accurate results of the cyclic fuel injection in transient type of experiments.

3- It was observed that the governor kicked in at the same speed of 97.3 rad/sec regardless of the conditions of the experiments. It is desirable for the governor's action to be delayed under cold temperature conditions to produce a faster arrival to the steady state of the engine operation. During moderate temperature conditions it is desirable that the governor kicks in very early to limit white smoke formation and emission.

4- The calculations of white smoke from measured data showed that it depends heavily on timing. The earlier the timing, the less white smoke emitted.

5- The calculation of white smoke from measured data showed, contrary to popular belief, that white smoke decreases at lower temperatures due to the decrease of the total net injected fuel as the needle movements become more restricted and the viscosity of the fuel increases, to make the filling of the fuel pump plunger more difficult.

6- The calculations also show that more volatile fuels are likely to start faster and to produce less white smoke.

RECOMMENDATIONS

1- Currently used opacimeters are not fit for white smoke measurement because (i) the temperature of the exhaust gases is not constant, (ii) the measurements are location dependant, (iii) the possibility of particles agglomeration and condensation and (iv) the failure of the opacimeters to detect fuels in vapor form.

2- A study of particle size and their mass fraction breakdown has to be conducted before any optical method can be chosen or designed.

3- The measurement of the instantaneous fuel injection which was calculated by the model from cylinder pressure, fuel line pressure and needle lift need more experimental verification. An average of the fuel consumption in a larger number of cycles should be compared with the predictions of the model.

4- Measurement of white smoke (hydrocarbons) by using a flame ionization detector method and compare it with the computer model results.

5- The heat release model by which the fuel burned was calculated assumes that the wall temperature is constant and equals the ambient temperature during the entire starting period. The model should be modified to allow the change of the wall temperature between one cycle and the next.

6- An alternative approach to study the effect of timing and fuel line pressure on startability and white smoke formation is the use of a fuel injector with an electronically controlled needle lift. This would provide more control over the start of fuel injection, duration of the fuel injection and fuel line opening pressure.

7- Experiments should be conducted without the engine governor to determine the effect of the governor's intervention on starting and white smoke.

8- Study engine startability with different fuels under different ambient conditions with a variety of engine parameter settings. From this study develop maps for engine combustion failure, white smoke, optimum timing, the most efficient governor intervention time, and the shape and the rate of fuel injection. These maps can be utilized for future optimization of engine design.

REFERENCES

1. Akram R. Zahdeh, "Diesel Engine Startability and White Smoke Formation Under Cold Temperature Conditions", PhD dissertation, 1990, Wayne State University.
2. Akram R. Zahdeh & Naeim Henein & Walter Bryzik, "Diesel Cold Starting: Actual Cycle Analysis Under Border-line Conditions", SAE paper 900441
3. Akram R. Zahdeh "Diesel Engine Cold Starting: P-C Based Comprehensive Heat Release Model, Part I: Single Cycle Analysis", ASME paper 91-ICE-15
4. Ramkrishna Phatak & Tadoa Nakamura, "Cold Startability of Open-Chamber direct-injection Diesel Engines- Part 1: Measurement Technique and Effects of Compression Ratio", SAE paper 831335
5. Ramkrishna Phatak & Tadoa Nakamura, "Cold Startability of Open-Chamber Direct-Injection Diesel Engines- Part 2: Combustion Chamber Design and Fuel Spray Geometry and Additional Air and Glow Plug as a Starting Aid", SAE paper 831396.
6. Toshiaki Tanaka, Kiyoshi Kobashi, Yoshihiko Imamura, "Development of White Smoke Measuring Method for Diesel Engine", JSAE vol 9, No. 4
7. A.E.W. Austen & W.T. Lyn, "Some Investigation on Cold-Starting Phenomena in Diesel Engines", Gas and oil Power, Annual Technical Review Number, 1959
8. Brian Y. Taniguchi and Jack D. Benson, "Cold Weather Fuel Requirements of Oldsmobile Diesels", SAE 800223.
9. C.M. Urban & J.T. Gary, "A Study of Marginal Compression Ignition", SAE paper 670948
10. D.F. Dolan and D.B. Kittelson, "Diesel Exhaust Aerosol Particle Size Distributions - Comparison of Theory and Experiment", SAE 780110.
11. Daniel H. Gerke, "Real-Time Measurement of Diesel Particulate Emissions with a Light Extinction Opacity Meter", SAE 830183.
12. H. Kanesaka "New Starting Aid For Low Compression Ratio Diesel Engine", ASME 80-DGP-8

ACKNOWLEDGMENTS

The authors acknowledge the invaluable assistance of Louinda Zahdeh in preparing and editing the manuscript of this paper. Special thanks to the US Army Tank Automotive Command for their financial support, and in particular to Dr. Walter Bryzik for taking a keen interest in this research. Mahmoud Yassine of Wayne State University also made a substancial contribution by conducting some of the data analyses.

19th ARMY SCIENCE CONFERENCE

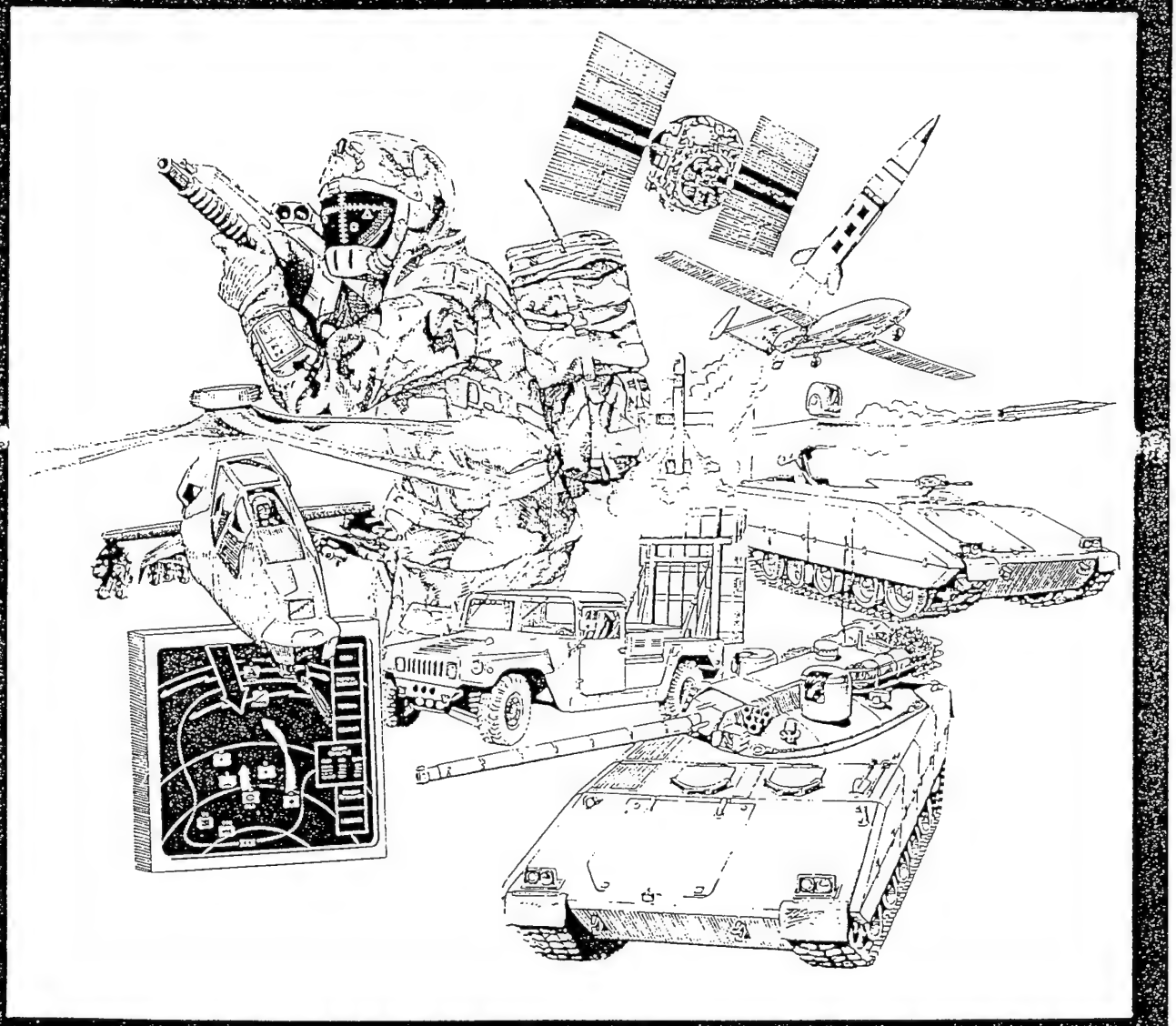

Assuring the Competitive Edge

20-23 June 1994

Orlando, Florida

INVITATION TO ATTEND

Fundamental Cold Start Phenomena Within Advanced Military Diesel Engines

Dr. Walter Bryzik *
U.S. Army Tank-Automotive Command
Warren, MI 48397-5000

Professor Naeim A. Henein
Wayne state University
Detroit, MI 48202-3489

INTRODUCTION:

The Army's fleet of ground vehicles is required to operate in a global environment of extremely wide temperature ranges. Battlefield success and soldier safety is critically dependent upon optimum vehicle performance and reliability under these extreme temperature ranges. The vast majority of U.S. Army tactical and combat vehicles, as well as those of our allies, utilize advanced diesel engines. Commercial diesel engines are likewise critically dependent upon operation over wide temperature ranges (especially during cold start conditions), and thus the high dual use relevancy and importance of the paper's material is also very apparent. Based on the above, the overall merit of the paper's content to the Army's mission can be judged as extremely significant. The paper's multidisciplinary elements involved a complex interaction of unsteady combustion (both premixed and diffusion burning), heat release phasing, autoignition phenomena, and residual gas dilution/combustion failure characteristics. A developed mathematical model features pure instantaneous characteristics such as: angular velocity, dynamic blowby losses, burning rates, and transient injection characteristics. Selected experimental work was performed on different engines under controlled dynamic conditions in a specially designed cold room using state-of-the art instrumentation and data acquisition systems. This paper investigates the fundamental causes of combustion instability and quantifies a lack of its randomness by both theoretical and experimental means over a wide range of engine and fuel related variables.

COMBUSTION INSTABILITY

The instability of combustion during cold starting is characterized by a complete or partial misfiring after a successful combustion and engine acceleration. Complete combustion failure may be due to lack of autoignition caused by very slow preignition reactions and the failure to form autoignition nuclei in the spray. Combustion failure can also be caused by the inability of the autoignition nuclei to burn the surrounding mixture. This may be caused by the lack of formation of a combustible mixture or its formation at low temperatures. Misfiring occurs also, if the reactions do not produce enough net energy to overcome the frictional losses, and supply the energy needed to accelerate the engine to the idle speed. If the frictional losses exceed the work done by the gases on the piston, the engine decelerates and fails to start.

Fig. (1) shows the cylinder pressure and angular velocity traces for a single cylinder, direct injection, 4-stroke-cycle, air cooled diesel engine running on diesel fuel at ambient air temperatures varying from 30°C to -10°C. At 30°C, the engine fired in the first cycle and produced stable combustion in the following cycles every four strokes. The engine accelerated during the first 22 cycles, after which the governor reduced the fuel and brought the engine to the idling speed. At 0°C, the engine was cranked for one cycle, fired every eight strokes for 3 cycles, after which it fired every four strokes with occasional 8-stroke-cycle operation. At -10°C the engine was cranked for 29 cycles, and fired every 12 or 8 strokes.

COMBUSTION INSTABILITY IS NOT A RANDOM PROCESS

Engine operation in both an eight and 12-stroke-cycle mode has been found to be

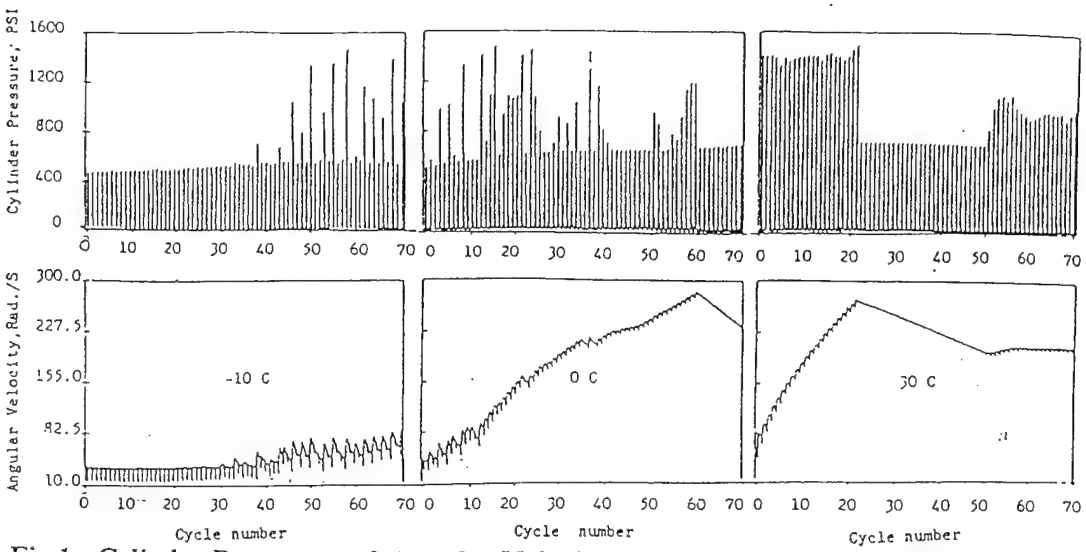

Fig.1 Cylinder Pressure and Angular Velocity Traces at Different Ambient Temperatures with Diesel Fuel.

reproducible for many test variables. A sample of traces for several sets of three consecutive cycles is illustrated in Figs (2) and (3). The engine was run on JP5 at a -10°C ambient temperature for this data.

COMBUSTION INSTABILITY IS NOT FUEL SPECIFIC

The data shown in Fig (4) is representative of tests performed using a variety of fuel types including: diesel fuel JP5, REF1, and REF2. REF1 and REF2 fuels represent military reference

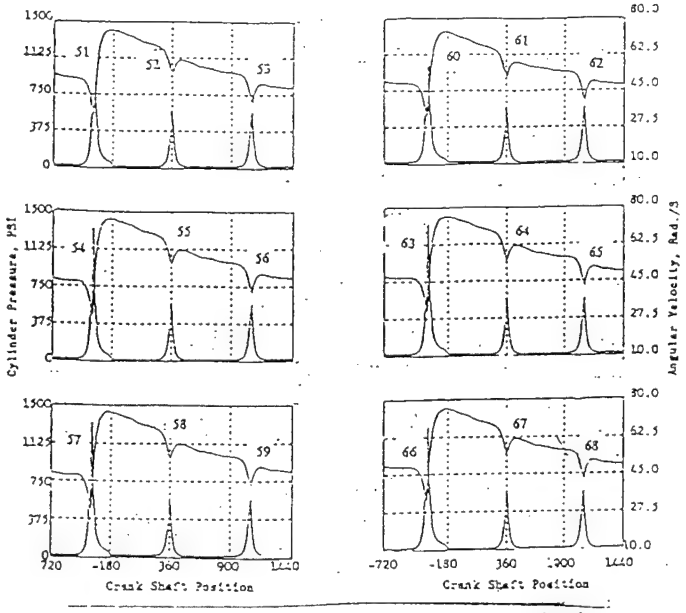

Fig.2 Cylinder Pressure and Angular Velocity Traces for 12 Stroke Cycle Operation with JP5 Fuel at -10°C.

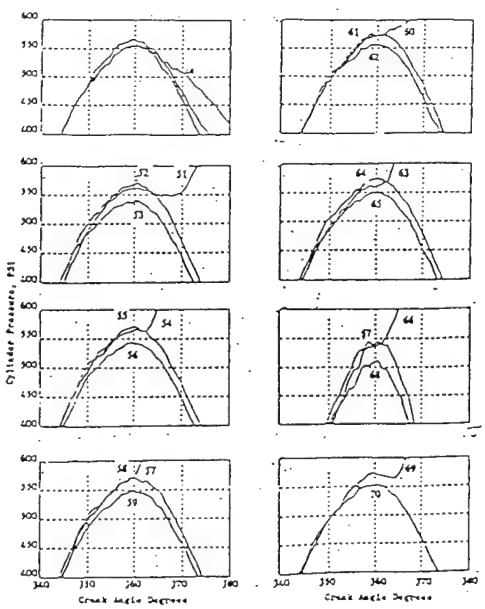

Fig.3 Consecutive Cylinder Pressure Traces for 12 Stroke Cycle Operation with JP5 at -10°C.

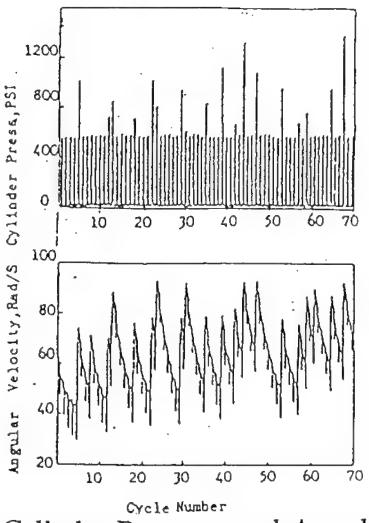

Fig.4 Cylinder Pressure and Angular Velocity Traces with REF1 at 0°C.

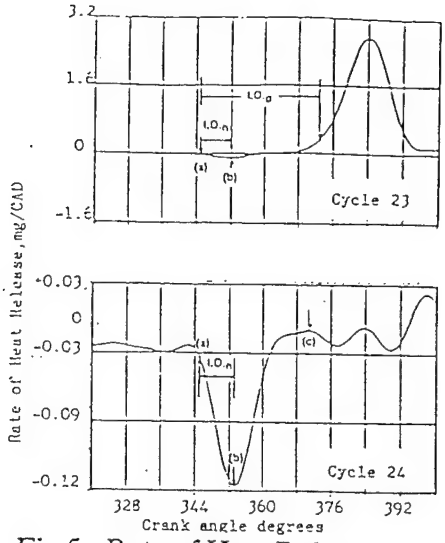

Fig.5 Rate of Heat Release for Cycles 23 and 24.

fuels which band wide ranges of properties including volatility, viscosity, specific gravity and cetane number. These multiple fuel testing showed that the quantification of 8, 12 and 16 stroke cycle during cold start was reproducible.

COMBUSTION INSTABILITY IS NOT ENGINE SPECIFIC.

The above described and reproducible "skip-fire" combustion phenomena was observed and quantified on these diesel engines of different individual designs. These engines included: 1) a TACOM single-cylinder research engine using direct fuel injection and water cooling, 2) a Deutz air cooled single-cylinder research engine, and 3) an optical access modified AVL single-cylinder engine. During the examination of cold start phenomena in all these engines, the probable causes of misfiring after acceleration were analyzed to determine the effect of engine speed, residual gases, fuel accumulation and ambient temperature.

THEORETICAL ANALYSIS

a- Autoignition

The autoignition reactions in diesel engines may be considered to take place in two stages. First, slow reactions forming intermediate radical compounds such as peroxides and aldehydes (1)*. Second, once a critical concentration of these intermediate compounds has been reached, very fast chain reactions occur and lead to the formation of autoignition nuclei. If the critical concentration is not reached in any part of the spray, the autoignition reactions will fail to form ignition nuclei and the whole combustion process will fail. The ignition delay $I.D._i$ may be considered to end once the critical concentrations for the intermediate compounds are reached. If we deal with the autoignition reactions as one lumped reaction between the fuel and oxygen, the following relation applies.

$$[F] + [O_2] \rightarrow [I.C.] \rightarrow \text{ignition nuclei} \qquad (1)$$

Hence, the rate of formation of the intermediate compounds can be given by an Arrhenius-type relationship in terms of the fuel and oxygen concentrations

* Number in parenthesis refer to the list of reference.

$$\frac{d[I.C.]}{dt} = k[F]^n[o_2]^m \qquad (2)$$

where k = reaction velocity constant, [F] = fuel vapor concentration, $[O_2]$ = oxygen concentration, [I.C.] intermediate compounds concentration, n and m = order of the reaction with respect to the fuel and oxygen, respectively, t = time. k can be expressed as:

$$k = c_1 e^{\frac{-E_i}{RT}} \qquad (3)$$

where c_1 = constant, E_i = apparent or global activation energy for the autoignition reactions, R = universal gas constant, T = absolute temperature. The ratio of the oxygen to fuel vapor concentrations can be given in terms of the fuel-air ratio or the equivalence ratio, Φ, and equation (2) can be reduced to

$$\frac{d\,[I.C.]}{dt} = c_2 e^{\frac{-E_i}{RT}} [F]^{n_1} \Phi^{-n_2} \qquad (4)$$

where c_2, n_1 and n_2 = constants.

The critical concentration of the intermediate compounds which is enough to produce the ignition nuclei, and start the combustion process may be considered constant for any fuel. The time taken to form the ignition nuclei or the ignition delay I.D. can be expressed as follows:

$$I.D._i = A_1 e^{\frac{E_i}{RT}} [F]^{-n_1} \Phi^{n_2} \qquad (5)$$

where A_1 = constant which depends on the state of the combustion system.

b- Combustion

Once ignition nuclei are formed, flamelets propagate in the surrounding combustible mixture releasing the energy of combustion. Part of the fuel burns in a premixed mode and the rest is burned in diffusion controlled mode. The cylinder gas pressure increases if the rate of energy released from the premixed combustion exceeds the sum of the rates of energy consumed in fuel evaporation, endothermic reactions, heat transfer and blowby losses. In addition, the work due to the change in the gas volume should be accounted for. This work will add energy to the gases during compression and consume energy from the gases during expansion.

Figure (5) shows also the rate of heat release in cycle 23 of Fig (4) where combustion took place. The rate of heat release is shown in terms of the equivalent mass of fuel burned in mg per crank angle degree. Injection started at 345° or 15° before top dead center. At 352°, the sum of the energy production rates from combustion and the compression work was equal to the sum of the rates of all other losses. After 352°, the rate of the energy released by combustion exceeded that of the other losses. At 373°, the pressure rise due to combustion was detected. The energy released after ignition depends on the amount of the premixed, fuel-vapor and air available for combustion. If the fuel evaporation or mixing was not fast enough, autoignition may occur but combustion would fail. Figure (5) shows the rate of heat release in cycle 24 when combustion failed. Fuel injection started at point (a). Point (b) shows the point at which the rate of energy released by premixed combustion was equal to the rate of the losses. The period between the start of fuel injection and point (b) will be referred to as ID_b (2). After point (b), the energy produced from the premixed combustion started to exceed the other losses. After point (c), the combustion process failed to produce energy in excess of the energy consumed in the other process. While

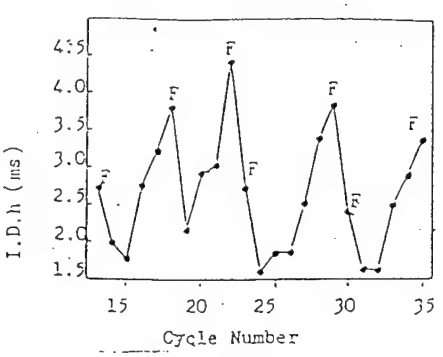

Fig.6 Ignition Delay $I.D._h$ for Cycles 13 to 35.

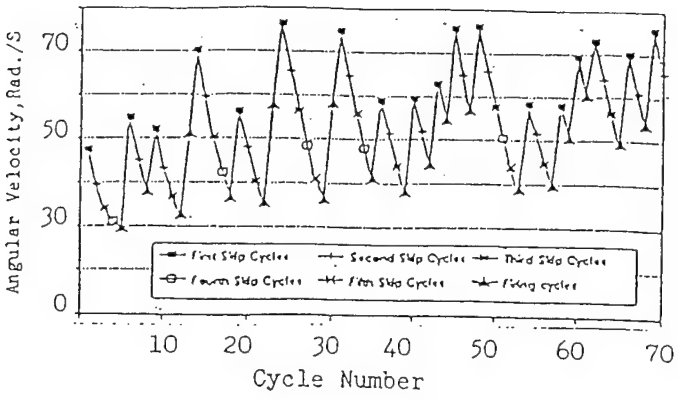

Fig.7 Minimum Angular Velocity for 70 Cycles.

ignition took place in cycle 24, the expansion work and the other losses chilled the reactions.

Fig (6) shows the ignition delay ID_h for cycles 13 to 35 of Fig (4). The cycles with successful combustion (firing) are designated with letter F. It is observed that ID_h for the misfiring cycles was always shorter than ID_h for the firing cycles. This indicates that longer ID_h was caused by more fuel evaporation and mixing.

c- Pressure rise delay, I.D.p

The period of time between the start of fuel injection, and the start of pressure rise due to combustion is known as I.D.p. In direct injection diesel engines, I.D.p may be given by equation (6)

$$I.D._p = \frac{A e^{\frac{E_a}{\bar{R}T_m}}}{P_m^n} \qquad (6)$$

where A = a constant, E_a = the apparent activation energy for the global autoignition and premixed combustion reactions, n = an exponent, P_m = the integrated mean gas pressure during the ignition delay period and T_m = the integrated mean gas temperature during the ignition delay period.

FACTORS CONTRIBUTING IN COMBUSTION INSTABILITY:

1- Engine dynamics:

Fig (7) shows the minimum instantaneous angular velocity for the first 70 cycles of Fig. (4). It is noticed that, on the average, the minimum angular velocity occurred in the firing cycle following the skip cycles. The increase in engine speed after a firing cycle is expected to increase the compression temperature of the first skip cycle as a result of the reduced blowby and heat transfer losses (3). The mass average gas temperature was calculated for all the cycles at every crank angle degree. The calculations took into consideration the heat losses and the blowby losses (4). Fig (8) shows the mass average cylinder gas temperature at the start of injection in cycles 22 to 29. The temperature increased from about 660°K in cycles 22 and 23 to 670°K in cycles 24 and 25 and dropped progressively in the following cycles and reached 650°K in cycle 29 when the engine fired. The increase in temperature and pressure in cycles 24 and 25 should have

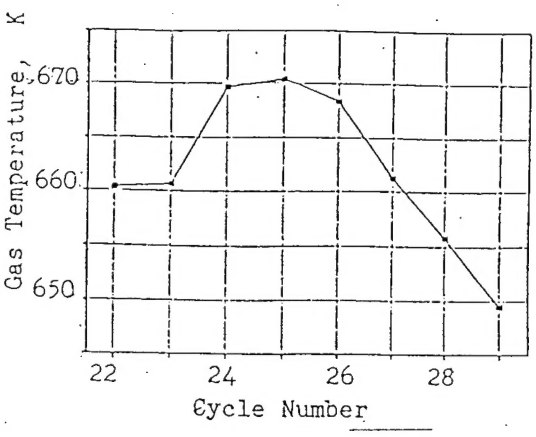

Fig.8 Cylinder Gas Temperature at Start of Injection for Cycles 22 to 29.

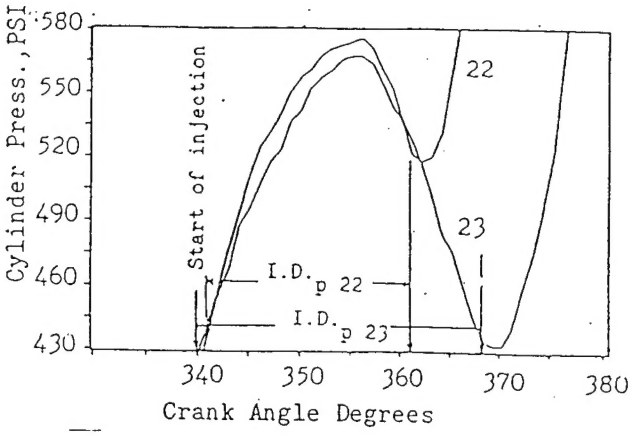

Fig.9 Ignition Delay I.D.p for Cycles 22 and 23.

increased the rate preignition reactions, shortened the ignition delay period, and enhanced combustion. However, combustion failed in cycle 24. The following analysis examines the effect of engine dynamics on combustion failure. The activation energy, E_0 for REFl fuel was calculated from correlations developed for fuels of different cetane numbers at different pressures (5). E_0 for REFl fuel is equal to 28 KJ/g.mol. (12,050 BTU/Mol).

The ratio between I.D.p in any cycle and another cycle may be given by equation (7).

$$\frac{I.D._{P1}}{I.D._{P2}} = \left(\frac{P_{m2}}{P_{m1}}\right)^{n} e^{\frac{E_0}{\bar{R}}\left(\frac{1}{T_{m1}}-\frac{1}{T_{m2}}\right)} \qquad (7)$$

I.D.p for cycles 22 and 23 were measured from Fig. (9) and found to be equal to 9.70 ms and 8.42 ms respectively. I.D.p in cycle 23 is 1.28 ms shorter than that in cycle 22. However, in terms of crank angle degrees, the I.D.p occupied 20 crank angle degrees (CAD) in cycle 22 compared to 28 CAD in cycle 23. Applying equation (7), the I.D.p for cycle 24 was calculated and found to be equal to 21 ms. In terms of CAD this is equal to 92°. This means that the pressure rise due to combustion would have started at 437 CAD. This is too late in the expansion stroke. While the increase in the temperature and pressure from cycle to cycle resulted in a shorter ignition delay, the increase in engine speed resulted in a drop of the available time for the premixed combustion reactions to produce enough energy to accelerate the engine.

2- Residual gas temperature

Residual gases from any cycle mix with the fresh charge of the following cycle and affect both the temperature and composition of the gases during the preignition reactions and combustion periods. The conditions in cycles 24 to 29 are expected to be as follows. The products of combustion of cycle 23, which were at a high temperature, mixed with the fresh charge and contributed to its higher temperature at the start of injection, as indicated in Fig (8). The misfiring, as explained earlier, was mainly the result of the sudden acceleration to a higher speed. The situation in cycles 25 to 28 was different than in cycle 24. Fig (10) is for the mass average cylinder gas temperature for cycle 25. At the opening of the exhaust valve the gas temperature was 297°K, compared to 318°K at inlet valve closing. This means that the residual gases of cycles 25 to 28 had a chilling effect on the following cycles. Cycle 29 is expected to have the greatest

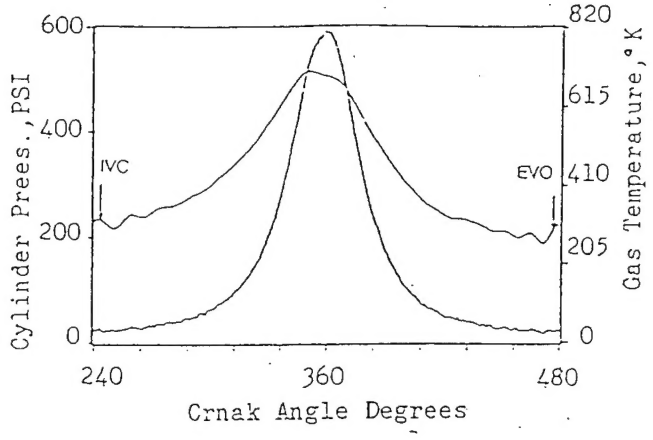

Fig.10 Cylinder Gas Pressure and Temperature for Misfiring Cycle No. 25.

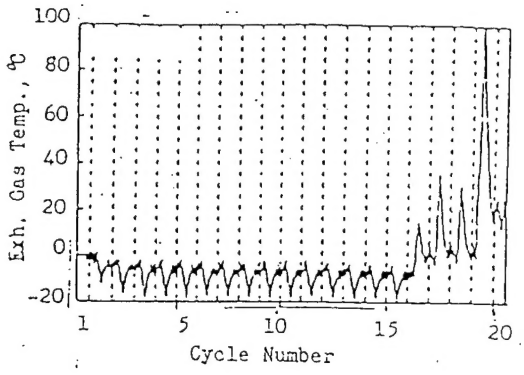

Fig.11 Exhaust Gas Temperature for the First 20 Cycles with JP5 at 0°C.

chilling effect. However, firing took place in cycle 29. Therefore the main cause of misfiring was not the drop in the gas temperature during the compression stroke.

Fig (11) shows the instantaneous exhaust gas temperature during starting on JP5 fuel at 0°C ambient temperature. The temperature dropped to -10°C in the first cycle, -16°C in the second cycle and kept dropping and reached -20°C in cycle 15. The engine fired in cycle no. 16. The autoignition and combustion in cycle 16 occurred in spite of the drop in the charge temperature. Therefore, factors other than the charge temperature contributed in enhancing the combustion process.

3- Residual gas composition

The exhaust gases, recirculated from one cycle to the next cycle, affect the composition during the compression stroke. It is not clear at the time of writing this paper if this factor played a major role in the failure or success of the autoignition and combustion processes. However, the present analysis might shed some light on this issue. The failure of combustion in cycle 24 of Figs (4) and (5), might be explained in terms of the dilution of the charge by the combustion products of cycle 23. If this was the case, the dilution would have been maximum in the first skip cycle and would have decreased in the following skip cycles. Dilution reached a minimum in cycle 29 when the engine fired. Researchers reported that a gasoline engine required a significant number of cycles, once ignition was turned off, to flush residual gas from the cylinder (6). If this is the case, in the present work, it took five cycles to flush the residuals of cycle 23. The recirculated gases from the fired cycles are expected to contain components of fuel and partial oxidation products. If these components exhibited a negative temperature coefficient (negative E_0 in equation (6)) under the higher temperatures and pressures of the first skip cycle, the ignition delay would have increased and resulted in the start of ignition late in the expansion stroke. The negative temperature coefficient behavior has been found to occur in the autoignition of many hydrocarbons (7,8,9).

4- Fuel Accumulation

Figure (12) shows the cyclic fuel injection during the starting process of Fig 4. The fuel injection per cycle was calculated from the needle lift and the fuel pressure in the high pressure line directly before the injector. The cyclic fuel injection varied from one cycle to the other. The cause of this variation may be attributed to the combined effects of speed and fuel viscosity. At

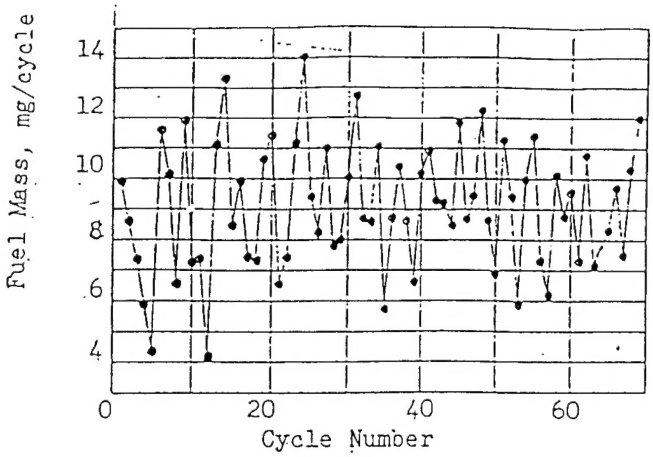

Fig.12 Injection During the Starting Process with REF1 Fuel at 0°C.

higher speeds, the time for filling the pump barrel would be less. This is particularly true for our engine, in which the flow from the tank to the pump is by gravity.

The fuel accumulation or the concentration of the fuel vapor in the cylinder during compression is expected to have played a role in the success of the combustion reactions. It is estimated that the fuel accumulated in the cylinder during cycle 29, as a result of the misfiring in cycles 24 to 28, amounted to 58 mg (10).

5- Ambient temperature

Fig (13) shows the gas temperature at the start of injection for the three ambient temperatures for the runs in Fig (11) As the temperature exceeded 640°K, the operation was on the 4 stroke cycle. Between 620°K and 640°K, the operation was on 8 stroke cycle till the temperature reached 640°K. Below 620°K, the engine misfired completely till cycle no. 28. In the following cycles, the temperature increased above 620°K and the engine operated on 12 stroke cycle and 8 stroke cycle.

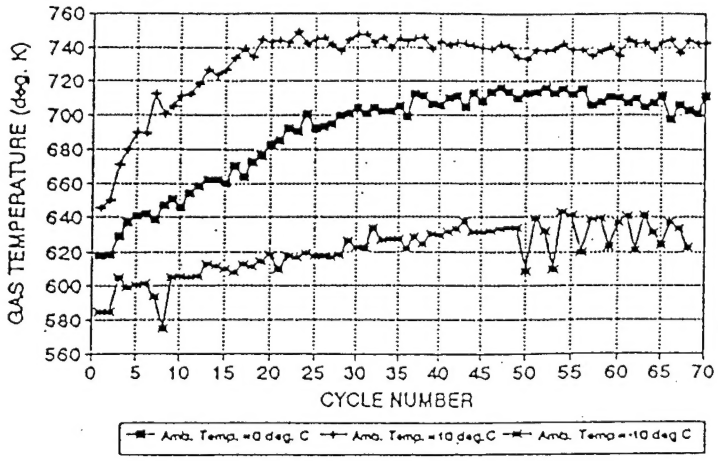

Fig.13 Cylinder Gas Temperature at Start of Injection with JP5 Fuel at Different Ambient Temperatures.

CONCLUSIONS

Significant findings to date include the following:

1. Combustion instability during diesel cold start is not a random phenomena. The mathematical quantification and subsequent experimental validation of borderline combustion allowed the actual fundamental definition of 16, 12 stroke and 8 stroke cycles within the engine start up phase, while after warm up a more conventional 4 stroke cycle operation became apparent. No previous researcher has ever quantified this phenomena.

2. Engine deceleration after acceleration (due to firing) during cold start transients was not caused by autoignition failure.

3. The first combustion misfiring after instantaneous acceleration is caused by a combination of the following: i) the short period of time available for autoignition and combustion at top dead center before expansion, and ii) the charge dilution with the residual gases of the fired cycle.

4. The causes of sequential misfiring appear to be an imbalance between:
i) energy released from exothermic reactions which depend on: the concentration of fuel vapor, dilution with residual gases, and temperature, and ii) energy absorbed in evaporation of accumulated fuel, endothermic reactions, heat losses to walls, and blowby losses.

RECOMMENDATIONS:

1. Investigate the chemical factors which cause combustion instability by using the advanced laser based diagnostic techniques in the optical access engine.

2. Apply advanced electronic controls to eliminate or reduce combustion instability during cold starting.

REFERENCES

1-Livengood, J.C. and Wu, P.C., "Correlation of Autoignition Phenomena in Internal Combustion Engines and Rapid Compression Machines", Proceedings of Fifth Internal Symposium on Combustion," pp 347-356, Reinhold, 1955.
2-Itoh, Yasuhiko, "The Characteristics of Diesel Combustion and the Mechanisms of Misfiring Under Low Ambient Temperatures," M.S. Thesis, Wayne State University, 1990.
3-Henein, N.A. and Lee, C.S., "Autoignition and Combustion of Fuels in a Direct Injection Engine Under Low Ambient Temperatures," SAE 861230, Combustion Heat Transfer and Analysis, Vol. P-186 pp 109-122 and SAE Trans. Vol. 95, 1986.
4-Zahdeh, A., Henein, N. A. and Bryzik, W., "Diesel Cold Starting: Actual Cycle Analysis Under Border Line Conditions," SAE 900441, 1990.
5-Birdi, P.S., "General Correlation of the Ignition Delay Period in Diesel Engines," Ph.D. Dissertation, Wayne State University, 1979.
6-Galliot, F., Cheng, W.K., Cheng, C., Sztenderowicz, M., Heywood, J.B. and Collings, N., "In Cylinder Measurement of Residual Gas Concentration in a Spark Ignition Engine," SAE 900485, 1990.
7-Leppard, W.R., "The Chemical Origin of Fuel Octane Sensitivity," SAE paper No. 902137, 1990.
8-Benson, S.W., "The Kinetics and Thermochemistry of Chemical Oxidation with Application to Combustion and Flames," Prog. Energy Combust. Sci., Vol. 7 pp 125-134, 1981.
9-Hoskin,D.H., Edwards,C.F. & Stiebers, D.L., "Ignition Delay Performance Versus Composition of Modern Fuels," SAE 920109, 1992.
10-Henein, N. A., Zahdeh, A., Yassine, M. and Bryzik, W., "Diesel Engine Cold Starting: Combustion Instability," SAE Subzero Engineering Conditions Conference Proceedings, Paper No. 920005, P 248, pp 33-48, and SAE 1992 Transactions, Journal of Engines, 1993.